#1

A STATISTICAL ANALYSIS OF ELECTROPHYSIOLOGICAL DATA FROM AUDITORY NERVE FIBERS IN CAT

PETER R. GRAY

Loan Copy Only

451

TECHNICAL REPORT 451

JUNE 21, 1966

MASSACHUSETTS INSTITUTE OF TECHNOLOGY
RESEARCH LABORATORY OF ELECTRONICS
CAMBRIDGE, MASSACHUSETTS

The Research Laboratory of Electronics is an interdepartmental laboratory in which faculty members and graduate students from numerous academic departments conduct research.

The research reported in this document was made possible in part by support extended the Massachusetts Institute of Technology, Research Laboratory of Electronics, by the JOINT SERVICES ELECTRONICS PROGRAMS (U.S. Army, U.S. Navy, and U.S. Air Force) under Contract No. DA36-039-AMC-03200(E); additional support was received from the National Science Foundation (Grant GK-835), the National Institutes of Health (Grant 2 PO1 MH-04737-06), and the National Aeronautics and Space Administration (Grant NsG-496).

The Eaton-Peabody Laboratory of Auditory Physiology is jointly operated by the Massachusetts Institute of Technology and the Massachusetts Eye and Ear Infirmary.

The research reported in this document was made possible in part by support extended the Eaton-Peabody Laboratory by the National Institutes of Health under Grant NB-01344.

MASSACHUSETTS INSTITUTE OF TECHNOLOGY

RESEARCH LABORATORY OF ELECTRONICS

Technical Report 451 June 21, 1966

A STATISTICAL ANALYSIS OF ELECTROPHYSIOLOGICAL DATA FROM AUDITORY NERVE FIBERS IN CAT

Peter R. Gray

This report is based on a thesis submitted to the Department of Electrical Engineering, M. I. T., August 23, 1965, in partial fulfillment of the requirements for the degree of Doctor of Philosophy.

(Manuscript received April 1, 1966)

Abstract

Electrophysiological data from single auditory nerve fibers have been analyzed with the objective of developing a random-process model for the firing patterns of these fibers. This study differs from earlier attempts at modeling these data in that new data-processing methods have been employed in order to more directly test and refine assumptions relating to models. In addition to calculating conventional post stimulus time (PST) and interval histograms, various conditional probabilities associated with the firing patterns have been estimated. These analyses suggest that a fiber recovers from the refractory effects that follow a firing within 20 msec after the firing. The effect of the stimulus on a fiber that has apparently recovered can be studied by estimating the conditional probability of a spike in a particular interval of time, given some minimum time since the last firing. Analysis of these "recovered probabilities" allows a more direct comparison of some aspects of model and data than is possible with other calculations such as the PST histogram. Results from these and other conditional probability analyses are presented with particular emphasis on data obtained with short acoustic clicks as stimuli. The use of these calculations to study the nonrefractory aspects of the data has provided a somewhat simpler picture of the relation between these firing patterns and the mechanical motion of cochlear structures, but it has also exposed some unexpected phenomona. The implications of these results for possible models are reviewed.

TABLE OF CONTENTS

I.	INTRODUCTION	1
	1.1 The Peripheral Auditory System	1
	1.1.1 Mechanical Motion of the Cochlear Partition	2
	1.1.2 Transduction from Mechanical Motion to Neural Firings	3
	1.1.3 Axons	6
	1.2 Firing Patterns in Auditory Nerve Fibers	7
	1.2.1 Spontaneous Activity	8
	1.2.2 Tuning Curves	9
	1.2.3 Click Stimuli	10
	1.2.4 A Simple Model	13
	1.3 Models for Firing Patterns of Auditory Nerve Fibers	15
II.	DATA PROCESSING METHODS	18
	2.1 Post Stimulus Time Histograms	18
	2.2 Interval Histograms and Hazard Functions	20
	2.3 Conditional Probability Matrices	25
	2.4 Recovered Probability Histograms	27
	2.5 Conditional Probability Histograms	29
	2.6 Conclusions	31
III.	ANALYSIS OF CLICK DATA	33
	3.1 The Click Stimulus	33
	3.2 Statistical Regularity	34
	3.3 Recovery	38
	3.4 Click Rate	39
	3.5 Probabilities Associated with the Peaks of the PST Histograms	45
	3.6 Second Firings after 3/4 to 1 msec	49
	3.7 Recovered Probabilities on a Finer Time Scale	57
IV.	DATA OBTAINED WITH VARIOUS STIMULI OTHER THAN SIMPLE CLICKS	64
	4.1 Continuous Tones	64
	4.2 Tone Bursts	70
	4.3 Noise Bursts	77
	4.4 Clicks Plus Noise	82
V.	Summary and Conclusions	86
Acknowledgment		89
References		90

I. INTRODUCTION

In the last few years, a considerable amount of electrophysiological data collected from single afferent auditory nerve fibers has become available. Many aspects of these data appear to be rather simply related to the details of the anatomy, physiology, and mechanical properties of the peripheral auditory system as they are, at present, understood. This situation has encouraged efforts to develop some sort of abstract model to describe the transformation from acoustic stimuli to firing patterns of the auditory nerve fibers. The long term objective in trying to develop such a model is twofold. A manageable description of the output of the peripheral auditory system would be valuable, if not essential, in considering what kinds of processing of auditory information could be performed by the brain. And a model such as this could also provide new insights into the detailed processes within the peripheral auditory system which result in these firing patterns. At least two attempts to develop a model have recently been made, and this study represents the beginning of still another attempt. The distinguishing characteristic of this study is that the data have been processed in new ways in order to more directly test and refine the assumptions relating to models.

This report consists of five sections; the contents of each are described below. In Section I, background material relating to this study is presented; the discussion is divided into three sections. The first section consists of a rough, functional description of the peripheral auditory system. The next section contains a somewhat more detailed discussion of the firing patterns of auditory nerve fibers. Two other recent efforts at modeling the firing characteristics of these fibers are discussed in the last section. The data-processing methods that have been employed in this study are discussed in Section II. By far the most thoroughly studied stimulus in this work is the click, and results obtained with this stimulus are presented in Section III. Several other stimuli were also employed, though less extensively than the click. Results obtained with these stimuli are presented in Section IV. The results of this study are reviewed in Section V in terms of their implications for models. A completed model has not yet resulted from this study, and some of the problems involved in developing a model are also discussed in Section V.

1.1 THE PERIPHERAL AUDITORY SYSTEM

Figure 1 presents a schematic diagram of the peripheral auditory system. Sound, impinging on the outer ear, travels through the external auditory meatus and vibrates the tympanic membrane (eardrum). This vibration is transmitted by the middle-ear bones to the oval window of the cochlea, thereby setting the cochlear fluids and structures in motion. The fibers of the auditory nerve terminate at hair cells, which are located within the cochlear partition. Through the action of the hair cells, the spike activity of these fibers is influenced by the mechanical motion of the cochlear structures.

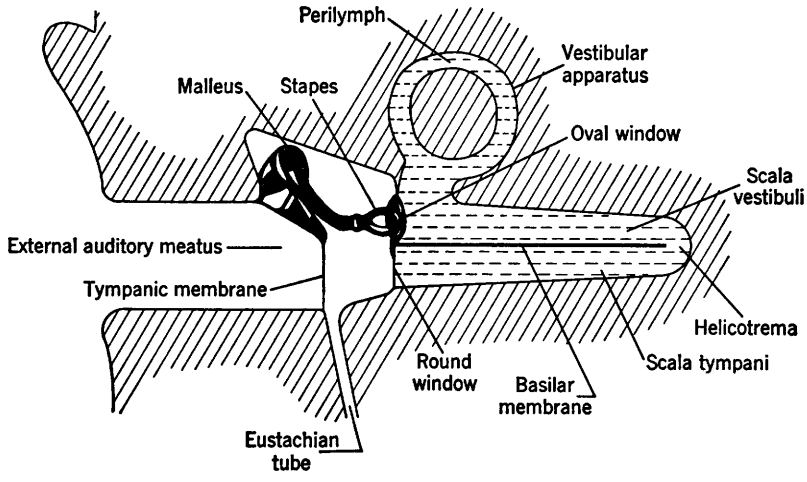

Fig. 1. Schematic drawing of the human ear. [From G. von Békésy and W. A. Rosenblith, "The Mechanical Properties of the Ear," Chap. 27 in Handbook of Experimental Psychology, S. S. Stevens (ed.), John Wiley and Sons, Inc., New York, 1951 (reproduced by permission of John Wiley and Sons, Inc.).]

The action potentials, or spikes, which are generated in the auditory nerve fibers, are propagated along these fibers and comprise the auditory input to the central nervous system.

These various stages in the transformation from acoustic stimulus to spike activity of the auditory nerve fibers will be discussed in some detail. This discussion is primarily a survey of the known anatomical, physiological, and mechanical features of the peripheral auditory system that are clearly relevant to the present study. Some topics such as the various potentials that have been measured with gross electrodes have been omitted from this discussion because these data have had little influence on the current study. This is not to suggest that these data are irrelevant; rather, for the sake of brevity and clarity, only that background which has thus far been involved in this study is presented.

1.1.1 Mechanical Motion of the Cochlear Partition

While driving the stapes sinusoidally, von Békésy measured the amplitude and phase of the resulting sinusoidal motion at several points along the cochlear partition.[1] His data suggest that for reasonable intensities the system that converts motion of the stapes into motion of a point on the cochlear partition may be regarded as linear and time-invariant, and hence completely described by a transfer function or frequency response. The transfer function presented in Fig. 2 illustrates the salient features of the transfer functions that he measured. For each point along the partition, there is some frequency, f_o, at which maximum amplitude of displacement occurs; the amplitude decreases smoothly as the frequency deviates from f_o. The "most sensitive frequency," f_o, varies, in an approximately exponential manner, with position along the cochlear partition; f_o is

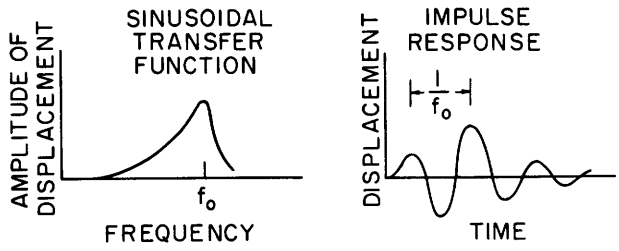

Fig. 2. Mechanical motion of one point on the cochlear partition. The sinusoidal transfer function is intended to be representative of von Békésy's data,[1] and the impulse response is intended to be representative of those calculated by Siebert[6] and Flanagan.[5] f_o decreases regularly as x, the distance from the stapes, increases.

highest near the stapes and lowest near the apex.

The transfer characteristics of the middle ear have also been measured by von Békésy[2] and by others.[3,4] It appears that the system that converts pressure at the eardrum to motion of the stapes may also be regarded as linear and time-invariant. The frequency response of this system is that of a lowpass filter that passes all frequencies below 1 kc or 2 kc, but attenuates higher frequencies. Conceptually, it is useful to combine the middle-ear and the inner-ear mechanical systems into one system, which transforms pressure at the eardrum into displacement of the cochlear partition. For the low-frequency region of the partition, the transfer function of Fig. 2 would also apply for the combined system. For the high-frequency region, this function would have to be modified to take account of the frequency-dependent attenuation of the middle ear.

A short acoustic click was used as a stimulus in much of this work. The mechanical motion resulting from this click can be calculated from the sinusoidal measurements discussed above. Since the mechanical system appears to be linear and time-invariant, a hypothetical impulse response of the system can be calculated from the frequency response (of course, this requires phase vs frequency information which von Békésy also measured). The response to a click, or to any other acoustic stimulus, can then be obtained by convolving the stimulus waveform with the impulse response. If the acoustic click is short compared with the impulse response, the click is effectively an impulse, and the mechanical motion is simply the impulse response.

The impulse response has been calculated by Flanagan[5] (with and without the middle ear) and by Siebert[6] (without the middle ear). The important features of the results of these calculations are represented in Fig. 2: the impulse response consists of a ringing, or oscillation, at the frequency f_o which decays to zero in a few cycles.

1.1.2 Transduction from Mechanical Motion to Neural Firings

Figure 3 presents a cross section of the cochlear canal. The cochlear partition is the region enclosed by the basilar membrane and Reissner's membrane. When the

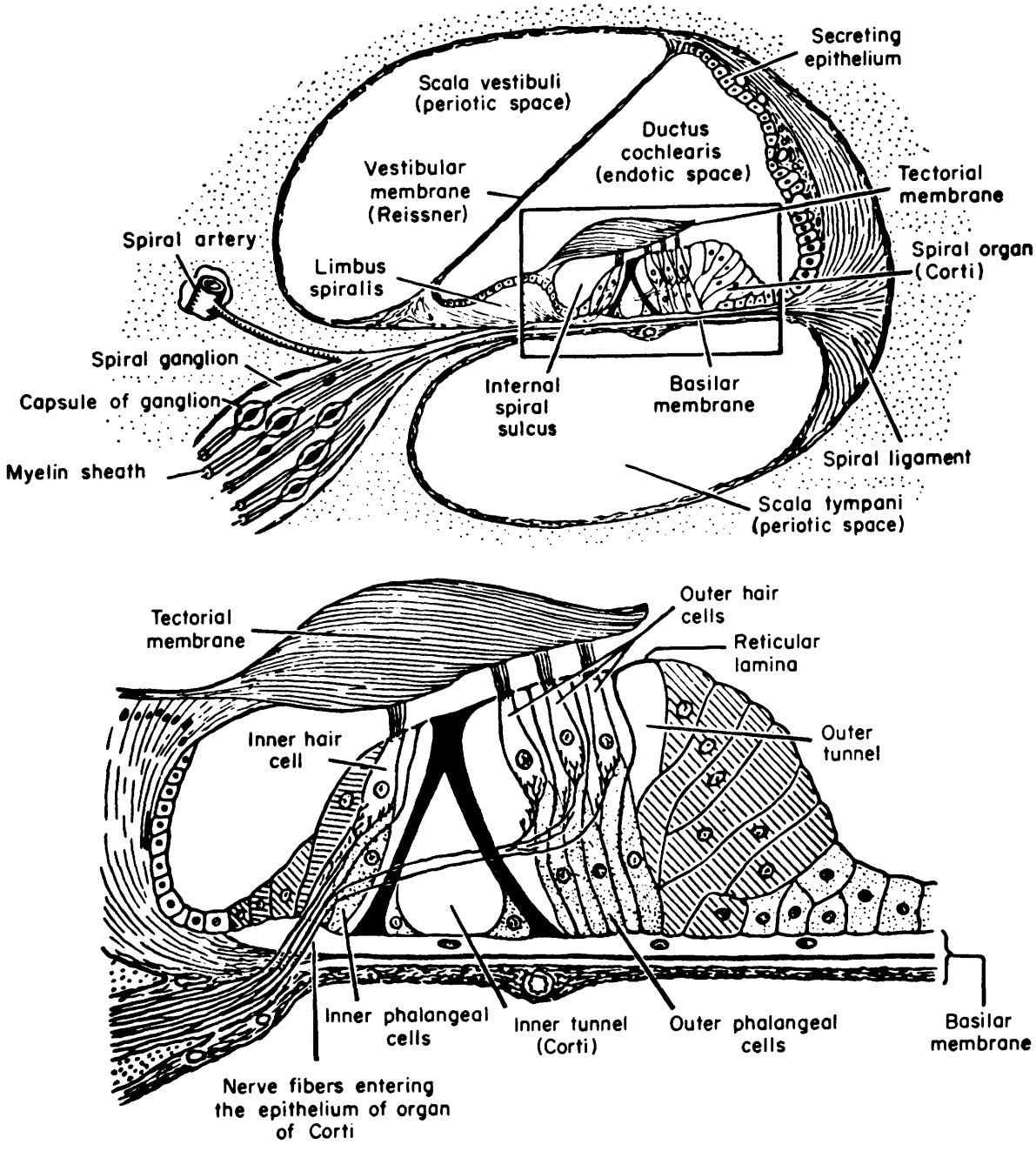

Fig. 3. Schematic diagram of a cross section of the cochlear canal with an enlarged view of the organ of Corti. [From A. T. Rasmussen, Outlines of Neuroanatomy, William C. Brown Company, Dubuque, Iowa, 3rd edition, 1943, as reproduced in S. Ochs, Elements of Neurophysiology, John Wiley and Sons, Inc., New York, 1965 (reproduced by permission of John Wiley and Sons, Inc.).]

cochlear partition is set in motion, there is some relative motion between the tectorial membrane and the hair cells, which results in the bending of the hairs. Presumably, the influence of the hair cells on the spike activity of the fibers varies with the bending of the hairs. The mechanical measurements referred to above were of the displacement of the cochlear partition as a whole. It seems reasonable (but not at all certain) that the bending of the hairs might be related in a simple way to the displacement of the cochlear partition. This possibility has not, however, been verified experimentally, although von Békésy has made some observations of the mechanical properties of the Organ of Corti.[7]

The details of the innervation of the hair cells by the auditory nerve fibers are not completely known. In order to give some idea of the complexity of the problem, the following paragraph from Kiang[8] is presented. The numerous references to the publications on which this paragraph is based are omitted here, but may be found in Kiang's monograph.[9]

> "The innervation of the cochlea has been described for a number of different species. The peripheral portion contains at least two main types of fibers, the radial and the spiral. Statistics are not available on the number and distribution of these fiber types, but it is usually said that (1) the innervation of inner hair cells is predominantly by radial fibers that end on only a few cells; (2) the innervation of outer hair cells is partially by radial fibers that go to a few cells and partially by spiral fibers that may run along as much as a third of a cochlear turn, innervating many cells; and (3) each spiral fiber thus supplies many hair cells, and each hair cell is connected to several fibers, radial or spiral. Electron microscope studies have given some information about the nerve endings in the cochlea but have not yet provided generally accepted descriptions of the detailed relation of fibers to endings." (pages 12-13)

In addition to these afferent-fiber endings at the hair cells, there are also endings of the efferent fibers of the olivo-cochlear bundle. (The efferent fibers conduct action potentials from the central nervous system to the periphery.) There are only approximately 500 fibers in the olivo-cochlear bundle of the cat[10] (as compared with approximately 50,000 afferent fibers[11]). But in some regions of the cochlea approximately half of the nerve endings at the hair cells are efferent.[12] Electrically stimulated activity in the efferent fibers has been observed to reduce the activity of the afferent fibers, and spike activity in response to acoustic stimuli has been recorded from the efferent fibers.[13] Thus, it appears probable that the efferent fibers have some influence on the spike activity of the afferent auditory nerve fibers.

Unfortunately, the functioning of the efferent fibers is not well understood, and very little information exists on the influence of the efferent fibers on the spike activity of a single afferent fiber. For this reason, the role of the efferent fibers is not specifically considered in this study. It is not yet clear whether or not this is a serious omission. Reasoning on the basis of the relatively small number of efferent fibers, Davis has suggested[16] that "the function of the efferents should be to produce a general increase or decrease in excitability as opposed to any detailed pattern of effects." The data of Fex[13] suggest that a latency of at least 15 msec could be expected for efferent effects. In most

of this study the firing patterns are examined for 10 or fewer milliseconds after the stimulus presentation, so that the efferent effects, if any, might well be of the kind Davis suggests. Finally, it is possible that the barbiturate anesthesia used in these experiments may considerably reduce the efferent activity.

The functioning of the hairs cells is not completely understood, partly because it has not yet been possible to make sufficiently microscopic measurements of the electrical and chemical activity of the hair cell. It is thought that the hair cell "excites" the auditory nerve fiber in some way that depends on the mechanical deformation of the hair cell. Whether the excitation is electrical or chemical in nature is unknown. Also, whether the hair cells that might excite a given nerve fiber are adjacent or distant (and therefore experiencing different mechanical motions) has not been resolved. Given this considerable uncertainty about the transformation from mechanical motion of the cochlear partition to the "excitation" of the auditory nerve fiber, a few comments are in order concerning the approach taken in this study.

Briefly stated, the approach is as follows. The simplest of the possible hypotheses that are consistent with the available information will be made, and these hypotheses will be tested and refined by considering the electrophysiological data available from auditory nerve fibers. Thus, until contradictions arise, it will be assumed that (i) each fiber is "excited" by only a few hair cells, each of which experiences effectively the same mechanical stimulus; (ii) the effective mechanical stimulus for a single hair cell is a linear transformation of the pressure waveform at the eardrum, and this transformation has a frequency response similar to that of Fig. 2; and (iii) the efferent effects, if any, are of the kind suggested above – an increase or decrease in excitability that does not change rapidly.

1.1.3 Axons

A good deal is known about the physiology of axons, and a discussion of their properties may be found in many physiological texts (see, for example, Ruch and Fulton,[14] or Ochs[15]). Although most of the relevant experiments have been done on much larger axons, where it is possible to place electrodes within the axon, and thereby both measure and control the potential across the axon membrane, it is thought that the auditory nerve fibers possess similar properties.

The functional importance of axons results from their ability to conduct "action potentials" (or "spikes" or "firings"). The action potential is a temporary depolarization of the membrane potential, which is propagated down the axon by means of some rather complex electrical and chemical processes. In the axon experiments, an applied current is used to depolarize the membrane potential from its resting value, and it is observed that when the membrane potential reaches a value called "threshold," an action potential occurs. The magnitude of the applied current determines the length of time that it takes for the membrane potential to reach threshold, but the size of the propagated action potential does not depend on the details of the applied "stimulus." This fact is

sometimes labeled the "all-or-none" law, and it implies that the information conveyed by a single axon is coded in the time pattern of action potentials, not, for example, in the particular wave shapes.

Immediately following an action potential there is a "refractory period" during which a stronger stimulus is required to initiate another action potential, i.e., the "threshold" is higher than its normal value. When all of the chemical and electrical changes associated with the action potential are over, so that, in particular, the membrane potential and threshold have returned to their resting values, the axon is said to have "recovered."

It is thought that the auditory nerve fibers are similar in many respects to other axons; however, the location and mechanism of the excitation of the fiber by the hair cells are not known. It might be that the fiber is depolarized by an electric current as in the axon experiments; alternatively, the depolarization might be effected by some chemical "transmitter substance." Presumably, the auditory nerve fibers (and perhaps also the hair cells) have refractory properties of the kind observed in the axon experiments. This being the case, the time pattern of firings in an auditory nerve fiber would be influenced by both the mechanically induced excitation of the hair cells and the refractory properties of the neural unit. One of the principal methods of this study has been to "remove" the refractory complications from the auditory-nerve data by considering the effect of the stimulus on fibers that have not fired for a period of time sufficient for recovery.

1.2 FIRING PATTERNS IN AUDITORY NERVE FIBERS

The discussion of the statistical analysis of the time pattern of action potentials in single auditory nerve fibers begins with a review of the data of Kiang and his co-workers.[8] There have been several other (less extensive) studies of the firing patterns of auditory nerve fibers in cats and other animals, and references to these may be found in Kiang[8] and in Davis.[16] The present study has been based primarily on data from Kiang's laboratory because (i) Kiang's results are in general agreement with those of other studies; (ii) Kiang's electrophysiological data have been available on magnetic tape for further processing in connection with this study; and (iii) it has been possible to obtain additional data needed for this study in the same laboratory and by employing the same techniques and equipment as Kiang and his co-workers used.

Following a brief statement of experimental methods, data obtained with various "simple" acoustic stimuli will be considered. Throughout this discussion an attempt is made to relate the statistical characteristics of the firing patterns of auditory nerve fibers to the characteristics of the peripheral auditory system, which were reviewed in the preceding section. Finally, these relations are summarized in an abstract model, which provides a framework for considering earlier modeling efforts and for beginning this one.

In these experiments the anesthetized cats were located in a soundproof room. The

acoustic stimuli were delivered by a condenser earphone, through a tube sealed into one external auditory meatus. The voltage waveforms applied to the condenser earphone were generated by equipment outside of the chamber and under control of the experimenter. The electrical signal from the microelectrode, as well as the stimulus timing information, were recorded on magnetic tape for later "off-line" processing. During the experiments performed specifically for this study, "on-line" computer processing of the data was used to provide information that was useful for choosing stimulus parameters. Details concerning experimental methods may be found in Kiang.[17]

1.2.1 Spontaneous Activity

Even in the absence of acoustic stimulation, action potentials occur in auditory nerve fibers. This "spontaneous activity" appears to be relatively easy to characterize statistically. Preliminary indications are that the times between "spontaneous" action potentials in a single fiber may be regarded as independent, identically distributed random variables.[18] This implies that the spontaneous activity is completely.specified (in

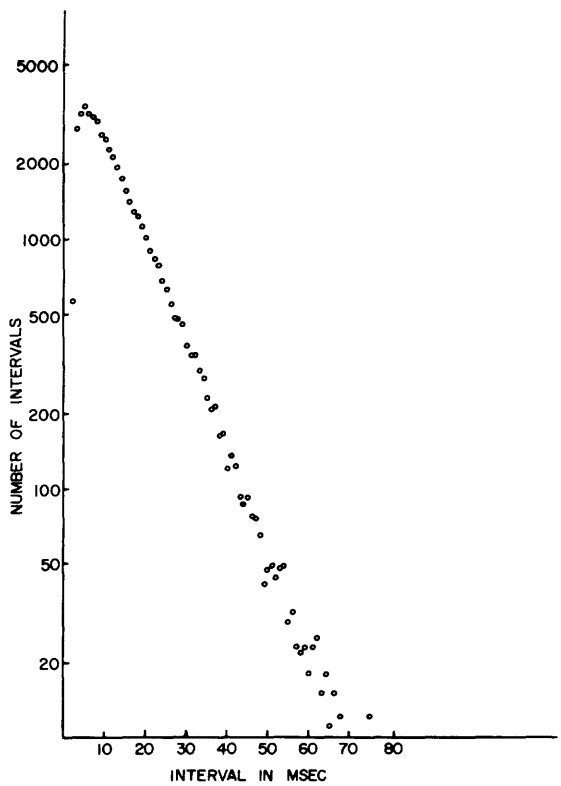

Fig. 4.

Unit 275-35. Interval histogram calculated from a long (11-minute) recording of spontaneous activity. Semi-logarithmic coordinates are used to emphasize the exponential decay of the interval distribution. [Fig. 8.5, page 98, in Kiang[8] (reproduced by permission of The M.I.T. Press, Cambridge, Mass.).]

a statistical sense) by the probability density function of these interevent times. An estimate of this density function is the interval histogram – a plot of the number of interspike intervals of each length in an observed period of activity. (For this and other histogram calculations, time is quantized into "bin-width" units, so that the k^{th} bar

corresponds to times between k and k + 1 "bin widths.")

A representative interval histogram of spontaneous activity is given in Fig. 4. The vertical scale is logarithmic, and the fact that the right-hand portion of this distribution is nearly a straight line implies that the interval distribution has an exponential "tail" when plotted on a linear scale. The spontaneous rate can be calculated from the interval histogram: it is equal to the reciprocal of the average interval length. Although spontaneous rates vary among fibers from less than one per second to more than 100 per second, it appears that all of the interval distributions may be characterized by a mode at less than 10 msec, followed by an exponential "tail."[19]

1.2.2 Tuning Curves

With continuous tone stimulation of appropriate intensity and frequency, the firing rate of auditory nerve fibers increases. (Rupert et al.[20] reported that the intensity and frequency of the applied tonal stimulus can be chosen in such a way that a firing rate that is below the spontaneous level is maintained; however, other workers, including Kiang,[21] have looked for and failed to observe this phenomenon.) If the tonal stimulus is sufficiently high in frequency (roughly, 5 kc or higher) no stimulus-related time structure can be found in the firing patterns, and the time pattern of events is statistically similar to the spontaneous case. (The interevent distribution is, of course, changed from that of the spontaneous case since the firing rate is increased, but it still has a mode at less than 10 msec, followed by an exponential "tail.") At lower frequencies a stimulus-related time structure is observed in the firing patterns; this structure appears as a tendency for the fiber to fire during only one-half of the period of the sine wave. In Section IV the firing patterns occurring with sinusoidal stimuli are discussed in more detail, with emphasis on the variations with stimulus intensity. In the present section only sinusoidal data in the form of "tuning curves" are considered.

The tuning curve of an auditory nerve fiber is a plot of its "threshold" (lowest intensity for which a change in rate from the spontaneous level can be detected by the experimenter*) against frequency. Several tuning curves obtained from different units in the same cat are presented in Fig. 5. These curves are representative in that (considering only moderate intensities) each has a single minimum. The frequency at which this minimum occurs is called the characteristic frequency (CF). These neural tuning curves are qualitatively similar to the mechanical tuning curves obtained by von Békésy; however, the neural tuning curves are somewhat narrower than the corresponding mechanical tuning curves.

The similarity of the neural and mechanical tuning curves suggests that the

*Normally the electrical signal from the microelectrode is displayed on an oscilloscope screen and presented audibly through a loudspeaker. Both cues are used by the experimenter in detecting a change in rate. It is much easier to detect a change if tone bursts rather than continuous tones are used, and it has been demonstrated that the tuning curves obtained by both methods are essentially equivalent.[22]

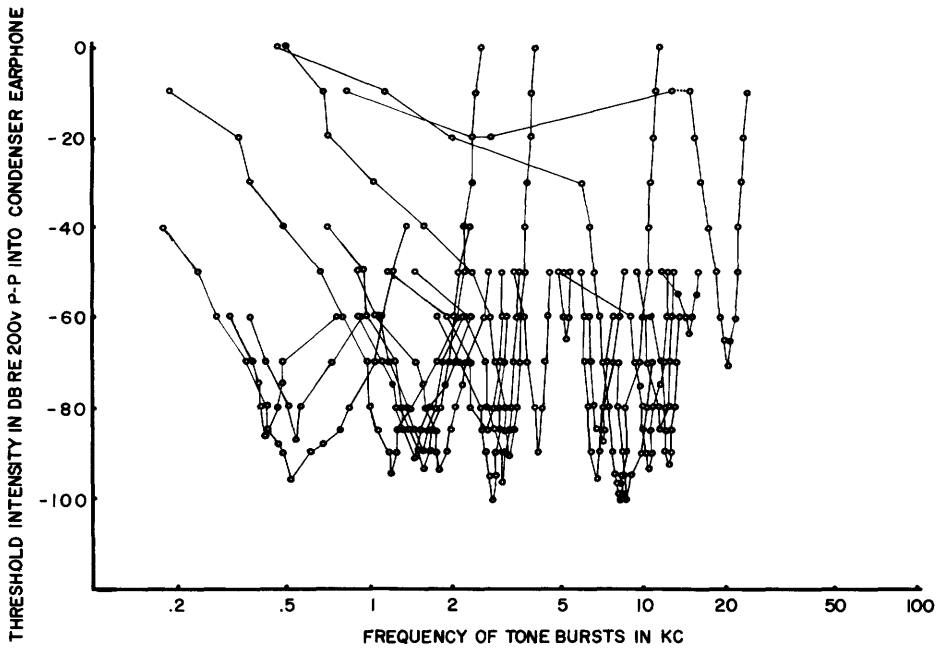

Fig. 5. Cat 296. Tuning curves. [Fig. 7.3, page 86, in Kiang[8] (reproduced by permission of The M.I.T. Press, Cambridge, Mass.).]

relationship between the mechanical motion and the firing rate of the fiber may not be overly complicated. For example, if a single fiber were affected by the mechanical motion at a single point on the cochlear partition, and a fixed amplitude of displacement corresponded to the "threshold" of the unit, then the mechanical and neural curves would be congruent. If, instead of depending on the displacement at a single point, the fiber were affected by some spatial average or derivative of the displacement, or the velocity, along the partition, then narrower tuning curves might result.

1.2.3 Click Stimuli

When short acoustic clicks are used as stimuli,* a time structure that is related to the time of the click presentation may be observed in the firing patterns of the fibers. This time structure consists of certain "preferred firing times" following the click presentation. One useful measure of the time structure of the firing patterns is obtained by calculating the post stimulus time (PST) histogram. The PST histograms for several units from cat 296 are presented in Fig. 6. The horizontal axis of the PST histogram represents time measured from the click. The height of any bar in the histogram is the number of spikes occurring in a one "bin-width" interval located at the time

*The click stimulus is generated by applying a 100-μsec voltage pulse across the earphone. This results in an acoustic pulse of 200-250 μsec duration. Reversing the sign, or polarity, of the voltage pulse reverses the polarity of the acoustic click.

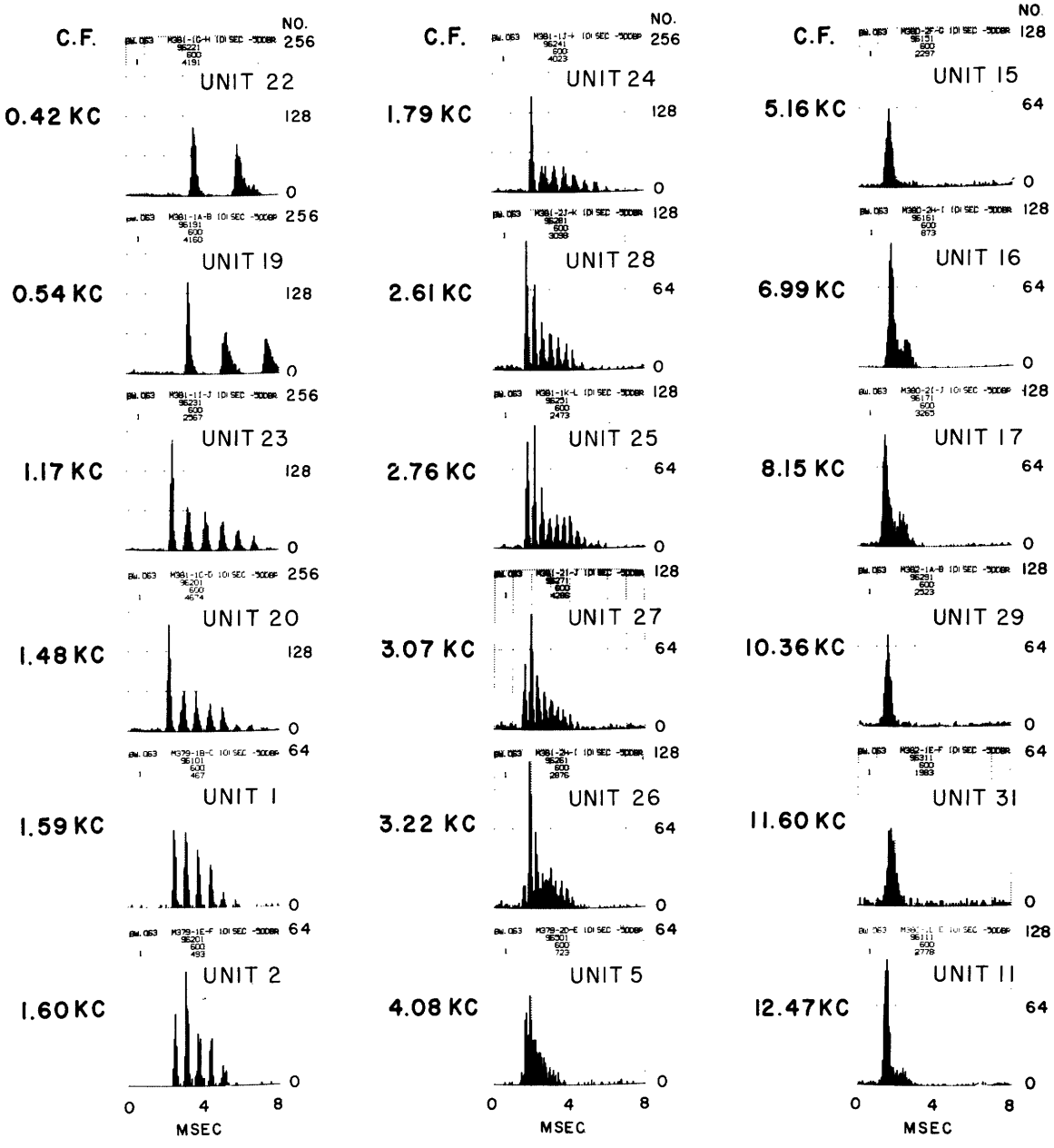

Fig. 6. Cat 296. PST histograms (bin width 0.0625 msec; 128 bars). Stimuli: 10/sec, -50 db rarefaction clicks, 1 minute. [Fig. 4.7, page 28, in Kiang[8] (reproduced by permission of The M.I.T. Press, Cambridge, Mass.).]

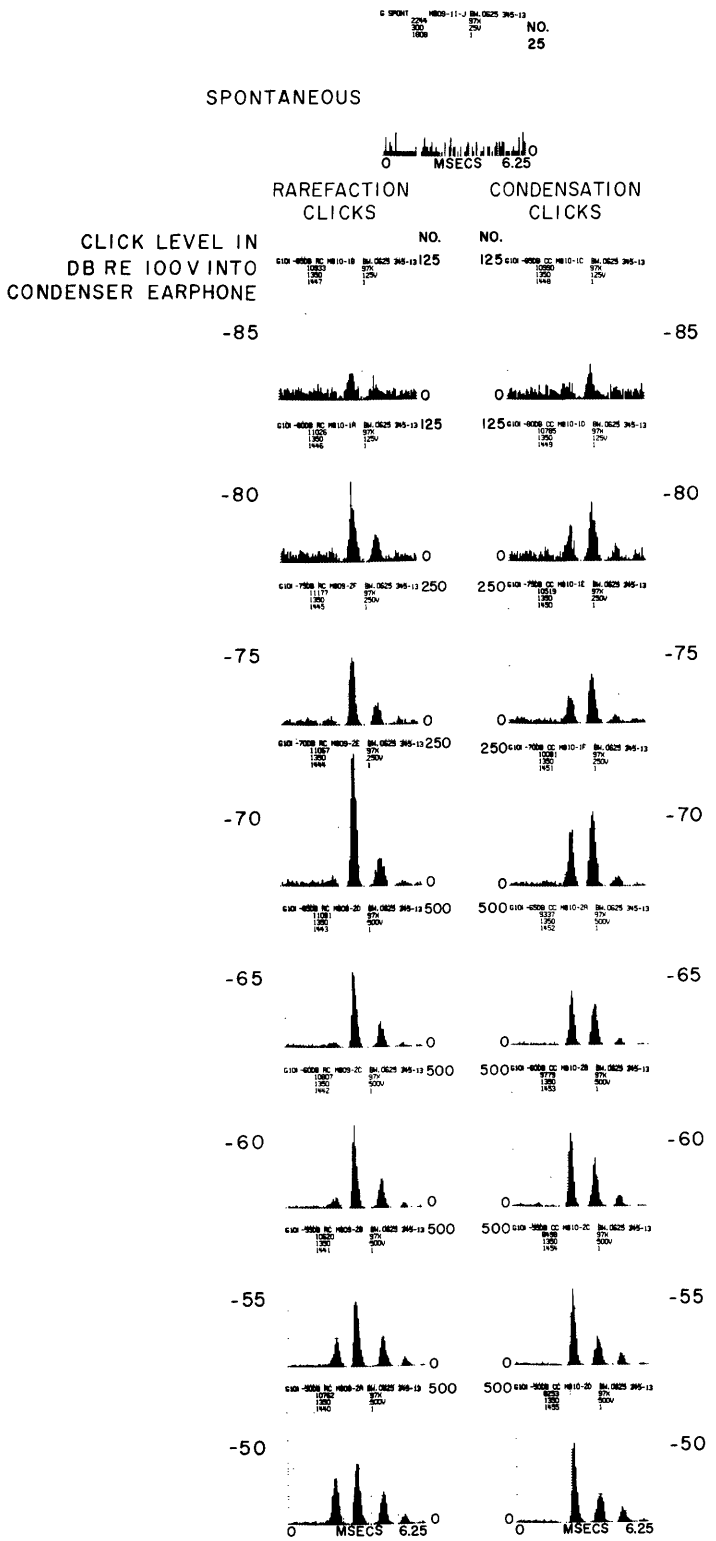

Fig. 7.

Unit 345-13. PST histograms (bi width 0.0625, 100 bars). Stimuli 10/sec rarefaction and condensation clicks, several intensities 2.25 minutes. Length of spontaneous run: 30 seconds.

corresponding to the horizontal coordinate of the bar. Thus, a particularly tall bar, or a "peak" consisting of adjacent relatively tall bars, indicates a preference for firing at that particular time after the click. Close examination of the first two columns of Fig. 6 indicates that the spacing of the peaks in these histograms is approximately equal to the period of the characteristic frequency. This correspondence also suggests that the relationship between mechanical motion and the spike patterns of these fibers may be relatively simple. To illustrate, if a fiber were affected by the mechanical displacement at a single point in the low-frequency region of the cochlear partition, the CF of the fiber would be expected to equal the most sensitive frequency for that point on the partition, and the mechanical motion of this point in response to a click would be simply the impulse response associated with that point – a ringing, or oscillation, at the CF. If only one polarity of motion stimulated firings, the preferred times of firings would be separated by the period of the CF. The units with higher CF, which are presented in the right column, do not necessarily contradict this picture, since compared with the impulse responses corresponding to these units, the acoustic clicks are not short enough to be regarded as impulses. Incidentally, at the present time, it is not clear (and, for this study, not important) whether the lack of time structure in the click response of the high-frequency units is due to (i) the wave shape of the actual acoustic click, (ii) a limit on the frequency at which these units can "follow," or (iii) limitations on the time resolution of the tape recorders and related equipment used in these experiments. Of course, the continuous-tone stimulus provides a more direct way of exploring the limits on the "following ability" of these units, but this stimulus has not yet been fully exploited for this purpose.

In Fig. 7, an intensity series is presented for both polarities of clicks. It may be observed that with increasing intensity the peaks grow in size and new ones appear, but the latencies of the peaks do not change. Another observation from Fig. 7 is that the peaks in one column are located, in time, between the peaks of the other. Both of these observations are consistent with the notion that only one polarity of the mechanical motion stimulates firings, for, changing the intensity of the click would then have no effect on the location of the preferred times of firing, but changing the polarity of the click, and hence the polarity of the mechanical motion, would shift the preferred times by one half of the period of the CF.

1.2.4 A Simple Model

This discussion of the statistical characteristics of the firing patterns of auditory nerve fibers may be summarized in terms of the functional model given in Fig. 8. This model consists of three stages: a mechanical system, a rectifier, and a probabilistic device. This abstract model is suggested by the discussion of the peripheral auditory system and of the firing patterns of auditory nerve fibers, and it is hoped the model can be refined to describe correctly the transformation from the pressure waveform at the eardrum to the spike patterns in the fibers. It is not crucial, however, that

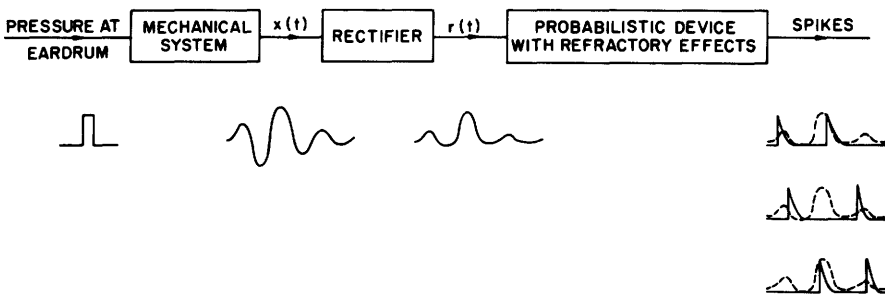

Fig. 8. Simplified model for generation of spikes in auditory nerve fibers. Indicated on the figure are waveforms corresponding to a click stimulus. Three of the many possible spike patterns are given to emphasize the probabilistic nature of the probabilistic device.

any of the intermediate model variables (i.e., the output of "mechanical system," and the output of "rectifier") correspond to any identifiable physical variables. For example, it might turn out that the output of the model mechanical system corresponds to the displacement of the cochlear partition at a single point, to the velocity of the cochlear partition at a single point, or to some local spatial average of displacement and velocity.

The (model) mechanical system is assumed to be linear and time-invariant and to have a frequency response and impulse response similar to that of Fig. 2. As the intermediate model variables are not constrained to be physically identifiable, the model mechanical system could have a frequency response narrower than the physical tuning curves measured by von Békésy. The rectifier, which operates on the output of the mechanical system, is only assumed to have a non-negative output that is a nonlinear, no-memory function of its input. (This assumption seems consistent with the data presented above, but will prove unworkable in Section III, where other aspects of the data are examined.) Finally, the output of the rectifier is taken as the input to the probabilistic device. This device has the property that the probability of a spike increases with the input, but decreases temporarily after each spike. The last property is intended to represent the refractory characteristics of the neural unit.

To illustrate that this model is consistent with the data discussed above, it is useful to consider each of the stimulus situations that were discussed. For the spontaneous case, the output of the mechanical system would be zero, the output of the rectifier would be a small positive constant, and the time patterns of spikes would be determined by the refractory characteristics of the probabilistic device. With continuous tone stimuli, the output of the mechanical system would be sinusoidal, with amplitude and phase depending on the frequency of the applied tone. The output of the rectifier would be similar to a half-wave rectified sine wave. The frequency sensitivity reflected in the neural tuning curves would be a direct consequence of the frequency response of the mechanical system. Finally, with clicks, the output of the mechanical system indicated in Fig. 8 might apply. The output of the rectifier would be increased from the spontaneous level when the displacement is positive, and might be decreased (though remaining non-negative)

when the displacement is negative. Changing the polarity of the clicks, and hence the output of the mechanical system, would move the preferred times of firing by the desired half period. Increasing the amplitude of the click, and hence the amplitude of the output of the mechanical system, would have two kinds of effects on the PST histogram. There would be a tendency for the peaks to grow in size, since the probability of a spike increases with the output of the mechanical system. Countering this effect, there might be a reduced probability of firing in the later peaks, because of the refractory characteristics of the device. For example, if the unit fires during the first peak, the probability of firing during the second is reduced. Thus it is possible that the size of the second peak might even diminish with increasing intensity.

Although this model appears to be consistent with the data discussed above, it does not appear capable of describing some of the complex interactions that occur with certain stimuli other than clicks and single sine waves. These interactions are often called "inhibitory" effects and are discussed by Kiang[23,24] and others.[25] A typical "inhibitory" situation is one in which the firing rate in the presence of two tones is less than that obtained with either one alone. In order to handle the "inhibitory" phenomena it would probably be necessary to modify this model, perhaps by removing the assumption that the fiber is affected by the mechanical motion at only one point on the cochlear partition.

The two-tone interactions have been excluded from consideration in this study for three reasons: at the time this study began, only a limited amount of data on two-tone interactions was available; the "simple" stimuli provide sufficient difficulties in terms of refining the model that it seems prudent to concentrate on them; and even if the model must eventually be generalized to handle the two-tone interactions, it is hoped that the model will reduce to the form considered here in the case of the "simpler" stimuli, and therefore the knowledge gained by studying the "simpler" stimuli will be of value in a wider context.

1.3 MODELS FOR FIRING PATTERNS OF AUDITORY NERVE FIBERS

While the model of Fig. 8 is incompletely specified, it does help to summarize the data described above and serves as a useful starting point for the development of a more refined model. There are quite different ways in which the probabilistic device might be defined, which depend in part on how explicitly the appropriate physiological variables are involved. One approach to the definition of this device is represented by the work of Weiss,[26] which was also based on Kiang's data.

Weiss formulated a model that relates the spike activity of auditory nerve fibers to acoustic stimuli. This model falls into the general framework of the model of Fig. 8, but Weiss is more specific about both the characteristics and the physiological significance of the various components of the model. He refers[26] to

> "... the major functional constituents of the peripheral system ... [as] ... (i) a linear mechanical system intended to represent the outer, middle, and the mechanical part of the inner ear; (ii) a transducer intended to represent the action of the sensory cells; and (iii) a model neuron intended to represent the nerve excitation process."

In terms of Fig. 8, his items (i), (ii), and (iii) are the mechanical system, the rectifier, and the probabilistic device. In Weiss' model neuron (probabilistic device), the output of the transducer (rectifier) is filtered and then added to Gaussian noise; the resulting waveform is identified as the neural membrane potential. When this potential exceeds some threshold, a spike occurs, and the threshold is set to a larger value. The threshold decays from this larger (refractory) value toward a resting level, until it is again exceeded by the membrane potential, at which time this sequence is repeated.

This description of the form of Weiss' model leaves some further details to be specified, such as the form of the rectifier, the bandwidth of the noise, and the time constant of the threshold decay. After making the necessary assumptions about such details, Weiss simulated the model on a large digital computer and found partial agreement between the PST and interval histograms obtained by simulation and those obtained from the electrophysiological data.

Weiss' work is of interest in this study because it illustrates one approach to refining the simplified model of Fig. 8. His model has served the purpose of demonstrating that certain assumptions about the nerve-excitation process, combined with what is known of the peripheral auditory system, yield results that are similar to the electrophysiological data. (There are difficulties, however, in obtaining the correct variations with intensity.) Unfortunately, it is a difficult model to refine further because its constituents cannot at the present time be measured directly. It is very difficult, for example, to improve on the form of the rectifier by comparing the simulated histograms with those obtained experimentally.

Another approach to completing the model of Fig. 8 could be described as phenomenological, as opposed to mechanistic. The phenomenological model would differ from that proposed by Weiss in the number and kind of physiological variables that are explicitly involved in the model. In this approach, the mechanical motion might be explicitly involved, as it is thought to be reasonably well understood. Variables like membrane potential and threshold, however, would probably not be, since they are neither clearly defined physiologically (for this neural system) nor directly measurable. The probabilistic device might then relate mechanical motion to the spike patterns without necessarily involving any intermediate variables that might be physiologically significant. This allows some freedom to choose a formulation that is more mathematically tractable than that of the threshold scheme used by Weiss. Of course, what is known, or guessed, about the excitation process could provide some hints about an appropriate mathematical scheme.

One example of the phenomenological approach is the model reported in a very preliminary way by Siebert and Gray.[27] Though this model has been contradicted by some

of the results of this study, it does provide a useful illustration of the phenomenological approach, and it gives some indication of the perspective with which this study was undertaken.

The model reported by Siebert and Gray describes the probability of firing in an incremental unit of time as proportional to the current value of a (suitably defined) "stimulus function" and to the current value of a "recovery function." The recovery function is assumed to have a fixed form, and its argument is taken as the area under the stimulus function since the last event, so that the rate of recovery is faster if an attempt is made to stimulate the unit. One consequence of these assumptions is that under an appropriate transformation of the time axis (determined by the "stimulus function") the process becomes a stationary renewal process (i.e., the times between events are independent identically distributed random variables). From this property follows a great deal of analytical simplicity in the description of statistics of this process. It can be shown, for example, that the expected bar heights ("expected" in the probabilistic sense) in a PST histogram are proportional to the "stimulus function," with refractory effects entering only as an over-all scale factor. (For this reason, it happens that if the model were "correct," the PST histograms would be a particularly useful way in which to present data.) Decision theoretic formulations and calculations for psychophysical experiments, of the type discussed in the author's Master's thesis,[28] and recently illustrated by Siebert,[29] are relatively easy, again, as a consequence of the particular form of the model.

Both the mechanistic and the phenomenological models described above were based on Kiang's data, as they were presented in interval and PST histograms. In Weiss' model, the histograms were such complicated results of the model assumptions that computer simulations were necessary to obtain them. In the model reported by Siebert and Gray, the assumptions implied that the PST histogram would be the same shape as the "stimulus function," but the examination of PST histograms alone could neither verify nor contradict these assumptions.

In many cases it is possible to process the data in other ways so as to more directly test and refine the assumptions of the model. This work began as an effort to develop still another model by testing and refining the basic assumptions with appropriate processing of the data. The orientation of this work is strongly phenomenological. It became apparent early in this study that the model reported by Siebert and Gray was not consistent with these data, and, in its present form, must be abandoned. In trying to develop another model, however, it remains an ideal of mathematical manageability. Though this study is not directed specifically toward a model of the kind reported by Weiss, many of the results provide new and stronger constraints on possible assumptions for that kind of model, too.

II. DATA PROCESSING METHODS

In the analysis of the firing patterns of auditory nerve fibers, three kinds of calculations have been particularly useful. All three will now be defined and illustrated. The first two – the post stimulus time (PST) histogram and the interval histogram – have been used extensively by others and have been described elsewhere.[30] Calculations of the third kind – estimates of various conditional probabilities associated with the generation of event times – were developed as part of the present study. While the discussion here is specifically oriented toward auditory nerve data, many of the techniques discussed may also be useful with other electrophysiological data. There are certain characteristics of the auditory nerve data which motivate and justify these probability calculations, and these are discussed below. The extent to which these techniques could be useful with other data would depend on some of the detailed characteristics of the data.

All of the calculations considered here are directed toward a random-process description of the firing patterns. Such a description is appropriate because the patterns of event times following identical stimuli are not identical, but certain averages performed over several stimulus presentations do show regularities. In the application of these methods there is an implicit assumption that the data are statistically regular in a sense that justifies treating all stimulus presentations identically. If, for example, on 600 repetitions of a stimulus, the calculations performed on data from the first 100 yielded significantly different results from those based on the last 100, it would not seem appropriate to treat all 600 presentations in the same way. This assumption does not preclude nonstationarities that are locked to the stimulus, but it does exclude – or at least assume to be negligible – nonstationarites that are not related to individual presentations of the stimulus. Fortunately, this assumption can be tested, and with the auditory nerve fibers, at least, adaptation and other effects are small enough that the assumption seems justified.

In the discussion that follows, there is a potential confusion between "true" probabilities and the estimates of these, which are based on calculations. Where it seems necessary, the distinction between probabilities and estimates of probabilities is made explicitly. As a matter of convenience, however, much of the discussion depends on context to indicate whether probabilities or their estimates are intended.

2.1 POST STIMULUS TIME HISTOGRAMS

With short acoustic clicks presented 10 times per second, certain regularities in the firing patterns of auditory nerve fibers may be observed. Figure 9 shows several samples of the microelectrode recording, each beginning at the time of a click presentation. Note that the waveforms are not identical, but that there do appear to be certain preferred times of firing. These preferred times of firing show up more clearly in the post stimulus time (PST) histogram, which also appears in Fig. 9. In the PST histogram, z_k, the height of the k^{th} bar, is equal to the total number of spikes which occurred

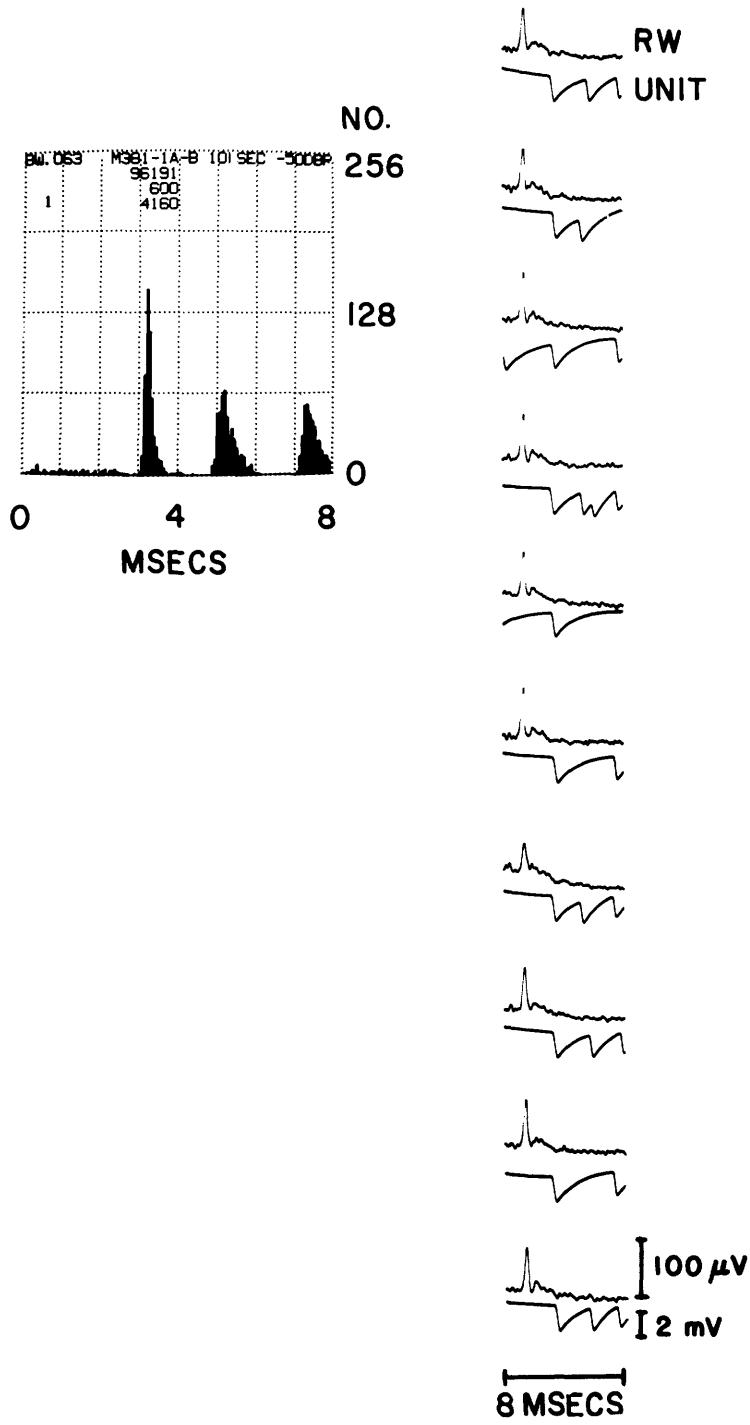

Fig. 9. Unit 296-19. PST histogram (bin width 0.0625 msec, 128 bars). Stimuli: 10/sec, -50 db rarefaction clicks, 1 minute. Also indicated are the recordings from the round window electrode and the fiber itself. The ten samples all begin at the time of a click presentation. [Fig. 4.1, page 21, in Kiang[8] (reproduced by permission of The M.I.T. Press, Cambridge, Mass.).]

between $k\Delta$ and $(k+1)\Delta$ time units after a stimulus presentation. (Δ is called the "bin width" of the calculation.) The calculation of the PST histogram can be described in the following way. At each stimulus presentation a clock is set to zero; the clock advances by one unit every Δ time units; at each spike the bar corresponding to the current clock reading is increased in height by one. Often it is convenient to normalize the PST histograms by dividing all of the bar heights by the number of stimulus presentations; these histograms are referred to as "normalized PST histograms."

The PST histogram can be useful in studying spike patterns that have a time structure related to the stimulus presentation, but there are some important aspects of the data that are discarded in the calculation of the PST histogram. For example, it cannot be determined whether or not most of the spikes that occurred in the interval corresponding to the second peak of the histogram were preceded by a spike in the interval corresponding to the first peak. Some further information could be obtained by calculating the interval histogram, but many important questions would remain unanswered even with both of these calculations.

2.2 INTERVAL HISTOGRAMS AND HAZARD FUNCTIONS

The interval histogram is simply a plot of the first-order distribution of the time intervals between events; that is, the height of each bar represents the number of intervals of that length. More precisely, let Δ be the "bin width" of the calculation and y_k, $k = 0, 1, 2, \ldots$, the height of the k^{th} bar, then y_k is the number of intervals of length greater than $k\Delta$ and less than or equal to $(k+1)\Delta$. (It is convenient though not strictly correct to speak of intervals being "of length $k\Delta$," rather than to detail the condition "between $k\Delta$ and $(k+1)\Delta$.")

It should be emphasized that the interval histogram involves only first-order statistics of the data. Any tendency for long intervals to follow short intervals, or for short intervals to come in bursts, is not directly reflected in this calculation. To explore such a sequential dependence between intervals it would be necessary to perform higher order calculations. One could, for example, count the number of intervals of length $k\Delta$ that are followed immediately by an interval of length $n\Delta$. If carried out for all n and k, this calculation would provide an estimate of the second-order density function for interevent times. This particular calculation has been performed on data from auditory nerve fibers and preliminary results suggest that the times between spontaneous events may be regarded as independent random variables.[18]

A process characterized by independent identically distributed interevent times is called a "renewal process." In the case of a renewal process, the interval histogram takes on special significance, for if a process is known to be a renewal process, the only information needed to completely characterize it is the interval distribution (or some equivalent function). Of course, the interval histogram may be an interesting statistic of other processes, but it is only in the case of a renewal process that it is clearly the one useful abstract of the data.

The number of intervals of length $k\Delta$ has been defined as y_k. The (estimate of the) probability that a given interval is of length k is

$$p(k) = \frac{y_k}{\sum_{n=0}^{\infty} y_n}. \tag{1}$$

In the literature of renewal theory (see, for example, Cox[31] or Parzen[32]) a function related to p(k) is often discussed. In the current notation this function is defined by

$$\Phi(k) = \frac{p(k)}{\sum_{n=k}^{\infty} p(n)}. \tag{2}$$

Equations 1 and 2 are combined to give

$$\Phi(k) = \frac{y_k}{\sum_{n=k}^{\infty} y_n}. \tag{3}$$

Equation 2 may be interpreted as follows: p(k) is the probability of an interval being of length $k\Delta$; $\sum_{n=k}^{\infty} p(n)$ is the probability of an interval being at least of length $k\Delta$; and $\Phi(k)$ is the conditional probability that an interval is of length $k\Delta$, given that it is at least of length $k\Delta$. Stated another way, if it has been $k\Delta$ time units since the last event, the conditional probability of an event occurring now (actually during the next Δ) is $\Phi(k)$. Similarily, in Eq. 3, $\sum_{n=k}^{\infty} y_n$ is the number of intervals that are at least $k\Delta$ in length, and $\Phi(k)$ is the fraction of these intervals that are exactly $k\Delta$ in length.

$\Phi(k)$ is an estimate of the conditional probability of an event during the next Δ, given that it has been $k\Delta$ time units since the last event. In renewal process discussions, $\Phi(k)$ has been referred to as the hazard function, as the age specific failure rate, or as any of several other names. In a neurophysiological context, Goldberg, Adrian, and Smith[33] calculated $\Phi(k)$ and referred to this calculation as a conditional probability analysis. In this study, however, the calculation of $\Phi(k)$ represents only one of several conditional probability analyses. The term "hazard function" is selected for this discussion, since it is the shortest, commonly used term that is not ambiguous.

In Fig. 10 the interval histogram calculated from a long recording of the spontaneous activity of an auditory nerve fiber is presented along with the corresponding hazard function (also in the form of a histogram). Several features of these two histograms deserve comment. The interval histogram starts at zero, rises to a mode at approximately 5 msec, and then decays in an exponential manner toward zero. The hazard function starts near zero, implying that the probability of an event in the next Δ is small if it has only been a millisecond or two since the last event. With increasing

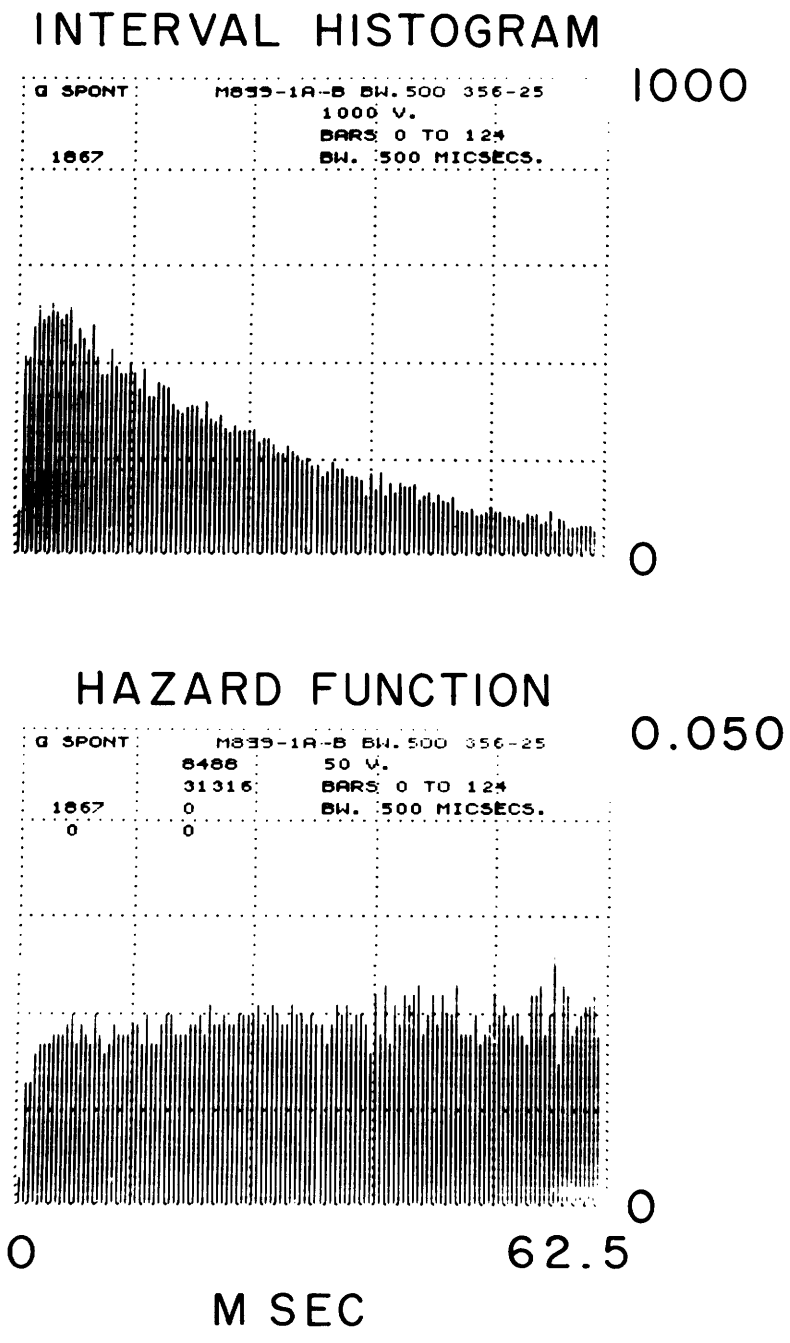

Fig. 10. Unit 356-25. Interval histogram and hazard function (bin width 0.5 msec, 124 bars) calculated from a long (approximately 14 minutes) recording of spontaneous activity.

values of time, the hazard function increases toward an asymptotic value of approximately 0.02. It appears that this asymptote is reached somewhere between 20 and 25 msec. This curve implies that the probability of an event in the next Δ is the same for any time-since-the-last-event greater than 20-25 msec. Finally, the curve is "noisy" for statistical reasons at large times, since the denominator of $\Phi(k)$, $\sum_{n=k}^{\infty} y_n$, is small.

It is easy to show that an exponential decay of the interval histogram implies a constant value of the hazard function, for all times after the exponential decay begins. It was pointed out in Section I that all interval histograms obtained from spontaneous activity of auditory nerve fibers seem to be characterized by a mode at less than 10 msec, followed by an exponential decay. This suggests that the hazard function of Fig. 10 is typical of auditory nerve fibers in that it levels off at a constant value, and does so in 20-25 msec. The value of this constant is, of course, related to the spontaneous rate of the fiber.

The hazard function of Fig. 10 is reproduced in Fig. 11, together with the hazard functions calculated from the spontaneous activity of four other units. For the purposes of comparison, all of the histograms in Fig. 11 have the same vertical and horizontal scales. For the units with the higher spontaneous rates, relatively few long intervals are available for estimating the hazard functions at the corresponding times. Hence the hazard functions are somewhat "noisy" in the right halves of these histograms.

These histograms appear to be consistent with the suggestion above that the hazard functions calculated from the spontaneous activity of auditory nerve fibers level off at a constant value within 20-25 msec. With these data, however, this cannot be a very precise statement, and, by way of illustration, the following hypothetical case would not be regarded as a contradiction: The hazard function achieves 90% of its maximum within 20 msec, but does not reach the full maximum for another 100 msec.

If the hazard function does in fact assume a constant value within a certain time after firing, then the following is implied: Provided it has been long enough since the last firing, the probability of a firing in the next Δ does not change with time, until, of course, another firing occurs. This suggests that the unit "recovers" from a previous firing in a period of roughly 20 msec. The words "recovery" and "refractory effects" are used in this discussion to refer in a general way to the processes that take place shortly after a firing. It should be emphasized, however, that the definitions of these terms are strictly operational and do not necessarily coincide with any underlying physiological phenomena. The neural unit is considered "recovered," i.e., the "refractory" effects are considered no longer present, when the probability of firing is no longer a function of the time-since-the-last-firing. Conceivably, the neuron could still be undergoing major chemical changes and still appear "recovered" by this definition. It has already been suggested that auditory nerve fibers "recover" from spontaneous firings; that they also "recover" in the presence of certain stimuli can be demonstrated by appropriate calculations. In this study it has been useful to calculate the effects of

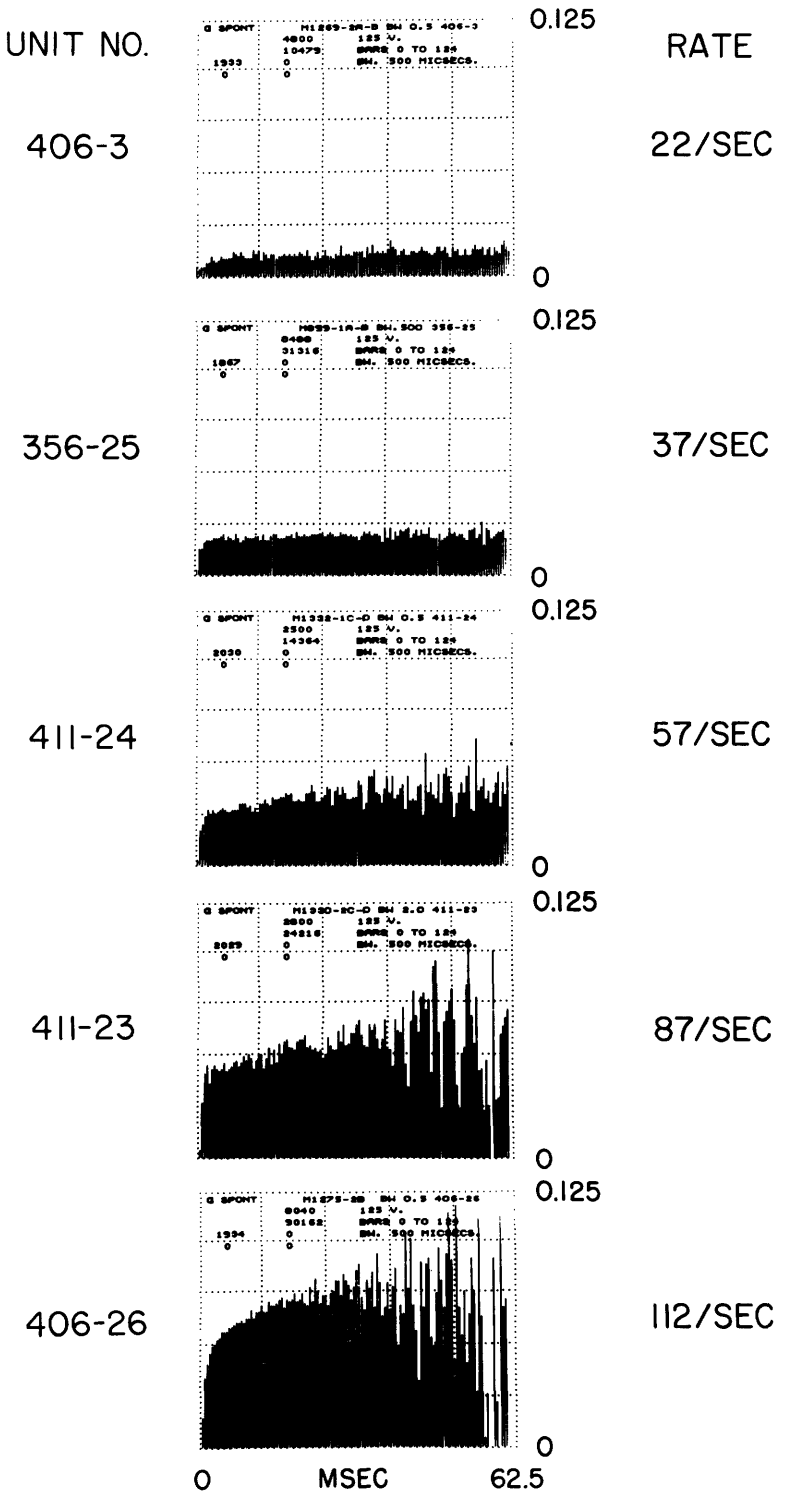

Fig. 11. Several units. Hazard functions (bin width 0.5 msec, 124 bars) calculated from long runs of spontaneous activity.

stimuli on "recovered units"; a discussion of these and other conditional probability calculations will now be given.

2.3 CONDITIONAL PROBABILITY MATRICES

In a stimulus situation such as the click example in the PST histogram discussion, where there is a preferred-time structure in the spike pattern, there are several conditional probabilities that might be of interest. For example, what is the conditional probability of an event in the interval corresponding to the second peak of the PST histogram, given that the last event occurred during the interval corresponding to the first? How does this probability compare with the conditional probability of an event, given that it has been a long time since the last event? The calculations described below have been used to estimate conditional probabilities such as these.

Several time intervals are defined relative to the onset of the stimulus presentation. For each pair of these intervals the conditional probability of an event in the later one, given that the last event was in the earlier one, is estimated. This is done on a simple relative frequency basis. To illustrate, suppose that in n of the stimulus presentations there was an event in interval 5, but no event in intervals 6 or 7. In other words there were n trials in which the last event before interval 8 occurred in interval 5. Furthermore, suppose that, considering only these n trials, on m of these there was also an event during interval 8. Then the estimate of the conditional probability of an event in interval 8, given that the last event was in interval 5, is m/n. A convenient way to present the results of these calculations is in matrix form with, for example, the entry in the 8^{th} column of the 5^{th} row being the conditional probability of an event in interval 8, given that the last event was in interval 5. Because of this natural scheme of presentation, this calculation is referred to as the "conditional probability matrix" calculation or simply the "matrix calculation."

By using the matrix calculation, the probability of an event in a specific interval of time relative to the click may be studied with the time-since-the-last-firing as a controlled variable. Calculations of this kind on eighth-nerve data yield results that are consistent with the notion that the unit recovers from previous firings within 20 or 25 msec, not only in the spontaneous situation but also under acoustic stimulation. In other words, in both situations, the probability of an event does not depend on exactly how long it has been since the last event, provided it has been at least 25 msec. Conditional probabilities based on a sufficiently long time since the previous firing are referred to as "recovered probabilities." As pointed out earlier, this involves a purely operational definition of "recovery," but it has proved very useful in analyzing these data.

Some typical results of the matrix calculations are presented in Fig. 12, together with the corresponding PST histograms, which were computed from the same data. In this figure, all probabilities are conditional on no event for 30 msec before interval A. Thus p(A) is the conditional probability of an event during interval A, given that the last event was at least 30 msec earlier. Similarly, p(B/A') is the conditional probability of

an event in B, given that the last event was at least 30 msec before interval A (so, in particular, there was no event during A).* p(B/A) is the conditional probability of an event in B, given that there was an event in A (and no event for 30 msec before A). The

(RECOVERED PROBABILITIES)

	p(A)	p(B/A')	p(B/A)	p(B)
-60 DB	0.32	0.61	0.32	0.52
-50 DB	0.76	0.87	0.56	0.64

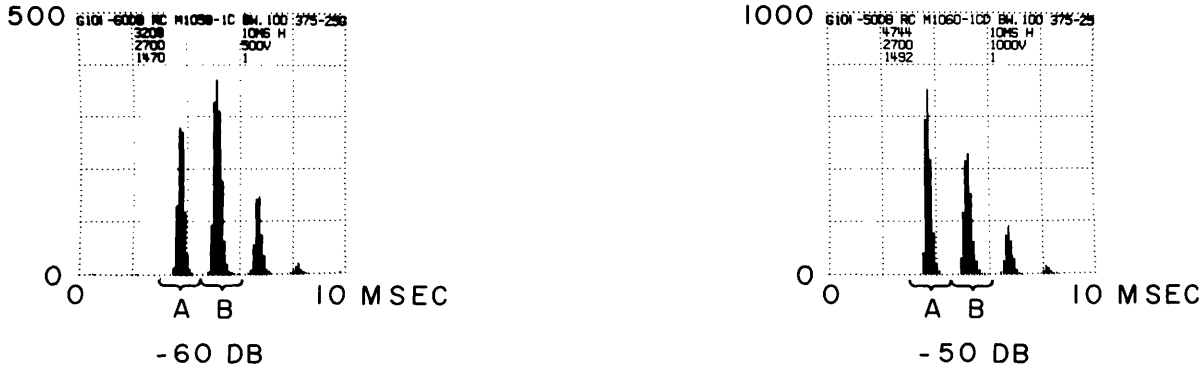

Fig. 12. Unit 375-25. PST histograms (bin width 0.1 msec, 100 bars) and various conditional probabilities. Stimuli: 10/sec, -50 db and -60 db rarefaction clicks. All probabilities are conditional on no spike for 30 msec before interval A. A(B) is the event: a spike during interval A(B). p(B) is calculated from $p(B) = p(A)\,p(B/A) + [1-p(A)]\,p(B/A')$.

conditional probability of an event in B, given only that no event occurred in the 30 msec immediately before interval A, is p(B), and this is calculated from the following equation.

$$p(B) = p(B/A)\,p(A) + p(B/A')\,[1-p(A)].$$

With these definitions, p(A) and p(B/A') are recovered probabilities, and p(B) and p(B/A) are not. In examining Fig. 12, it should be noted that the recovered probability for B is larger than that for A at both intensities, the probability of an event in B is smaller if the unit has fired in A than if it has not, and all of the probabilities are higher at the higher intensity.

As well as presenting some typical results of the matrix calculations, Fig. 12 illustrates some inadequacies of the conventional PST histogram. The fact that peak A is

*In fact this number cannot be determined with the "matrix calculation," and the number given is really the conditional probability of an event in B, given an event in A, without any condition on what happened in the 30 msec before A. This number is probably very close to the desired number, but even if it were not, the qualitative conclusions intended from this example would presumably still apply.

larger than peak B in the -50 db run could be misleading if the PST histogram were interpreted as a direct measure of the strength of an effective stimulus. In terms of recovered probabilities, peak B is larger than A, but if there has been an event during A, the unit is "refractory" during interval B and a smaller probability (p(B/A)) applies. Since, at the -50 db intensity, the unit is likely to fire during interval A and hence be "refractory" during interval B, the size of peak B in the histogram is smaller than would be expected from the recovered probability alone. As the recovered probabilities are presumably free of any refractory complications, it seems reasonable to regard them as a measure of an effective stimulus. In these terms, the PST histogram reflects a somewhat complicated combination of both the characteristics of the effective stimulus and the refractory characteristics of the neural unit.

2.4 RECOVERED PROBABILITY HISTOGRAMS

The calculation to be described now is, in principle, a specialization of the conditional probability matrix calculation, but for practical reasons it is employed separately, and it seems appropriate to discuss it separately. The concept of a recovered probability has already been introduced. The conditional probability of an event in an interval of time defined relative to the stimulus, considered as a function of the time since the last event, appears to reach an asymptote in approximately 20 msec. This asymptotic value is defined as the recovered probability. By definition, the height of each bar in the recovered probability histogram represents the recovered probability of an event at that time. More precisely, if the "recovered condition" is -20 msec, let m_k be the number of stimulus presentations on which there was no event during the interval from -20 msec to $+k\Delta$. (-20 msec refers to the time 20 msec before the stimulus presentation.) Considering only these m_k trials, let n_k be the number on which there was an event between $k\Delta$ and $(k+1)\Delta$. (So $m_{k+1} = m_k - n_k$.) Then n_k/m_k is an estimate of the recovered probability of an event in the interval $k\Delta$ to $(k+1)\Delta$, and x_k, the height of the k^{th} bar in the recovered probability histogram, is defined to be equal to n_k/m_k.

It is interesting to compare the recovered probability histogram with the conventional PST histogram for the same data; this is done in Fig. 13. To facilitate comparison of two histograms, rather than displaying the customary bar graph, a smooth curve representing the straight-line interpolation between the tops of the bars is given for each histogram. The heavy line represents the recovered probability histogram, hence the height of the curve at a particular time represents the recovered probability of an event occurring within a bin width of that time. The lighter curve is a conventional PST histogram which has been normalized by dividing by the number of stimuli. Its height, therefore, represents the fraction of stimulus presentations on which there was a spike during the indicated bin width. In comparing these two curves, it may be observed that they are much the same for the small first peak and for the first half of the larger second peak, but that the PST histogram returns toward zero sooner than the recovered probability histogram. Furthermore, the recovered probability histogram rises for the second

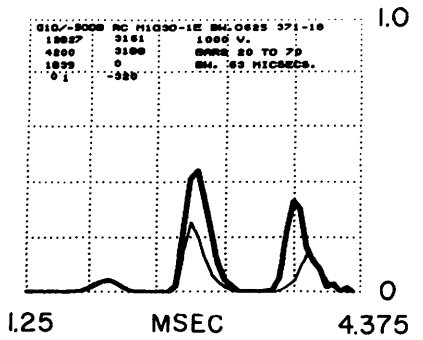

Fig. 13. Unit 371-18. Recovered probability histogram (heavy line) and normalized PST histogram (light line), (bin width 0.0625 msec; straight-line interpolations between tops of bars 20-69; recovered condition: -20 msec). Stimulus: 10/sec, -50 db rarefaction clicks, 7 minutes.

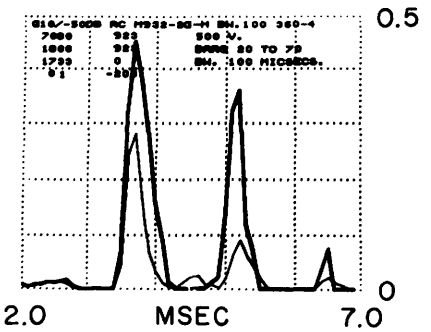

Fig. 14. Unit 360-4. Recovered probability histogram (heavy line) and normalized PST histogram (light line), (bin width 0.10 msec; straight-line interpolations between tops of bars 20-69; recovered condition: -20 msec). Stimulus: 10/sec, -50 db rarefaction clicks, 3 minutes.

peak before the conventional PST histogram does. The apparent discrepancy between these two curves can be understood qualitatively in terms of the refractory characteristics of the neuron. The probability of an event during the first half of the second peak is sufficiently large that on most stimulus presentations the unit fires somewhere during the early part of the peak and is "refractory" – and hence less likely to fire – for a period of time afterward. The portion of the PST histogram corresponding to the time when the unit is usually refractory is diminished by this refractory effect. The recovered probability histogram is not affected by the refractoriness, since in estimating the recovered probability of an event at some time in the second half of the first peak, none of the stimulus presentations that involved an event during the first half are used.

Another kind of discrepancy between the recovered probability histogram and the conventional PST histogram is illustrated in Fig. 14. There is a small peak in the PST histogram that does not appear in the recovered probability histogram. Considering that the recovered probability is essentially zero in this region, it is curious that the conventional PST histogram shows so many events. For this to happen it is necessary that some "unrecovered" probability be larger than the negligible value of the recovered probability. This rather unexpected situation can be studied by using the calculations described below.

2.5 CONDITIONAL PROBABILITY HISTOGRAMS

The height of each bar of the conditional probability histogram represents the conditional probability of an event at the corresponding time, given that the last event occurred in the specified "conditioning interval." The recovered probability histogram is a special case of the conditional probability histogram where, for example, the conditioning interval might include all times at least 20 msec before the stimulus. In calculating the conditional probability histogram, the only stimulus presentations that are used are those on which there was an event during the conditioning interval. If m_k is the number of these trials that involved no event between the conditioning interval and $+k\Delta$, and n_k the number of these that involved an event before $(k+1)\Delta$, $(m_{k+1} = m_k - n_k)$, then x_k, the height of the k^{th} bar, is n_k/m_k. Slightly restated, m_k is the number of stimulus presentations on which there was an event during the conditioning interval, but no event between the conditioning interval and $+k\Delta$. Considering only these m_k stimulus presentations, x_k is the fraction of these that involved an event between $k\Delta$ and $(k+1)\Delta$. Hence x_k is an estimate of the conditional probability of an event at $k\Delta$, given that the last event occurred during the conditioning interval.

In Fig. 15 the normalized PST histogram, the recovered probability histogram, and a conditional probability histogram for three intensities of click runs on the same unit are presented. The conditioning interval is defined to correspond to the first peak. Several conclusions can be drawn from this figure. In the left column, the recovered probability histogram appears as the heavy line and the normalized conventional PST histogram as the light line. Both curves show several peaks spaced at the period of the

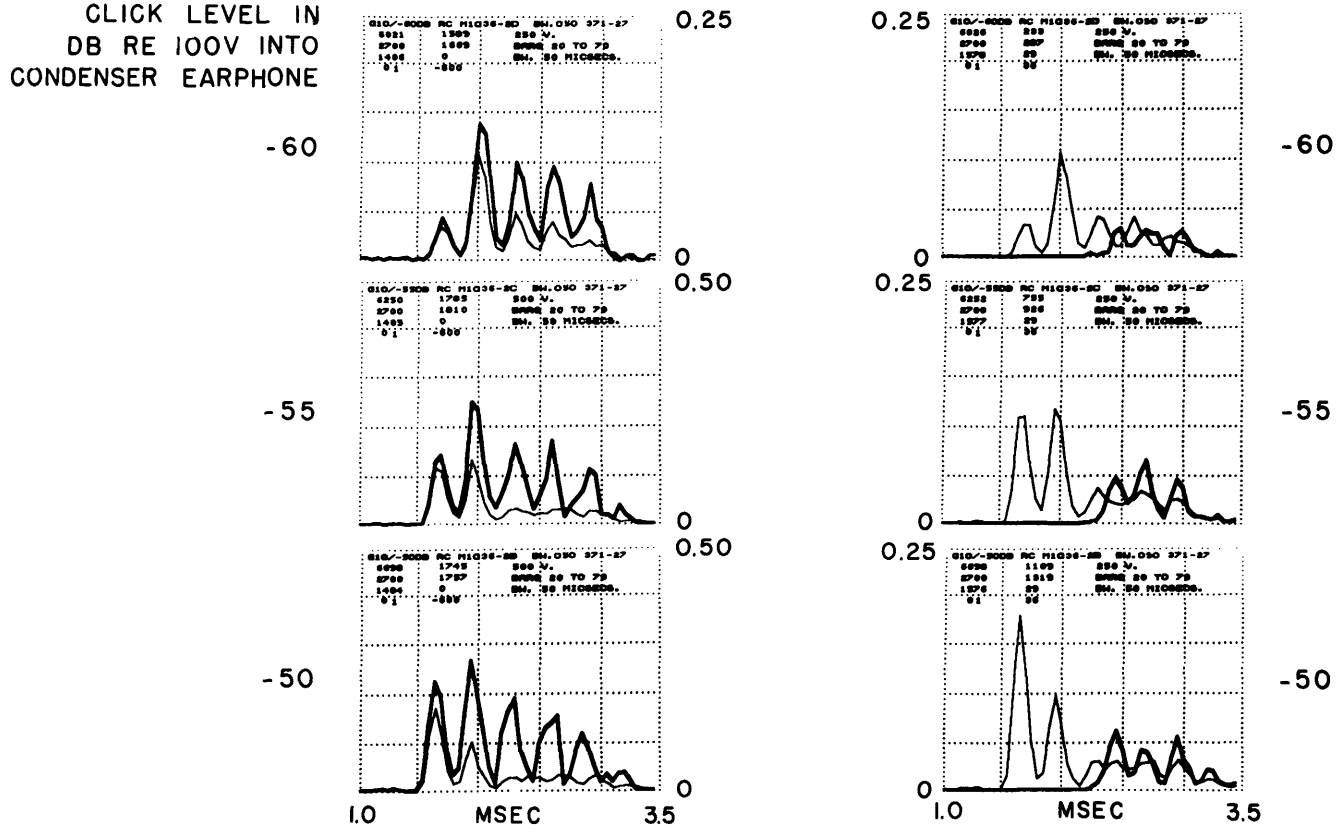

Fig. 15. Unit 371-27. Left column: recovered probability histograms (heavy lines) and normalized PST histograms (light lines). Right column: conditional probability histograms (heavy lines) and normalized PST histograms (light lines), (bin width 0.05 msec; straight-line interpolations between the tops of bars 20-69; recovered condition: -30 msec, conditioning interval: 1.5-1.8 msec). Stimuli: 10/sec, -60, -55, and -50 db rarefaction clicks, 4.5 minutes.

3.27-kc characteristic frequency of this unit, but the separate peaks are much clearer in the recovered probability curve than in the PST curve. This is because the unit often fires a second time during the displayed interval of time and the second firings do not have the same preferred time structure as applies to the first. This phenomenon can be studied by means of the conditional probability histograms shown in the right column.

At each time indicated on the horizontal axis, the height of the conditional probability curve represents the probability of an event within the next bin width, conditional on the last firing being during the first peak. The first peak of the conditional probability curve occurs approximately 3/4 msec after the first peak of the PST histogram. Examination of the pictures in the left column indicates that this time corresponds to the region between the third and fourth peaks of the recovered probability histogram. Because the time structure of the recovered probabilities does not in this case hold for the second firings, the separate peaks are much harder to distinguish in the PST histogram than in the recovered probability histogram.

Incidentally, the tendency to fire a second time, after approximately 3/4 msec, is apparently also the cause of the extra peak in Fig. 14. In fact, these calculations applied to several units have demonstrated that this phenomenon appears to be present in many auditory nerve fibers; its effect on the PST histogram depends on the relation between the 3/4 msec interval and the spacing of peaks in the histograms.

2.6 CONCLUSIONS

Within the general framework of conditional probability calculations, three specific calculations have been discussed: the conditional probability matrix, the recovered probability histogram, and the conditional probability histogram. It has already been pointed out that the recovered probability histogram is a special case of the conditional probability histogram, and that it, in turn, is a special case of the matrix calculation. Practical constraints imposed by limited computer memory preclude computing several conditional probability histograms simultaneously or having more than 10 or 20 intervals for the matrix calculation. The computer program currently in use performs three calculations simultaneously: a conventional PST histogram (with 125 bars), a conditional probability histogram (with 125 bars), and a conditional probability matrix (with 15 intervals).

A major consideration in employing these calculations, and in gathering the data on which they are based, is the statistical problem of estimating probabilities from a limited number of trials. For example, in calculating a recovered probability histogram, all stimulus presentations that are preceded too closely by an event are discarded, and in calculating the height of the k^{th} bar, all trials on which an event occurred during any of the first k-1 bin widths are discarded. For this reason, at moderate intensities it is often difficult to calculate recovered probabilities for any time after the first peak. In general it is necessary to obtain longer data runs to get reliable probability estimates than are necessary for reliable PST histograms.

The concept of a recovered probability was suggested by the exponential "tails" of the spontaneous interval histograms, and has been verified on data obtained under stimulation. The calculation of recovered probabilities is particularly useful because in a sense it removes the refractory complications from the data. From the standpoint of developing a model this can be very helpful. Most attempts at modeling these data treat the refractory properties of the neuron as a somewhat separable part of the model. In terms of testing or refining the nonrefractory portion of the model the recovered situation is a useful one. The comparison of model and data in terms of recovered probabilities is more direct than, for example, comparing the PST histograms predicted by the model with those obtained from the data. Of course, a complete model would have to include refractory effects, but it may be strategically wise in the construction of a model to begin by excluding the refractory complications.

In addition to providing a more direct measure of the nonrefractory aspects of the data, the recovered probability histograms have been useful for pointing out specific phenomena that occur shortly after firings. Some of the apparent discrepancies between recovered probability histograms and conventional PST histograms are reasonable in terms of the usual notion of a diminished probability of firing following a firing. Other discrepancies can be explained only in terms of a temporary increase in the probability of firing. These phenomena are suggested by the comparison of the recovered probability and PST histograms, but are best studied in detail by using the more general conditional probability calculations.

III. ANALYSIS OF CLICK DATA

The spike-discharge patterns that occur in auditory nerve fibers when short acoustic clicks are presented as stimuli will now be considered. We begin with a discussion of the usefulness and characteristics of the click stimulus. Included in this discussion are some comments about the model-oriented perspective that is used in examining these data. A brief discussion of the question of the statistical regularity, or stationarity, of the data is followed by a discussion of data relating to recovery. After a discussion of the influence of the rate of click presentation the main discussion of the click data begins with the presentation of conventional PST histograms, together with some probabilities associated with the peaks in these histograms. The emphasis here is on the variation with intensity of the recovered probability of firing in a time interval corresponding to a peak in the histogram. To examine the time structure of firing patterns in more detail, recovered probability histograms are employed. A digression is first made to consider the phenomenon of "second firings," which is a complication present in much of the click data. After this digression, the recovered probability histograms are contrasted with conventional PST histograms, and then considered by themselves as a function of intensity. From these data some important constraints on possible models are inferred.

3.1 THE CLICK STIMULUS

Classically, the click has been popular as a stimulus in both physiological and psychophysical experiments, and many data exist in both realms. To the communication engineer it is a familiar fact that a linear, time-invariant system is characterized by its impulse response, and that a click that is short compared with the time constants of the system is effectively an impulse. Because the first portion of the simplified model presented in Fig. 8 is to be a linear, time-invariant system, the click is an especially appropiate stimulus for studying the peripheral auditory system. Another appropriate stimulus for studying linear time-invariant systems is the continuous sine wave, and data obtained with this stimulus will be presented. There appear to be some long-term complications, however, with the continuous stimuli that are not present or at least less pronounced when clicks are presented at a low enough repetition rate. These complications will be discussed in greater detail, but, in some senses, their existence makes the click a simpler stimulus than the sine wave.

In obtaining the data discussed here, the stimulus was delivered by a condenser earphone, through a tube sealed into one external meatus. To present clicks, a 100-μsec voltage pulse was applied to the earphone, this resulted in a pressure waveform, measured at the eardrum, which was a pulse of 200-250 μsec length. In these experiments, it has not been possible to obtain an acoustic pulse any shorter than 200 μsec. Under the assumption that the mechanical system is linear and time-invariant, the motion of the cochlear partition in response to an acoustic pulse can be obtained by convolving the pulse with the appropriate impulse response. It is a well-known property of convolution

that if one waveform varies slowly as compared with the duration of the other, convolving the two of them will result in a waveform with the same shape as the slowly varying one. Therefore, in the low-frequency region, where the impulse response might have a period of 1 or 2 μsec, the 200-msec pulse is sufficiently short that the mechanical motion will have essentially the same shape as the impulse response. In the high-frequency region the impulse response might last only 50 μsec, in which case the mechanical motion would look more like the input pulse than the rapidly ringing impulse response.

The simplified model of Fig. 8 provides a useful framework for the discussion of the click data. In this discussion, it is assumed that the block diagram of Fig. 8 is essentially correct and that the indicated system is linear and time-invariant. The exact form of the impulse response of the system is not assumed. The form of the rectifier is not assumed, but it is intended that the output of the rectifier be some instantaneous function of the input. The form of the probabilistic device is not assumed either, except that presumably its refractory effects become less important as the time-since-the-last-firing increases. The major emphasis in the present discussion is on refining, or contradicting, this simplified model. For this purpose, the recovered situation proves quite valuable, and therefore most of the calculations presented below are of recovered probabilities.

3.2 STATISTICAL REGULARITY

All of the calculations employed here treat each presentation of the stimulus identically. This would not make sense if the properties of the unit that is being studied changed significantly with time. If the first portion of a long click run had different statistics from the last, or if, in the course of several runs on the same unit, repetition of an earlier stimulus condition did not yield the same results, then the validity of these data-processing techniques would be open to question. Three examples will now be presented, which suggest that these data are statistically regular in the sense that they possess only minor long-term variations in characteristics. (The words "long term" are used to distinguish these variations from the "short term" nonstationarities that are

Table 1. Unit 371-18. Probabilities associated with peaks of the PST histogram.

	p(A/R)	p(B/R)	p(B/A)	p(C/B)	p(D/C)	p(D/B)
First two minutes of data	0.17 (902)	0.87 (749)	0.72 (201)	0.53 (1014)	0.23 (664)	0.40 (482)
Last two minutes of data	0.17 (906)	0.89 (756)	0.74 (190)	0.54 (1039)	0.23 (682)	0.40 (481)

p(x|y) = conditional probability of an event in x, given last event was in y.
Numbers in parentheses represent number of trials on which the estimate is based.
Interval definitions: A, bars 26-40; B, bars 41-55; C, bars 56-70; D, bars 71-85; R, all times at least 20 msec before click.
"Bars x-y" refers to times larger than x/16 msec and less than or equal to y/16 msec.

related to the individual stimulus presentations.)

Data from a long run of -50 db, 10 per second clicks were recorded from Unit 371-18. (The PST and recovered probability histograms based on the entire 7-minute run were presented in Fig. 13.) Separate calculations were performed on the first and last two minutes of this run. Some of the probabilities from these calculations are presented in Table 1 and the PST histograms appear in Fig. 16. It seems clear from this table that the data obtained during these two intervals, which were separated by approximately four minutes, are not significantly different.

In the course of a long series of masking runs on Unit 371-23, two -60 db click runs were recorded. These runs were separated by approximately 25 minutes, during which

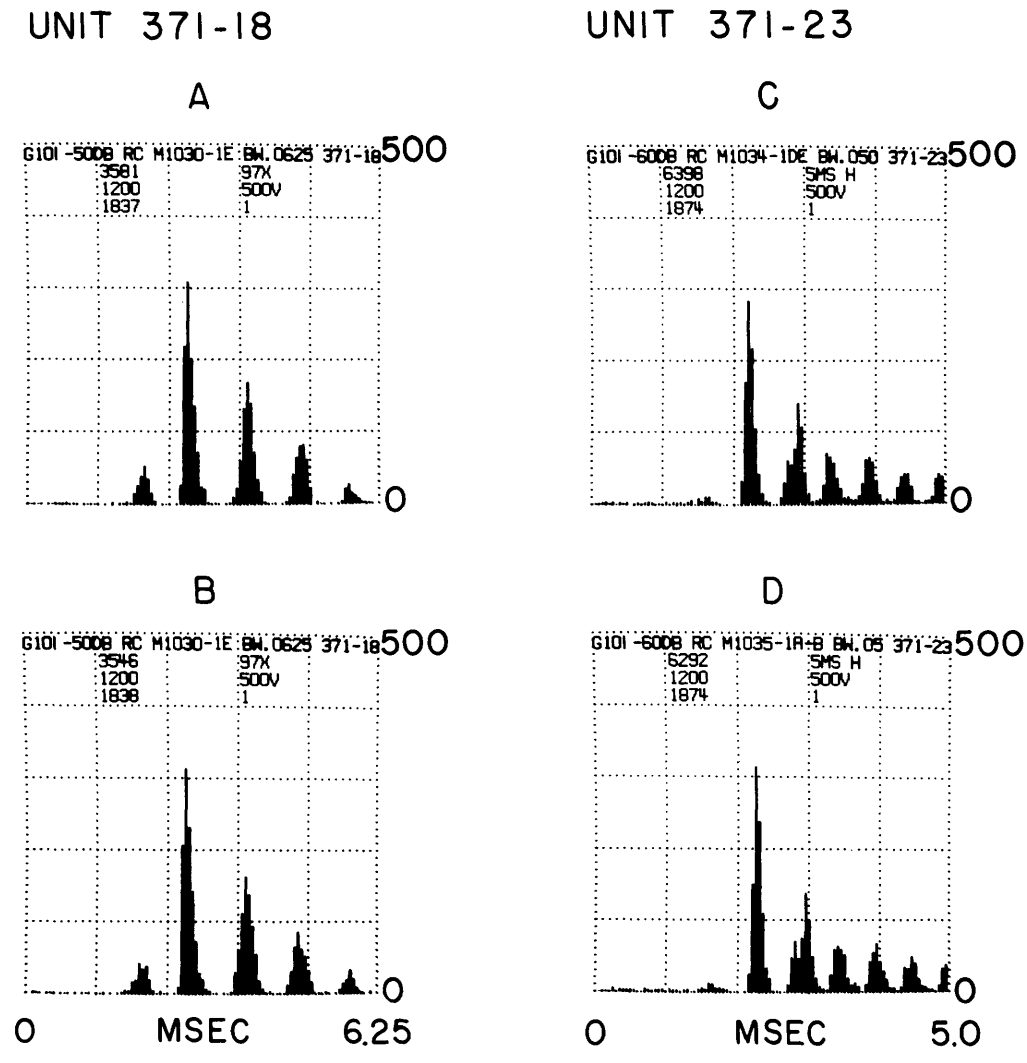

Fig. 16. A and B: Unit 371-18. PST histograms (bin width 0.0625 msec, 100 bars). Stimulus: 10/sec, -50 db rarefaction clicks. A is based on the first two minutes, and B on the last two minutes of a 7-minute run. C and D: Unit 371-23. PST histograms (bin width 0.05 msec, 100 bars). Stimulus: 10/sec, -60 db rarefaction clicks, 2 minutes. D is based on data taken 25 minutes after the data for C.

Table 2. Unit 371-23. Probabilities associated with peaks of the PST histogram.

	p(A/R)	p(B/A)	p(C/B)	p(C/A)
First -60 db run	0.82 (450)	0.41 (879)	0.13 (561)	0.32 (519)
Second -60 db run (25 minutes later)	0.82 (462)	0.40 (898)	0.14 (574)	0.33 (543)

p(x|y) = conditional probability of an event in x, given last event was in y.
Numbers in parentheses represent number of trials on which the estimate is based.
Interval definitions: A, bars 39-52; B, bars 53-64; C, bars 65-74; R, all times at least 20 msec before click.
"Bars x-y" refers to times larger than x/20 msec and less than or equal to y/20 msec.

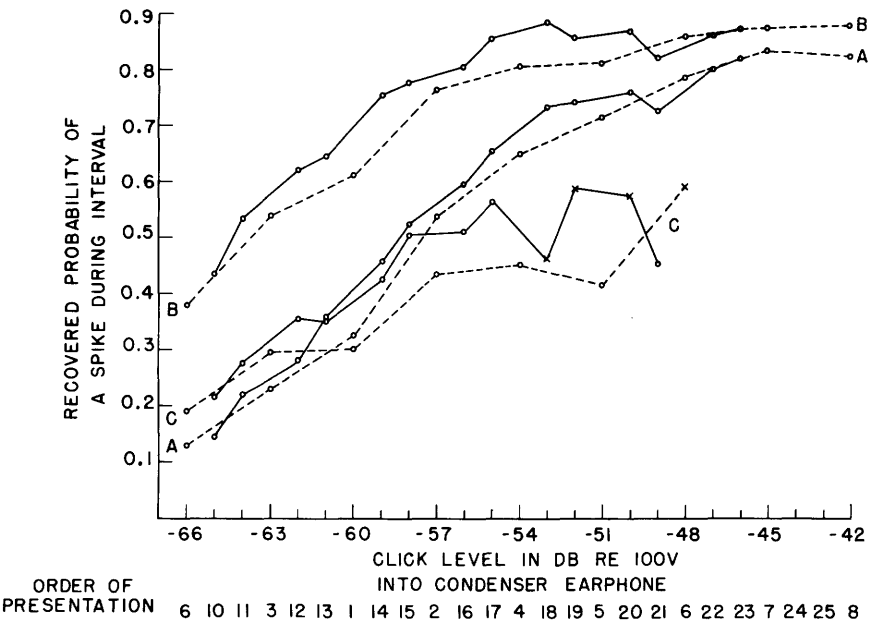

Fig. 17. Unit 375-25. Recovered probabilities associated with three peaks of the PST histogram (recovered condition: -29 msec). Stimuli: 10/sec rarefaction clicks, several intensities, 4.5 minutes. The order in which the various click runs were taken is indicated. Data points from the first 9 runs are connected with dashed lines, those from the next 14 with solid lines. When a probability estimate is based on between 50 and 100 trials, an "x" is used to designate the point; when fewer than 50 trials are available, no point is given.

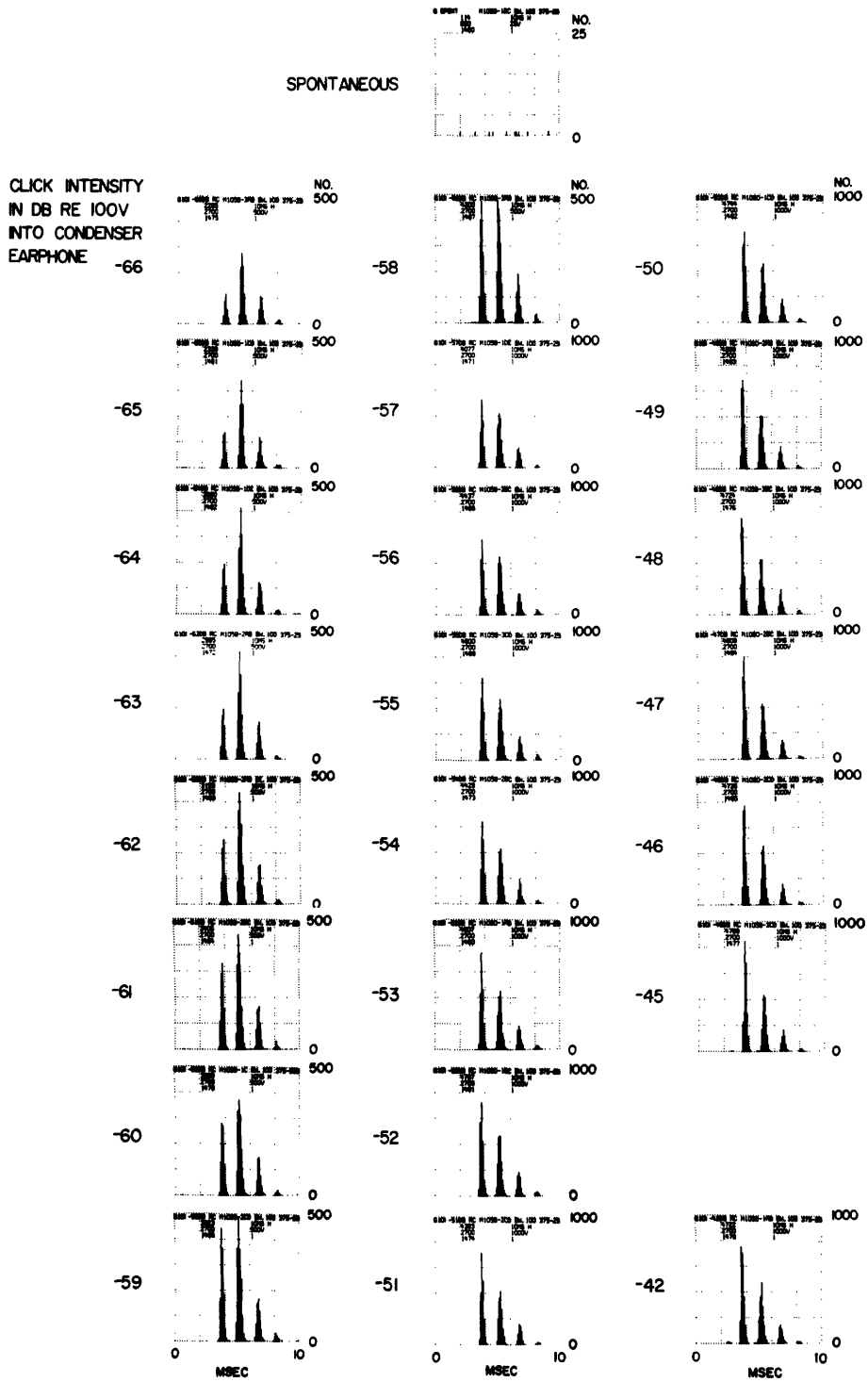

Fig. 18. Unit 375-25. PST histograms (bin width 0.1 msec, 100 bars). Stimuli; 10/sec rarefaction clicks, several intensities, 4.5 minutes. Length of spontaneous run: 1 minute.

time a variety of stimuli was presented. Some statistics of these two runs are presented for comparison in Table 2 and the PST histograms are presented in Fig. 16. Again it appears that the properties of these units do not vary significantly with time.

Finally, a somewhat negative example is presented in Fig. 17. In this figure the recovered probabilities for each of three intervals are plotted as a function of intensity for Unit 375-25. The corresponding PST histograms appear in Fig. 18. The data on this unit include 23 5-minute runs, each at a different intensity. The order in which the different runs were taken is indicated in this figure. Data points from the first 9 runs are connected by dotted lines, those from the next 14 are connected by solid lines. Examination of this figure indicates a significant difference between the first 9 and the next 14 runs. The direction of the discrepancy is a little surprising; the probabilities were generally higher in the last 14 runs than in the first 9 runs. While Fig. 17 indicates that some long-term variations are present, it also suggests that they may not be too serious. The dotted and solid lines are not identical, but they do have roughly the same shape, and they are not very far apart. This figure would be more disturbing if, for example, the solid line zigzagged across the dotted one. The long-term variations which are illustrated by Fig. 17 indicate that there are limits to the precision with which the properties of these units may be measured. If a data run is long enough to obtain adequate statistics for a desired level of precision, it may also be long enough to allow the properties of the unit to vary during the run.

These three examples have been presented to demonstrate that these data are reasonably regular and to give some indication of the magnitude of the long-term variations. It is felt that these data are reasonably typical, and several other similar examples could be presented. The one qualification that should be added is that all of these examples involve only moderate intensities. At high intensities there may be nonstationarities that depend on the stimulus history. For example, the unit may be less sensitive for several minutes following a high-intensity run.

3.3 RECOVERY

The concept of a recovered unit has been discussed in Section II. The exponential decay of the interval histograms obtained with spontaneous activity implies that, in this situation, these units recover from previous firings in the sense that the probability of firing in the next bin width does not vary after some operationally defined "recovery time." An appropriate recovery time seems to be approximately 20 msec, and this is the value used for most of this study. To confirm that the recovered concept also applies in the presence of click stimuli, the probability of an event in an interval of time that is defined relative to the click must be calculated as a function of the time since the previous firing. To justify saying that the unit recovers within 20 msec, it is necessary that this function achieve a constant value within 20 msec. Data are presented in Figs. 19 and 20 to indicate that this is approximately the case.

Conventional PST histograms calculated from long click runs on each of four units

are presented in Fig. 19. Two or three intervals are defined on each histogram, and the conditional probabilities of an event in each interval are plotted in Fig. 20, as a function of the location of the "conditioning interval." The "matrix calculation," described in Section II, was used to obtain these numbers. In this calculation several intervals are defined relative to the click presentation; the resulting probability estimates are conditional on the last spike being in one of these "conditioning intervals." In Fig. 20, the conditioning intervals before the click are represented by the minimum possible time between the click and a spike in the conditioning interval; the conditioning intervals after the click are represented by word-labels of the horizontal coordinates, e.g., "second peak." Different intervals were used for different units, so some care is necessary in interpreting Fig. 20. To illustrate the interpretation of this figure, the curve labeled "E" represents the probability of a spike in interval E (Unit 411-24), conditional on the last spike before E falling in the various conditioning intervals. For the point above -30 msec, the conditioning interval is -30 to -40 msec; above -40 it is -40 to -60 msec; and above -60 it is "before -60 msec" (i.e., -60 msec to $-\infty$).

Despite the long click runs employed (7, 9, 15, and 10 minutes), statistical fluctuations in these curves are appreciable, and these make precise inferences inappropriate. It does appear, however, that these curves level off somewhere in the region from 15 to 30 msec. That is, the probability of a spike in the designated interval does not depend on the time since the last spike, provided that the last spike preceded the click by at least 20 msec (30 msec would be a more conservative estimate).

The choice of a "recovery time" for recovered probability calculations is a compromise between large values which ensure recovery and small ones that allow more trials. The consistently short mode for all spontaneous interval histograms suggests that one recovery time may be sufficient for all units. The choice of 20 msec is somewhat arbitrary, and several other values, most of them at least 20 msec in length, have also been used in this study. It may be that the unit is only "nearly recovered" after 20 msec and it is not "fully recovered" until much later, but this would be very difficult to determine for statistical reasons.

Especially long runs were used in order to gather the evidence on recovery presented above. For statistical reasons, the shorter click runs which are normally employed provide less information about the time course of recovery. In all cases, the data from the shorter runs appear to be consistent with the hypothesis that the unit recovers within 20 or 30 msec.

3.4 CLICK RATE

In most of this study, a presentation rate of 10 per second was used for the click stimuli. This choice of rate is something of a compromise. On the one hand, it is desired to present clicks at a sufficiently low rate that each can be regarded as a separate stimulus, unaffected by previous clicks. On the other hand, the higher the click rate the greater the number of click presentations that are available for statistical

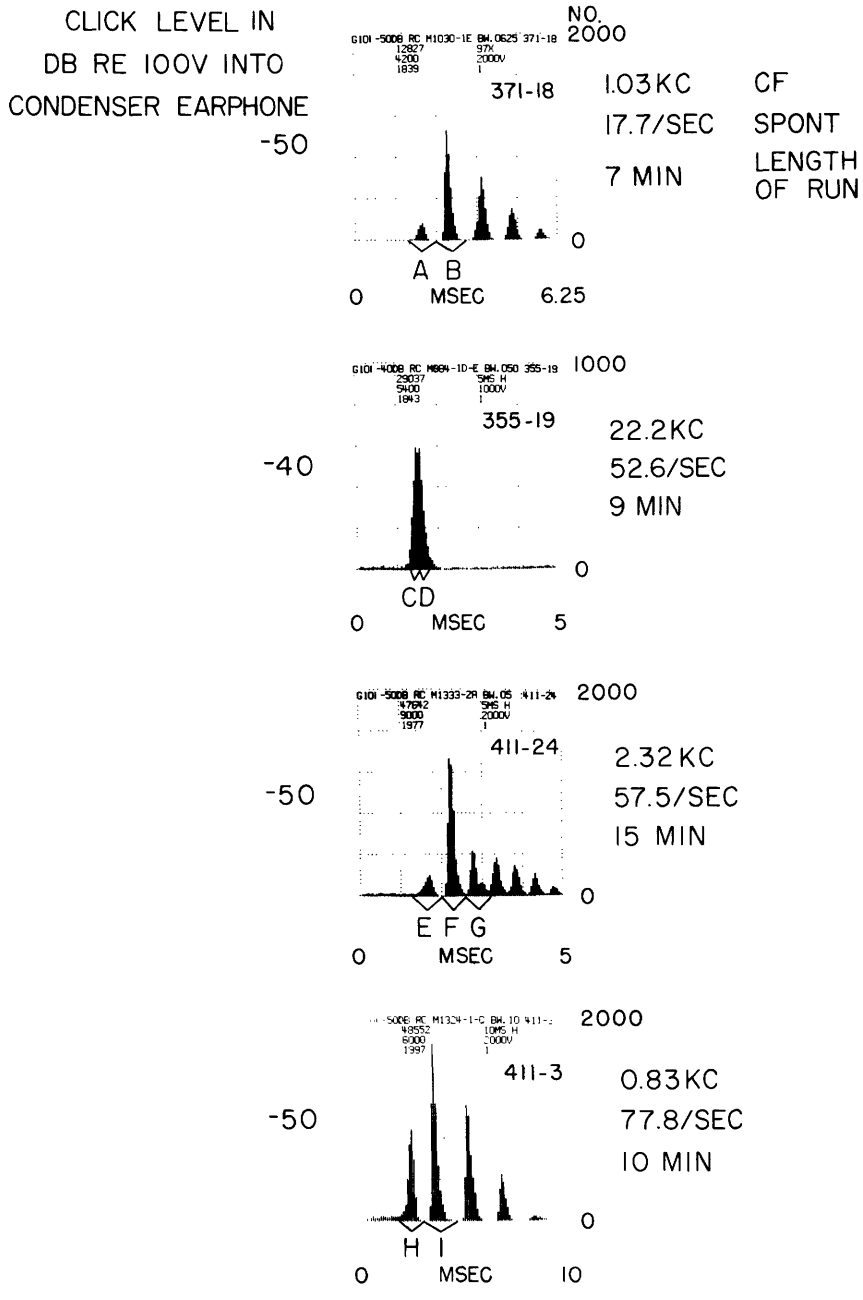

Fig. 19. PST histograms and interval definitions for Fig. 20. (All histograms display 100 bars, bin widths 0.0625, 0.05, 0.05, and 0.10 msec for Units 371-18, 355-19, 411-24, and 411-3, respectively.) Interval definitions: A = bars 26-40; B = 41-55; C = 27-30; D = 31-34; E = 26-40; F = 41-52; G = 52-63; H = 19-30; I = 31-45. Stimuli: 10/sec rarefaction clicks.

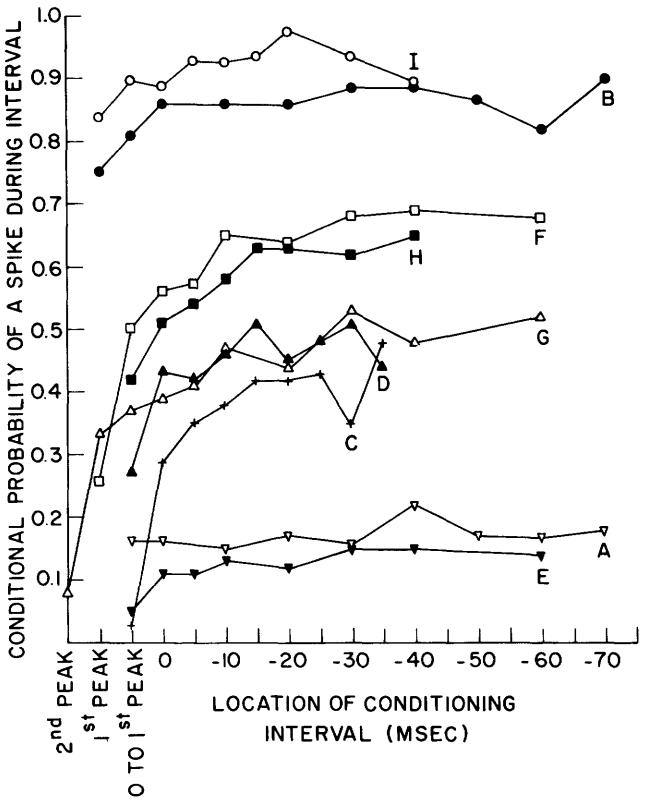

Fig. 20. Conditional probabilities as functions of the location of the conditioning interval. Stimuli: 10/sec rarefaction clicks. The curve labels (A-I) correspond to the interval definitions of Fig. 19. For conditioning intervals preceding the click, each point is plotted at the horizontal coordinate representing the conditioning interval's boundary which is closest (in time) to the click. The conditioning intervals following the click are labeled in terms of the peaks of the appropriate histogram.

estimates of the properties of a given unit. The rate of 10 per second appears to be low enough to exclude at least the major dependence on rate in the click data. This question has not been clearly resolved, however, partly because it is difficult at the lower rates to get enough stimulus presentations to yield statistically reliable results. Click data obtained at various rates from two different units are presented here in order to give some indication of the reasonableness of the 10/sec choice, as well as an indication of the effects that occur with higher rates.

In Fig. 21, the normalized PST histograms obtained with seven different click rates, ranging from 10/sec to 400/sec, are presented for Unit 309-27. The histograms are normalized to facilitate comparison, since different numbers of stimuli are involved in these histograms. On all histograms, the full vertical scale value is 0.25, corresponding to a spike in the bin on one-fourth of the stimulus presentations.

It is clear from this figure that both the absolute and the relative sizes of the peaks vary with click rate. The histograms from the two lowest rates are approximately equal.

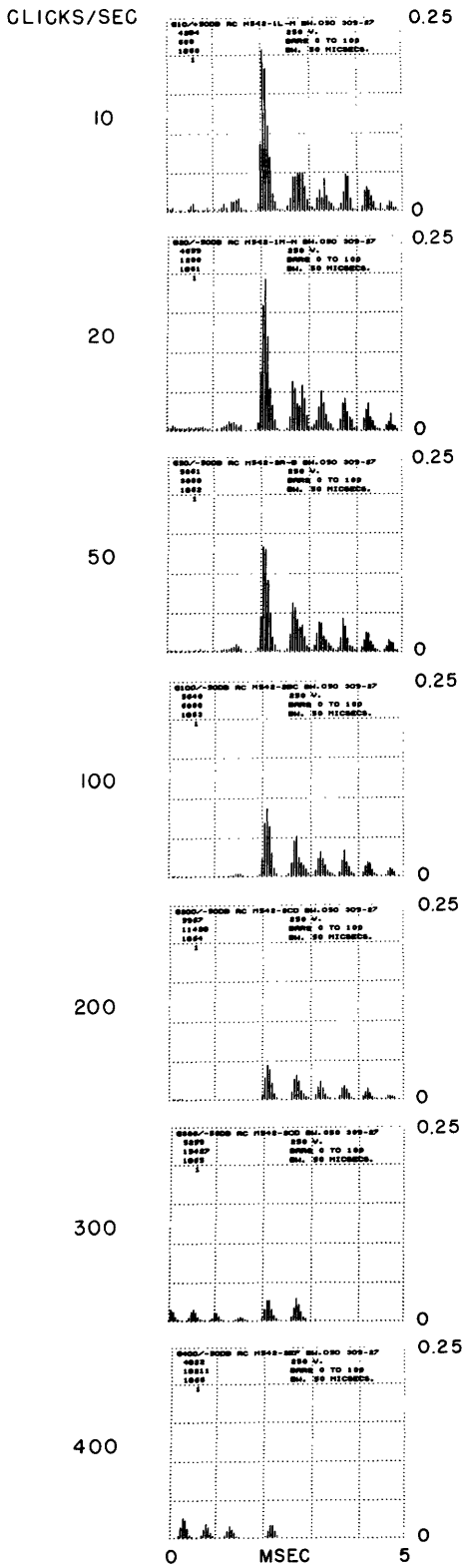

Fig. 21.

Unit 309-27. Normalized PST histograms (bin width 0.05 msec, 100 bars). Stimuli: −50 db rarefaction clicks, several rates.

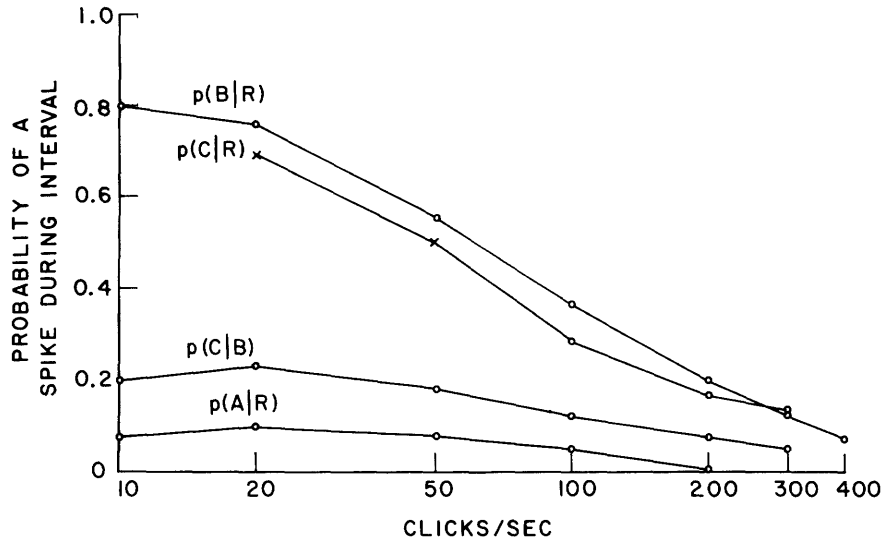

Fig. 22. Unit 309-27, recovered and conditional probabilities associated with three peaks of the PST histogram. The events A, B, and C are defined as the occurrence of a spike in the intervals defined by bars 36-50, 51-62, and 63-72, respectively (bin width 0.05 msec). The event R is defined as no spike since 20 msec before the click. When a probability estimate is based on between 50 and 100 trials, an "x" is used to designate the point; when fewer than 50 trials are available, no point is given.

It might be concluded from this figure that the histograms are not sensitive to click rate if the rate is 20 per second or less, and that 10 per second is sufficiently low for this purpose. Incidentally, the drastic changes that occur at the two highest rates are the result of the inter-click interval being smaller than the duration of the obvious response to the click.

Another view of the effect of click rate may be obtained by examining some probabilities associated with the peaks in these histograms. In Fig. 22, the recovered probabilities for three of the peaks, together with one conditional probability, are presented as a function of click rate. In general, the probabilities decrease with increasing click rate, but these curves do appear to level off in the region around 10 per second. Unfortunately, no data were obtained from this unit at rates less than 10 per second; such data might have confirmed this last suggestion.

Click data with lower presentation rates were obtained from Unit 411-4. The normalized PST histograms appear in Fig. 23, and some conditional probabilities are plotted in Fig. 24. In the PST histograms, there were not any obvious changes with click rate (as there were with the higher rates used on Unit 309-27), except that, for statistical reasons there is less continuity in the heights of the bars at the lower rates, where relatively few presentations are used.

The plot of the various conditional probabilities against click rate (Fig. 24) does indicate a gradual increase in the probabilities as the rate is lowered. This would suggest an error in trying to estimate the single-click probabilities for this unit from

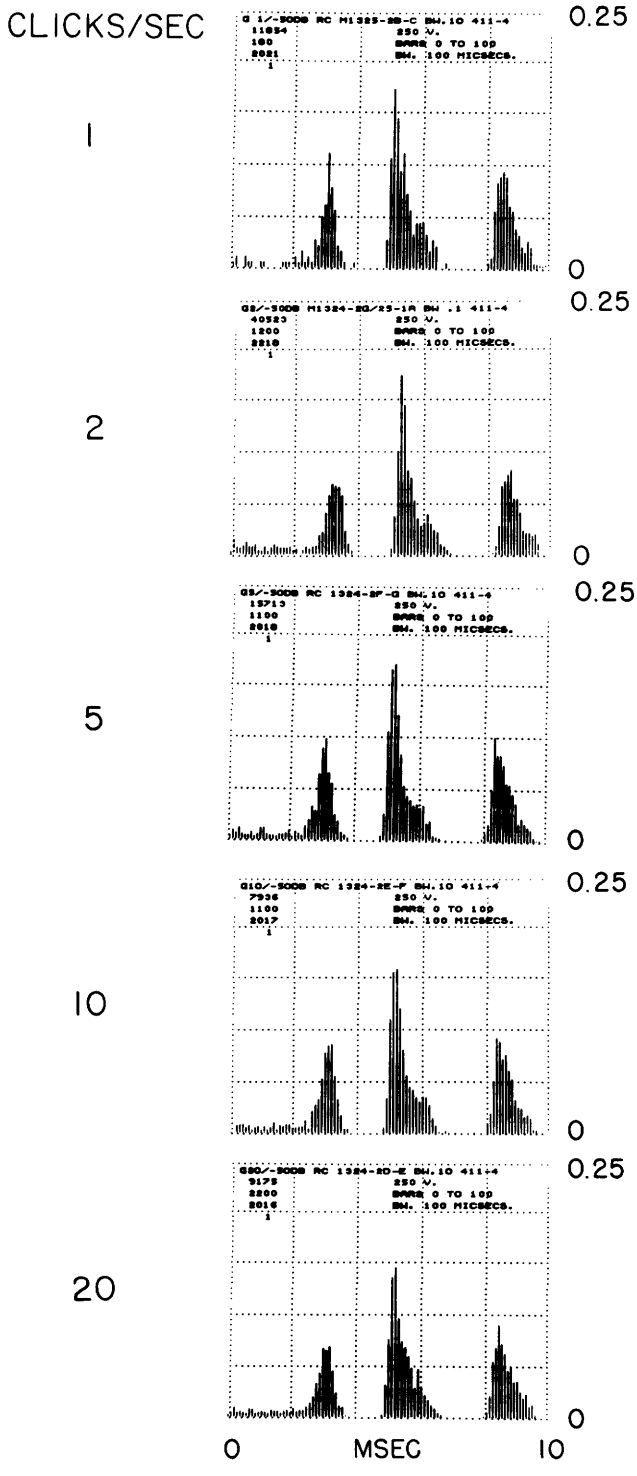

Fig. 23. Unit 411-4. Normalized PST histograms (bin width 0.05 msec, 100 bars). Stimuli: -50 db rarefaction clicks, several rates.

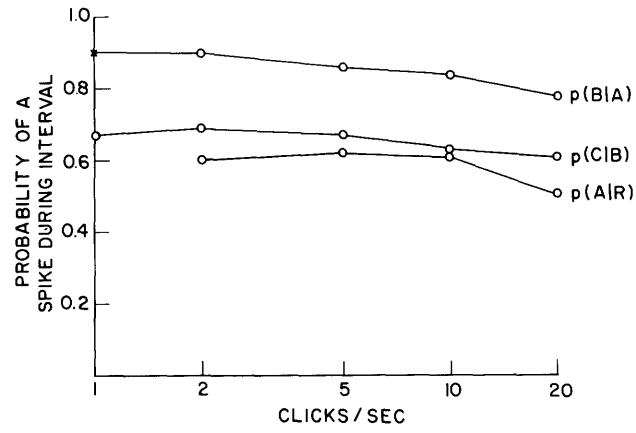

Fig. 24. Unit 411-4, recovered and conditional probabilities associated with three peaks of the PST histograms. The events A, B, and C are defined as the occurrence of a spike in the interval defined by bars 21-40. 41-66, and 80-100, respectively (bin width 0.05 msec). The event R is defined as no spike since 20 msec before the click. When a probability estimate is based on between 50 and 100 trials, an "x" is used to designate the point; when fewer than 50 trials are available, no point is given.

the 10/sec data of roughly 0.00, 0.05, and 0.06 for p(A|R), p(C|B), and p(B|A).

The data on Units 411-4 and 309-27 are representative of the data from many units that have been examined. In some cases the probabilities increase gradually as the rate decreases below 10 per second; in other cases, the probabilities do not seem to change with rate for rates below 10/sec. In all cases examined, increasing the rate considerably above 10 or 20/sec results in sizeable decreases in the probabilities.

Unfortunately, the influence of rate on the click data has not been clearly resolved, and a good deal more data may be necessary before it is. At rates of 5/sec and lower, very long runs are necessary to get reliable statistics, and the required length of these runs leads to difficulties. For one thing, in the period in which it is possible to "hold" a unit, there may not be time for more than two or three long runs. Furthermore, the question of stationarity, or statistical regularity, which was discussed earlier, may be a significant problem if comparisons have to be made of data based on long runs separated by other long runs.

A related question which has not been explored is the influence of intensity on the click-rate data. At higher intensities it may be that the dependence on click rate will be important at even lower rates.

3.5 PROBABILITIES ASSOCIATED WITH THE PEAKS OF THE PST HISTOGRAM

In the discussion concerning the statistical regularity of the data, the PST histograms and the recovered probabilities associated with each of the three peaks in the histograms were presented for Unit 375-25 (Fig. 17). For the present discussion, the general form of these curves should be noted. Also it should be noted that the recovered

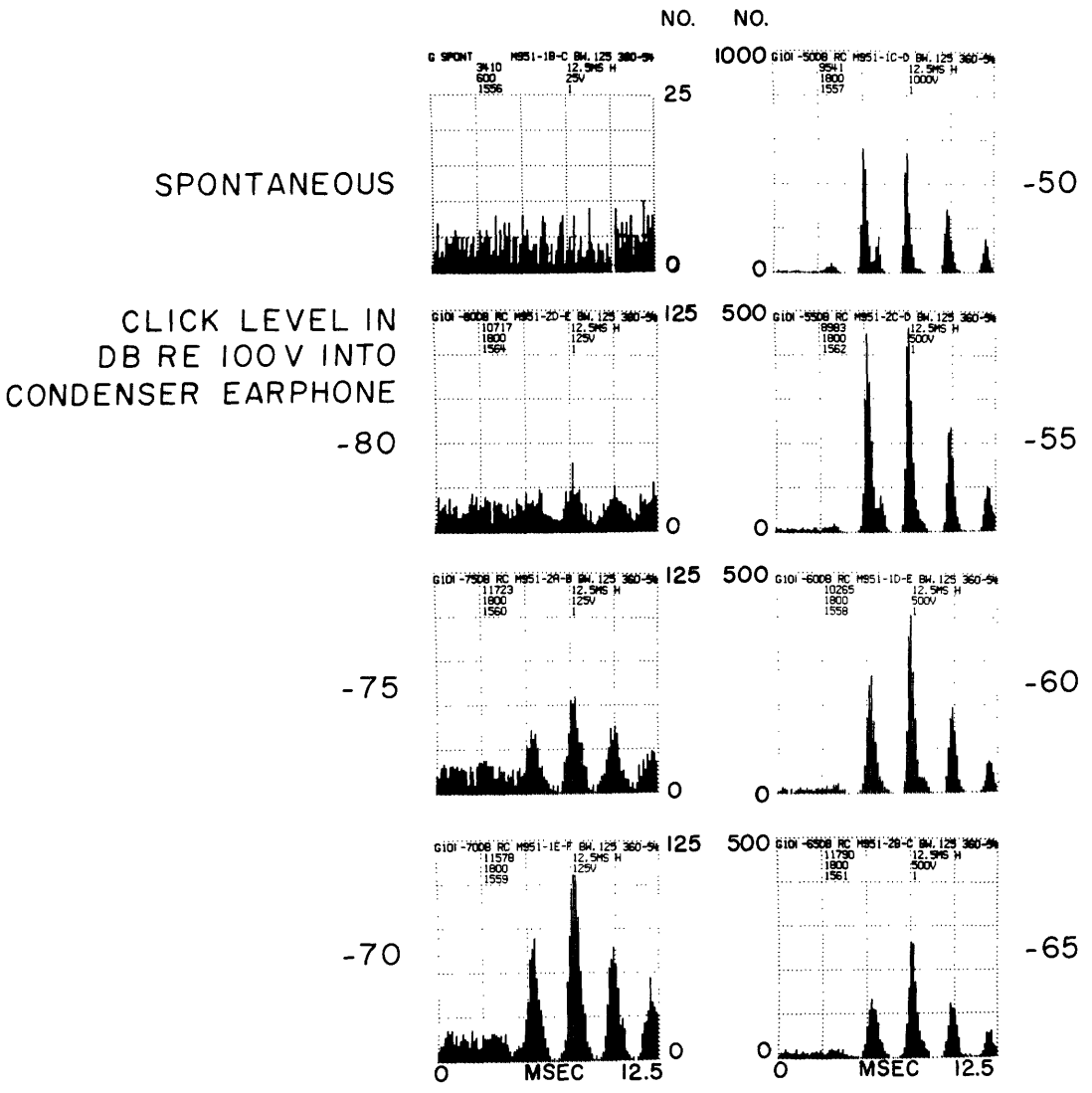

Fig. 25. Unit 360-54. PST histograms (bin width 0.125 msec, 100 bars). Stimuli: 10/sec rarefaction clicks, several intensities, 3 minutes. Length of spontaneous run: 1 minute.

probability for interval A is smaller than that for B at all intensities, whereas peak A of the histogram is larger than peak B at the higher intensities. This apparent discrepancy can be explained in terms of the refractory characteristics of the unit, and this was done in the discussion relating to Fig. 12.

In Fig. 25 the PST histograms from an intensity series on Unit 360-54 are presented. In Fig. 26 several conditional probabilities associated with the peaks in these histograms are plotted as functions of intensity. In this figure, recovered probabilities are plotted as solid lines and are labeled p(A/R), p(B/R), and p(C/R), for the first, second, and third peaks. The recovered probabilities for interval A are typically based on 600 trials. For later intervals there are, of course, fewer trials available. Where only between

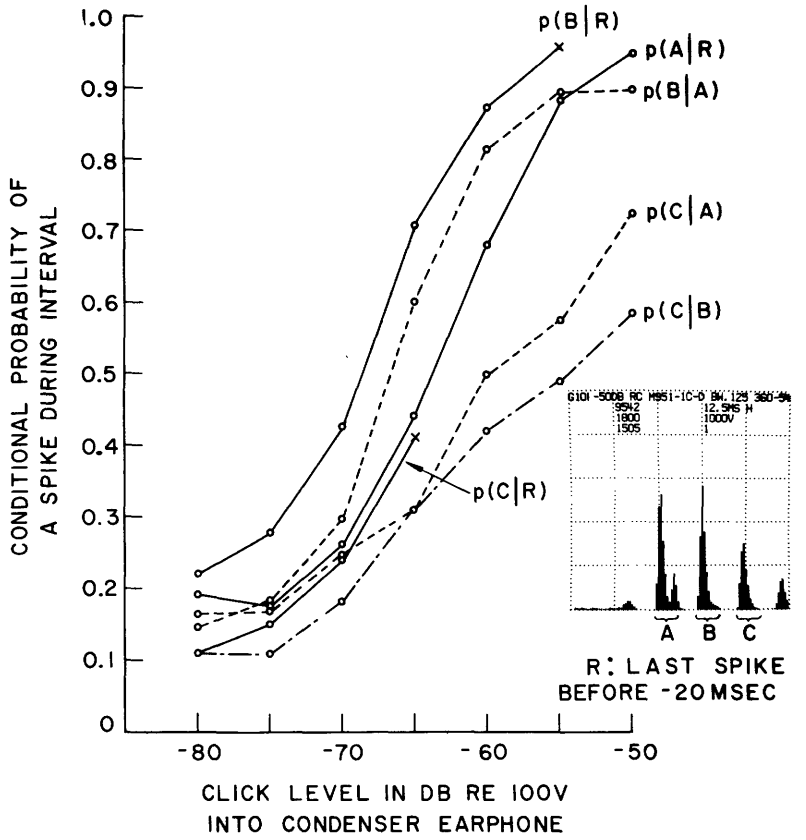

Fig. 26. Unit 360-54. Recovered and conditional probabilities associated with three peaks of the PST histogram. Stimuli: 10/sec rarefaction clicks, several intensities, 3 minutes. The events A, B, and C are defined as the occurrence of a spike in the first, second, and third peaks, respectively, of the PST histogram; the event R is defined as no spike since 20 msec before the click. When a probability estimate is based on between 50 and 100 trials, an "x" is used to designate the point; when fewer than 50 trials are available, no point is given.

50 and 100 trials are used to estimate a probability, the point is marked with an "x." If fewer than 50 trials are available, no point is plotted. Examination of this figure indicates that the largest recovered probabilities are associated with interval B, and that these probabilities increase from about 0.2 at -80 db to 0.9 at -55 db. The curve for interval A is similar in shape, but shifted to the right approximately 5 db. If the recovered probability associated with an interval depended only on the mechanical motion during that interval, and if the mechanical motion during interval B had the same shape as that during A but was 5 db larger, the recovered probability curves for A and B would be identical except for a 5-db horizontal shift. The curve for C is slightly smaller than A, but terminates at -65 db. No values of p(C/R) are given for intensities above -65 db because for these intensities there are fewer than 50 trials with no spikes from 20 msec before the click until the beginning of interval C.

In addition to the recovered probability curve for interval B, a curve representing

the conditional probability of an event in B, given that there was an event in A, p(B/A), is plotted as a dashed line. As would be expected from the refractory properties of the unit, p(B/A) is somewhat smaller than p(B/R). Finally, for interval C, p(C/B) and p(C/A), the conditional probabilities of an event in C, given that the last event was in B and A, respectively, are given. These curves are presented as typical of the probabilities associated with click stimuli, but, as there is considerable variation in the form of the curves, even with different units from the same cat, it is useful to examine several such plots.

The recovered probabilities from Fig. 26 are plotted again in Fig. 27, together with those from three other units from the same cat. The PST histograms for these three

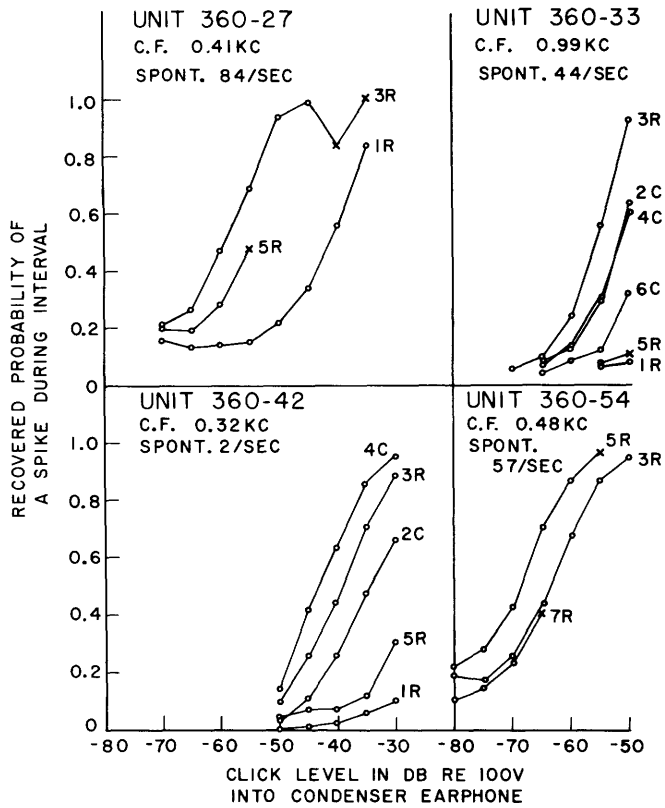

Fig. 27. Units 360-27, 33, 42, and 54. Recovered probabilities associated with peaks of the PST histograms (recovered condition: -20 msec). Stimuli: 10/sec rarefaction (R) or condensation (C) clicks, 3 minutes. Interval definitions: Unit 27 (bin width 0.125 msec), 1R = bars 21 through 30, 3R = 31-50, 5R = 41-50, 2C = 26-35, 4C = 36-45, 6C = 46-55; Unit 33 (bin width 0.10 msec), 1R = bars 21 through 30, 3R = 31-40, 5R = 41-50, 2C = 26-35, 4C = 36-45, 6C = 46-55; Unit 42 (bin width 0.125 msec), 1R = bars 21 through 40, 3R = 41-60, 5R = 61-82, 2C = 30-50, 4C = 51-74; Unit 54 (bin width 0.125 msec), 3R = bars 36 through 55, 5R = 56-75, 7R = 76-90. When a probability estimate is based on between 50 and 100 trials, an "x" is used to designate the point; when fewer than 50 trials are available, no point is given.

units appear in Figs. 28, 29, and 30. In Fig. 27 the intervals corresponding to peaks in the histograms are labeled in order, with odd numbers for rarefaction clicks and the corresponding even numbers for condensation clicks. A redundant R or C is also used to denote rarefaction or condensation. To illustrate, the first two rarefaction peaks with Unit 360-42 occur in intervals 1R and 3R; the first condensation peak occurs between these two intervals, in interval 2C.

Units 360-27 and 360-54 are similar in that the histogram peaks are located at approximately the same times and, in both cases, the recovered probability curves for the unit are roughly equal except for a horizontal displacement. Although the intervals 3R and 5R are essentially identical for these two units, with 360-27 the recovered probability for 3R is larger than that for 5R, while with 360-54 the reverse holds. Units 360-33 and 360-42 provide some more similarities and differences. It is interesting to note that Unit 360-33 has only one rarefaction peak larger than 0.12 in recovered probability.

These four sets of curves are presented as typical, but not exhaustive, examples of the recovered probabilities associated with click stimuli. These figures illustrate the rough equivalence with horizontal displacement of different curves from the same unit, and the variety of rank orderings of peak sizes which is possible with different units from the same cat.

3.6 SECOND FIRINGS AFTER 3/4 TO 1 MSEC

The calculations discussed above relate to the recovered probability of a firing in an interval corresponding to an entire peak in the PST histogram. Further information can be obtained by examining these probabilities on a finer time scale. This can be accomplished by calculating the recovered probability histogram, which gives the recovered probabilities corresponding to each bin width, or bar. These calculations provide some information about the shape of the peak and how this shape varies with intensity, which was not available from the calculations involving coarser time intervals. As part of the discussion of the recovered probability histogram in Section II, the conventional PST and the recovered probability histograms from the same data were contrasted in Figs. 13 and 14. Before considering in detail the recovered probability histograms obtained with click stimuli, the phenomenon of a second firing after 3/4 to 1 msec, which is evidenced by the "extra" peak in Fig. 14 and by the small additional peaks at the higher intensities presented in Figs. 25, 28, and 30, will be discussed. This phenomenon complicates many PST histograms obtained with clicks, and, while it is not well understood, it can at least be partially characterized. The term "second firing" is used to describe this phenomenon, and is indicative of some of its characteristics. Typically the "second firings" occur between 3/4 and 1 msec after an "ordinary" firing. The "ordinary" firing usually occurs when the effective stimulus (measured by the recovered probability) is moderately large, but the "second" firing may occur at a time when the effective stimulus is quite small. The second firing seems to be influenced more by the stimulus at the time of the previous firing than by the current stimulus, and the words "second

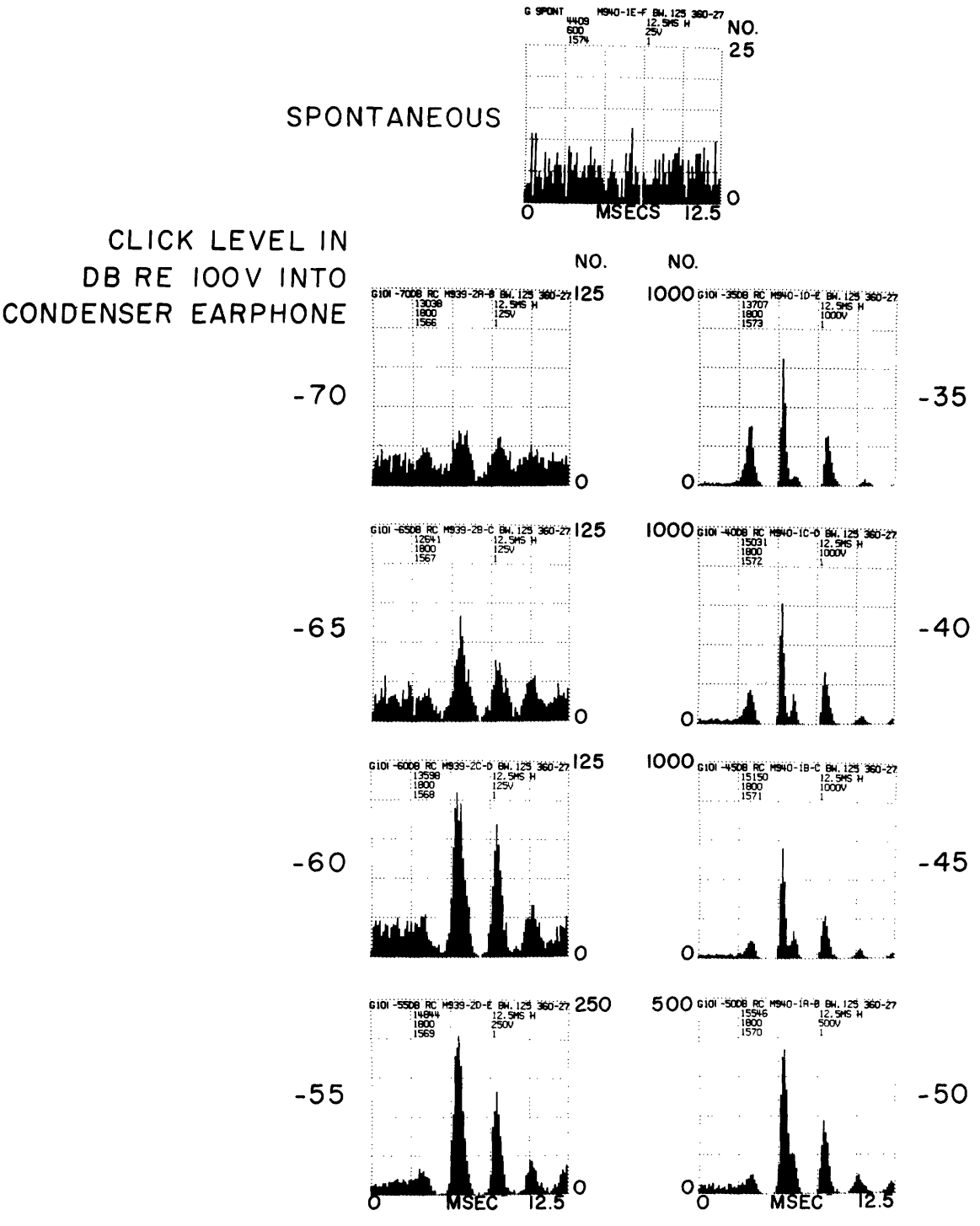

Fig. 28. Unit 360-27. PST histograms (bin width 0.125 msec, 100 bars). Stimuli: 10/sec rarefaction clicks, several intensities, 3 minutes. Length of spontaneous run: 1 minute.

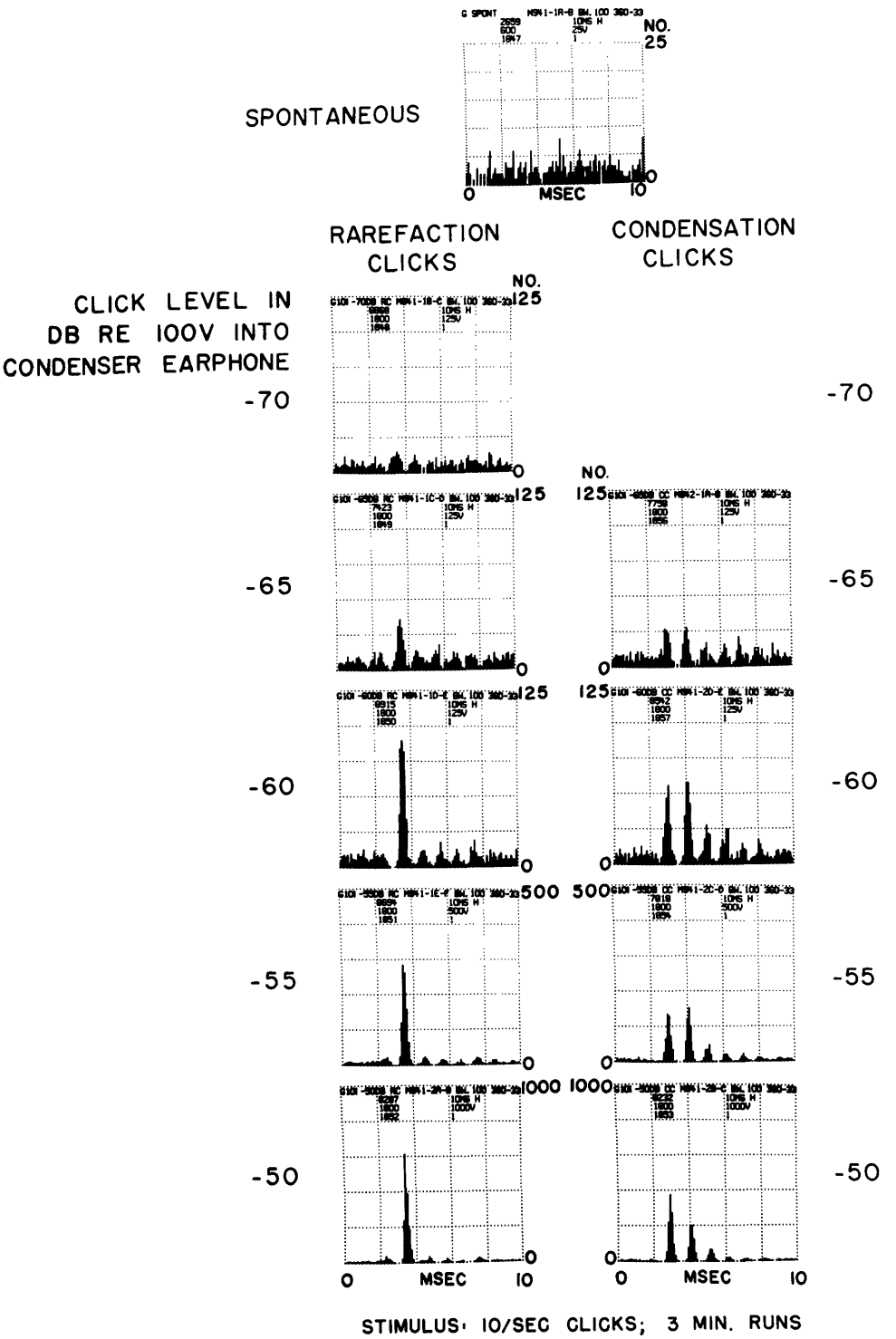

Fig. 29. Unit 360-33. PST histograms (bin width 0.1 msec, 100 bars). Stimuli: 10/sec rarefaction and condensation clicks, several intensities, 3 minutes. Length of spontaneous run: 1 minute.

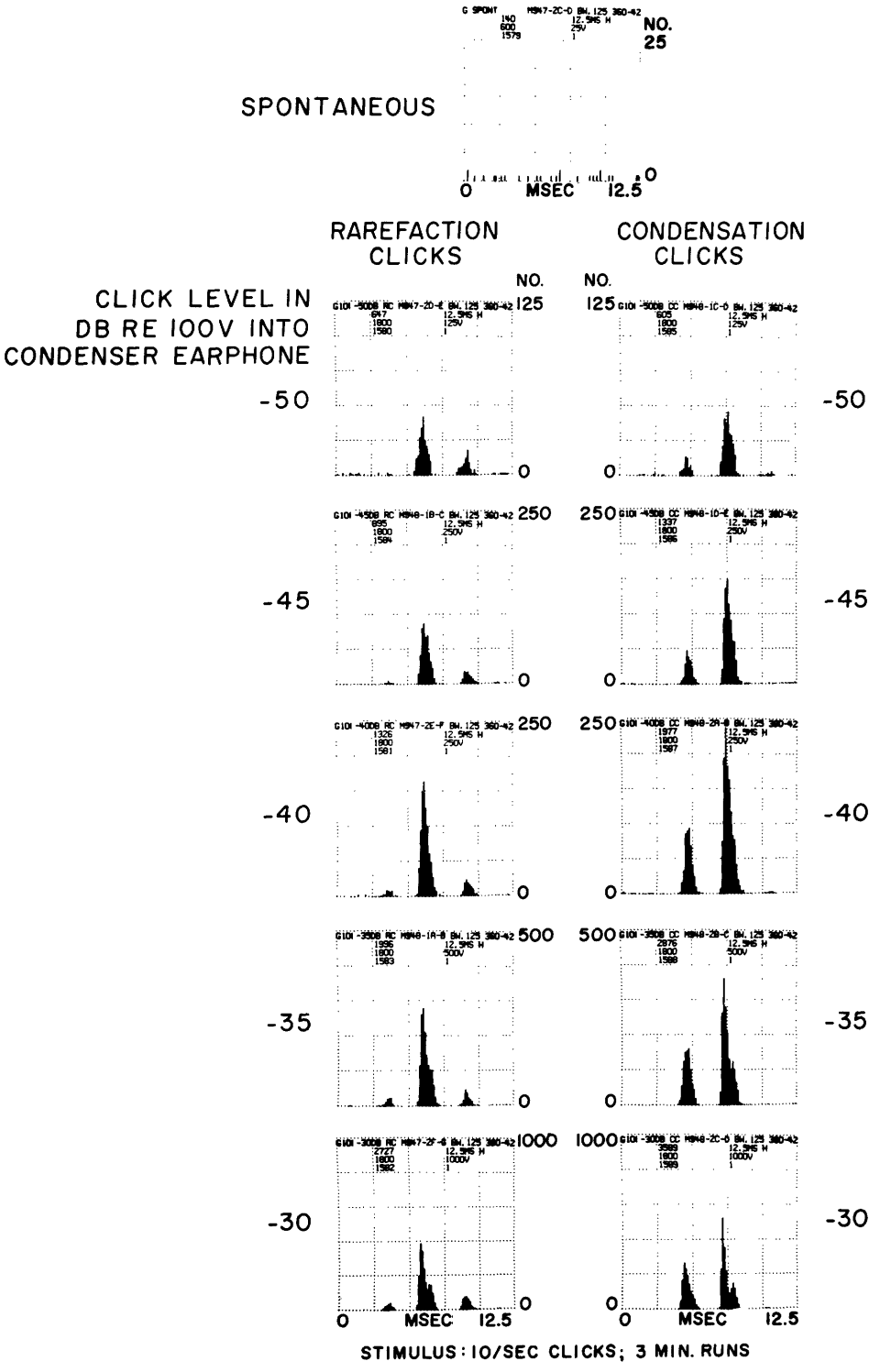

Fig. 30. Unit 360-42. PST histograms (bin width 0.125 msec, 100 bars). Stimuli: 10/sec rarefaction and condensation clicks, several intensities, 3 minutes. Length of spontaneous run: 1 minute.

firing" are intended to indicate this characteristic.

Some examples of the effect of this phenomenon are given in Fig. 31. Normalized PST histograms appear in the left column, and appear again on an expanded time scale, together with the recovered probability histograms in the right column. These histograms were selected from units with quite different CF's, to illustrate how the effect of the second firing on the histogram varies with CF. Beginning with the lowest CF, Unit 360-54 has a small extra peak at the end of the first large peak of the PST histogram, which does not appear in the recovered probability histogram. The same is true of Unit 371-11, which is somewhat higher in CF. Because Unit 360-4 has a still higher CF, the "extra" peak occurs almost midway between the two "legitimate" peaks. With Unit 371-23, the extra peak is on the late side of the second peak in the PST histogram. In these four examples, the extra peak consistently appears in the PST histogram approximately 3/4 to 1 msec after the first major peak. The position of this extra peak relative to the others depends on the spacing of the other peaks, which is inversely proportional to the CF.

Unit 371-27 was considered earlier in the discussion concerning Fig. 15. With this unit, the "second firing," 3/4 to 1 msec after an ordinary firing in the first peak, occurs between the third and fourth peaks of the recovered probability histogram. There are also second firings following firings in the other peaks, and, as these also tend to occur at times corresponding to local minima of the recovered probability curve, the time-locked structure of the response does not appear clearly in the PST histogram.

The curious characteristic about this "second firing" is that it often occurs at times corresponding to very low recovered probabilities. In fact, with this second firing, there are many situations in which the conditional probability of an event in the next bin width, given that the last event was 1 msec earlier, is larger than the corresponding recovered probability. Some sample probabilities associated with this phenomenon may be read from Fig. 15. For example, with the -50 db run, at 2.45 msec, the conditional probability of an event, given that the last event was during the first peak, is ~0.06. The corresponding recovered probability is ~0.02. Some further examples of the probabilities associated with this phenomenon are given in Tables 3 and 4.

Each entry in Table 3 is a conditional probability associated with a 0.2-msec interval that is located at a time corresponding to the extra peak. Each row corresponds to a different click level, each column to a different conditioning interval. The first three columns correspond to the last event being in a 0.2-msec interval located 0.6, 0.8, and 1.0 msec earlier than the considered interval. The fourth column corresponds to the last event being before the click. The PST histograms corresponding to these calculations are presented in Fig. 32.

Table 4 is similar to Table 3 except that it is based on Unit 360-54 and involves intervals that are 0.25 msec in duration. The first three columns in Table 4 correspond to intervals displaced from the considered interval by 0.5, 0.75, and 1.0 msec. The histograms corresponding to these calculations appear in Fig. 25.

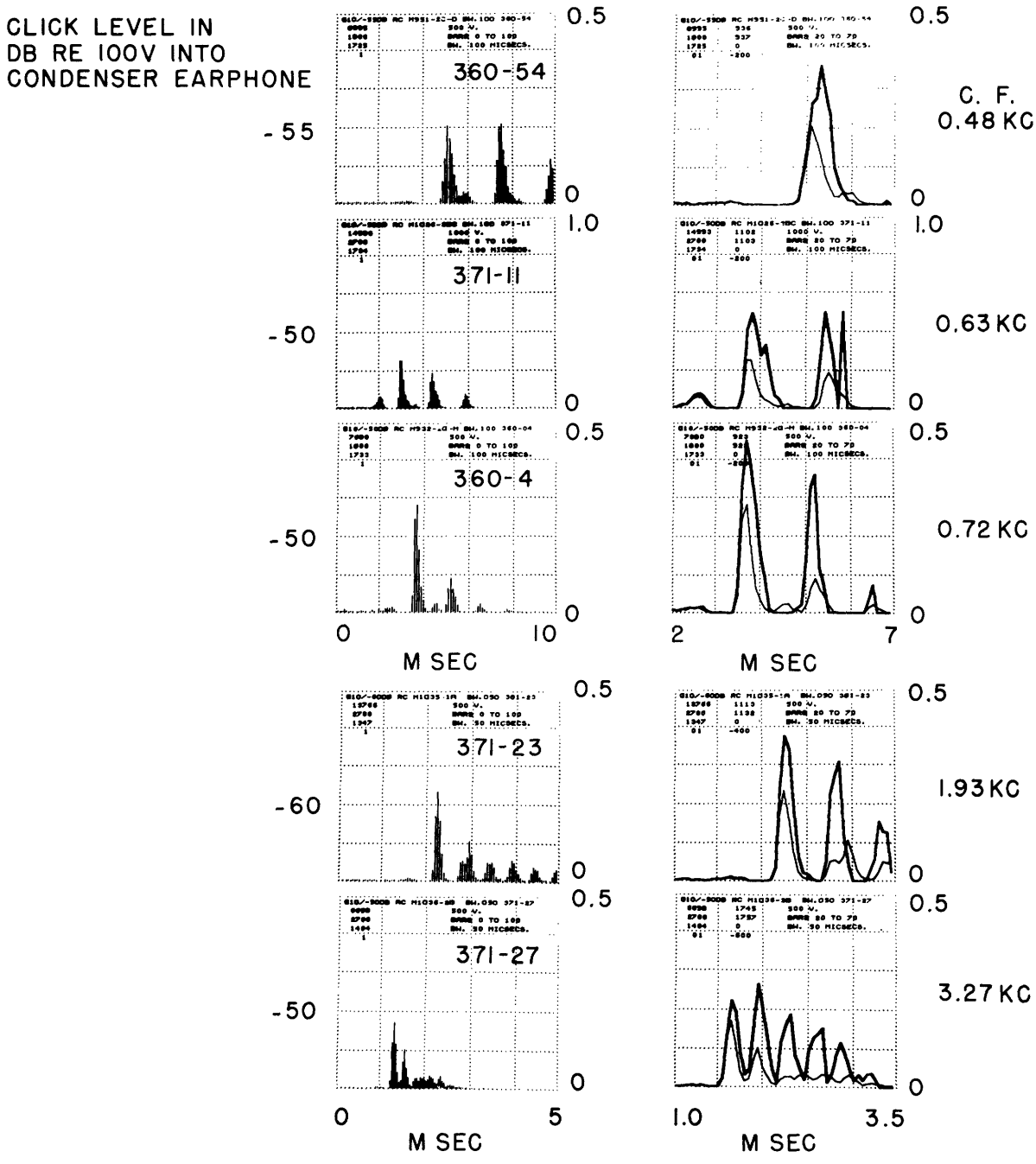

Fig. 31. Several units. Left column: normalized PST histograms (100 bars). Right column: normalized PST histograms (light lines) and recovered probability histograms (heavy lines) (straight-line interpolations between tops of bars 20-69). Bin width 0.1 msec in top three rows; 0.05 msec in bottom two. Stimuli: 10/sec rarefaction clicks. Recovered condition: -20 msec, except -30 msec for Unit 371-27.

Table 3. Unit 371-11. Conditional probability of an event during bars 46-47.

	Given last event during bars			
Click Level	40-41	38-39	36-37	$-\infty$-0
-65 db	0 (490)	0.00 (997)	0.01 (291)	0.00 (640)
-62 db	0 (398)	0.01 (1181)	0.01 (456)	0.00 (494)
-59 db	0 (336)	0.01 (1085)	0.03 (700)	0.00 (390)
-56 db	0 (340)	0.02 (1022)	0.04 (830)	0.01 (294)
-53 db	0 (279)	0.02 (946)	0.04 (1055)	0.00 (165)
-50 db	0 (297)	0.03 (1030)	0.06 (884)	0.00 (167)

"Bars x-y" refers to times larger than x/10, and less than or equal to y/10 msec. Numbers in parentheses represent number of trials on which the estimate is based.

Table 4. Unit 360-54. Conditional probability of an event during bars 47-48.

	Given last event during bars			
Click Level	43-44	41-42	39-40	$-\infty$-0
-80 db	0 (32)	0 (32)	0 (33)	0.02 (1216)
-75 db	0 (64)	0 (62)	0.01 (38)	0.01 (1177)
-70 db	0 (117)	0.04 (122)	0.06 (55)	.02 (1094)
-65 db	0 (220)	0.05 (242)	0.14 (94)	.02 (838)
-60 db	0 (281)	0.03 (514)	0.08 (213)	.02 (529)
-55 db	0 (305)	0.09 (789)	0.21 (342)	.02 (204)
-50 db	0 (168)	0.11 (704)	0.25 (642)	.05 (79)

"Bars x-y" refers to times larger than x/8, and less than or equal to y/8 msec. Numbers in parentheses represent number of trials on which the estimate is based.

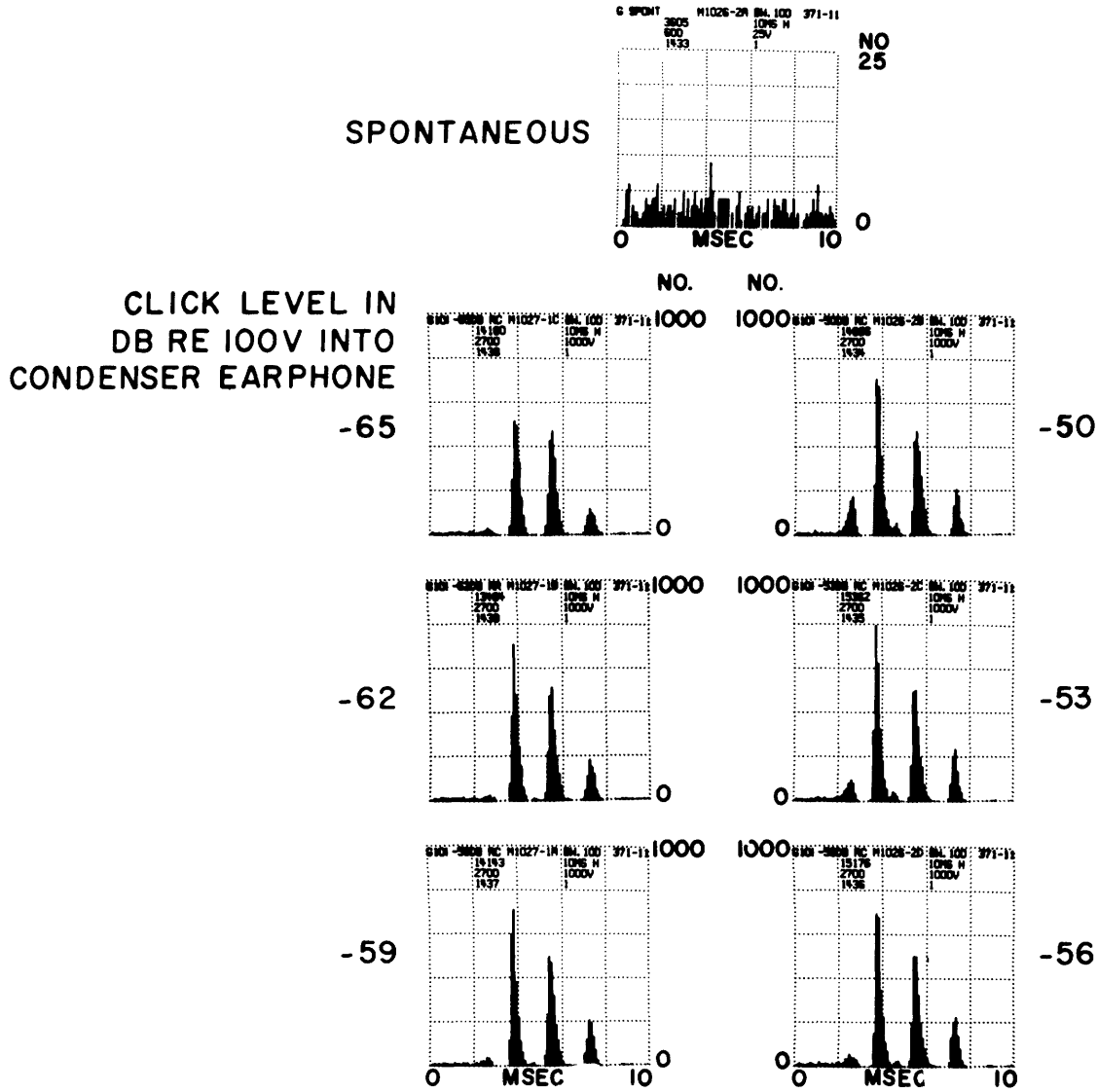

Fig. 32. Unit 371-11. PST histograms (bin width 0.1 msec, 100 bars). Stimuli: 10/sec rarefaction clicks, several intensities, 4.5 minutes. Length of spontaneous run: 1 minute.

No specific quantitative conclusions are intended from Fig. 15 and Tables 3 and 4; however, the probabilities presented may be regarded as representative. It should be noted that the probabilities associated with the 3/4 to 1 msec interval (column 3 of both tables) do increase with intensity, and that they are larger than the probabilities conditional on no event since the click – even at the lower intensities where, with Unit 360-54, the "extra" peak cannot be identified in the histograms.

This effect has been identified in roughly half of the units studied. It could be present, but undetected, in the other units, also. Where the CF is such that the 3/4 to 1 msec interval places the second firings in the middle of an existing peak, it would be difficult to isolate this effect. At lower intensities where the second firings may not be obvious

in the histograms (as with the -60 db run of Unit 360-54), it would also be difficult to identify the effect. No special effort has yet been made to identify this phenomenon in other stimulus situations, but it may well be present.

3.7 RECOVERED PROBABILITIES ON A FINER TIME SCALE

In the discussion concerning Fig. 13, it was observed that the apparent discrepancy between the normalized PST histogram and the recovered probability histogram could be understood in terms of the refractory characteristics of the unit. As the unit usually fires during the first portion of the peak, it is refractory during the later portion and hence relatively few firings occur. The refractoriness diminishes the PST histogram relative to the recovered probability histogram, since, in estimating the recovered probability at a time late in the peak, none of the trials that involved a firing earlier in the peak are used. It is interesting to examine this effect as a function of intensity. For this purpose, the PST and the recovered probability histograms for Unit 360-54 are presented in Fig. 33. These are based on the same data as the histograms presented in Fig. 25, but in this figure a somewhat smaller region of time is examined. Comparison of the recovered probability curves with the PST curves indicates that they are approximately the same at the lower intensities. But, beginning with the -60 db run, the early return to zero of the PST curve occurs and this becomes more pronounced as the intensity increases. This is, again, a refractory effect, which becomes important when the unit has a moderate to high probability of firing during the first part of the peak. This early return to zero of the PST curve could be misleading. Looking only at the PST histogram, it would appear that the peak narrows, and, since it does so by dropping off the later portion, it might also seem that its latency is shorter at higher intensities. Since the narrowing and the shortened latency occur only in the PST histogram, and not in the recovered probability histogram, they should be recognized as refractory effects.

Unfortunately, at the higher intensities there are relatively few trials with which to estimate the recovered probabilities for the later portion of the peak. Hence the curve is not statistically reliable in this region and may have some spurious peaks.

Because of the complications appearing in the PST histogram which are due to refractory effects and the tendency toward second firings, the recovered probability histogram appears to be a more useful measure of some properties of the unit. Referring to the simplified model of Fig. 8, consideration of recovered probabilities reduces the probabilistic device to its simplest state and provides a more direct measure of the mechanical system and the rectifier. It is tempting to regard the recovered probability as an effective stimulus, and to try to use this as an intermediate variable in the model, i.e., as the output of the rectifier. With this in mind, some further data on recovered probabilities as functions of intensity will be presented. Before considering these data, however, the hypothesis under consideration should be clarified.

This hypothesis includes the following assumptions. The output of the mechanical system, $x(t)$, is a linear transformation of the input. The output of the rectifier, $r(t)$,

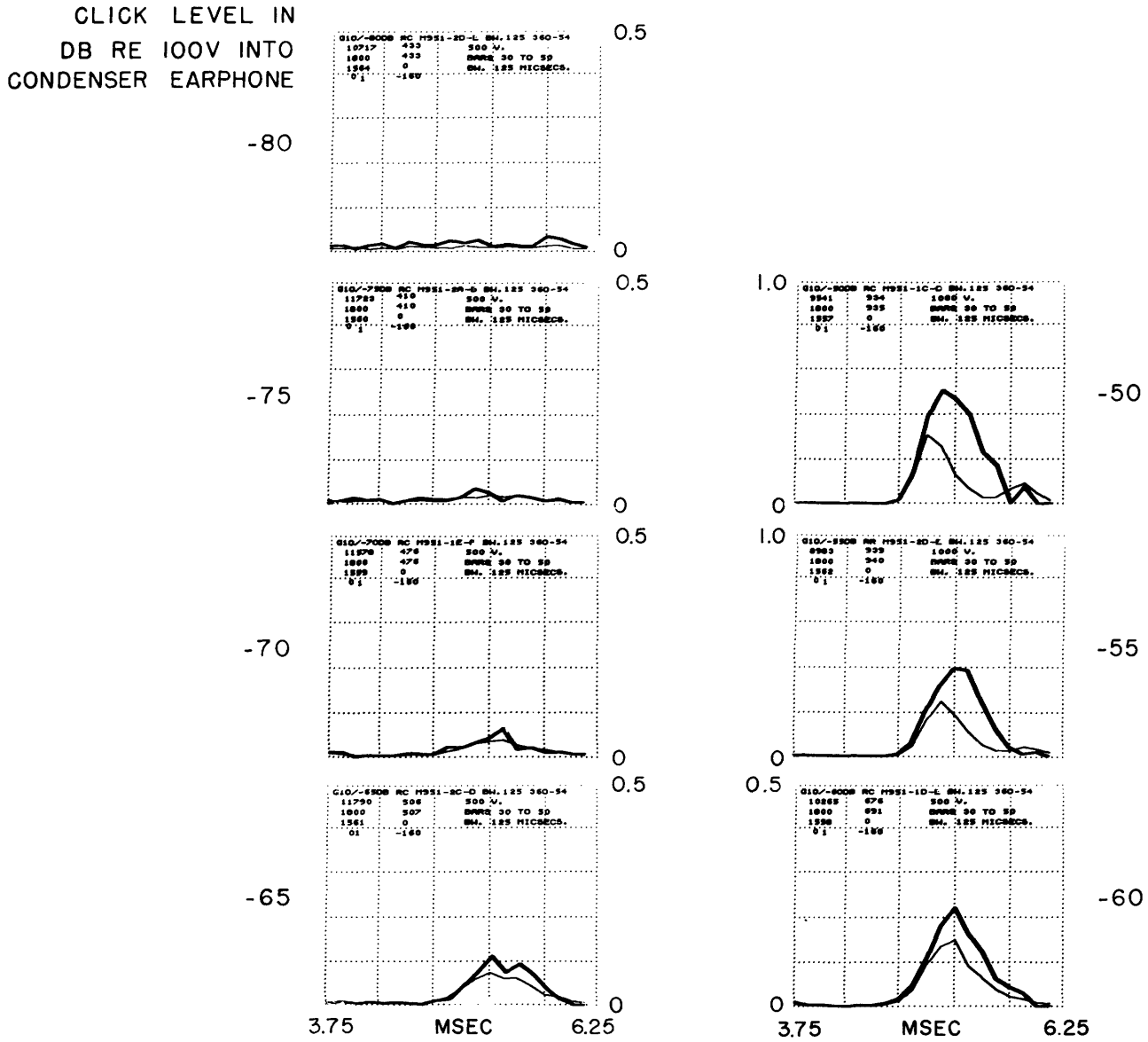

Fig. 33. Unit 360-54. Recovered probability histograms (heavy line); normalized PST histograms (light line); (bin width 0.125 msec, straight-line interpolations between tops of bars 30-49, recovered condition: -20 msec). Stimuli: 10/sec rarefaction clicks, several intensities, 3 minutes.

is an instantaneous function of x(t), i.e., r = f(x). Finally, it is assumed that r(t) represents "recovered probability per unit time," i.e., the recovered probability of an event in a short interval, Δ, is $r(t)\Delta$. From this assumption it is easy to show (in the same manner used in most derivations of the Poisson process) that the recovered probability of an event in the interval from a to b is $1 - e^{-\int_a^b r(u)du}$. (Of course, if Δ is sufficiently small, and $b = a + \Delta$, this reduces to $r(a)\Delta$, in agreement with the original assumption.)

In Fig. 34, the recovered probability curves of Fig. 33 are superimposed on one graph to facilitate comparison. Unlike the PST histograms, these curves remain reasonably symmetric with increasing intensity, except at the highest intensity where the second half of the peak is smaller than it should be to maintain the symmetry. This violation of the symmetry at the highest intensity suggests that the current hypothesis is incorrect. If the bin width, Δ, were sufficiently small that r(t) were essentially constant over a bin-width interval, the recovered probability associated with the k^{th} bin width would be $1 - e^{-\Delta r(k\Delta)} = 1 - e^{-\Delta f(x(k\Delta))}$. The linearity assumption implies that an amplitude change in the stimulus results in the same amplitude change in x(t). Thus two bin widths that have the same recovered probability (corresponding to the same value of x) at one intensity should have the same recovered probability at all intensities, and the superimposed recovered probability curves should maintain their symmetry. Actually, for the data of Fig. 34 it is not reasonable to say r(t) is essentially constant over a bin

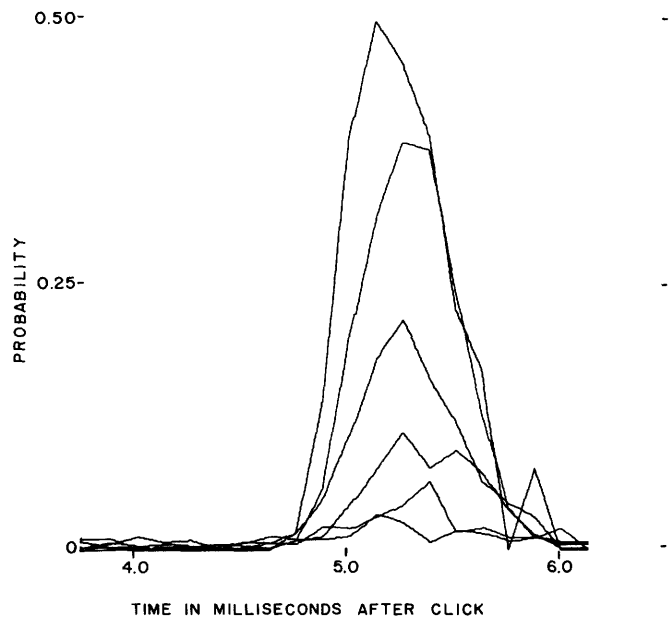

Fig. 34. Unit 360-54. Superimposed recovered probability histograms (bin width 0.125, straight-line interpolations between the tops of bars 30-49, recovered condition: -20 msec). Stimuli: 10/sec rarefaction clicks, several intensities, 3 minutes.

width interval, but this only complicates the argument,* it does not change the conclusion.

The data of Fig. 34 are presented in a different form in Fig. 35. Here the recovered probabilities for several individual bin widths, or bars, are plotted as a function of intensity. The vertical scale is a monotonic transformation of the recovered probability, which is related to the expression for the recovered probability, which has been given as $1 - e^{-\int_a^b r(u)\,du}$. The vertical scale is chosen to be the negative logarithm of 1 minus the recovered probability $\left(\int_a^b r(u)\,du\right)$. This vertical scale has the advantage that the shape of the curves is not very sensitive to the choice of bin width. For example, if two adjacent intervals are combined, the resulting curve is the sum of the original two.

Since Fig. 35 is a plot of $\int_{k\Delta}^{k\Delta+\Delta} r(u)\,du$ against intensity in db, the curves should be almost identical except for horizontal displacement. (The word "almost" could be eliminated if Δ were sufficiently small that the approximation $\int_{k\Delta}^{k\Delta+\Delta} r(u)\,du = \Delta r(k\Delta) = \Delta f(x(k\Delta))$ applied.) In particular, two curves that are equal for low intensities should be equal at higher ones also. With this in mind, inspection of the figure indicates that bars 42 through 44 seem too small at -50 db. Before considering the implications of this fact, additional data, which are more reliable statistically, should be considered. For this

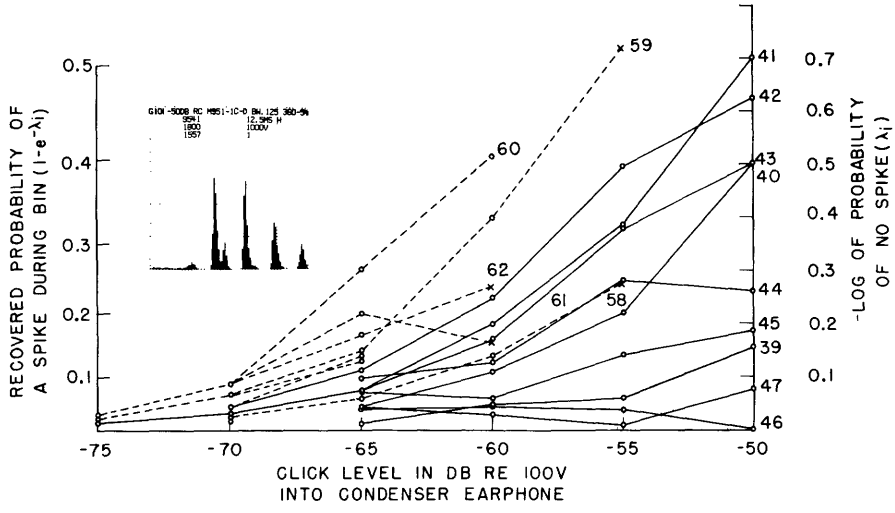

Fig. 35. Unit 360-54. Recovered probabilities associated with single bin widths (bin width 0.125 msec, recovered condition: -20 msec). Stimuli: 10/sec rarefaction clicks, several intensities, 3 minutes. Separate curves are identified by bar number (the dotted vertical lines in the PST histogram go through bar numbers 0, 20, 40, 60, 80, and 100). See text for explanation of vertical scale. When a probability estimate is based on between 50 and 100 trials, an "x" is used to designate the point; when fewer than 50 trials are available, no point is given.

*It is only necessary that r(t) be symmetric about the center of the peak (which appears to be roughly the case in Fig. 34), in order to argue that two symmetrically located bin widths should have equal recovered probabilities at all intensities.

purpose, an intensity series with longer runs and smaller increments in intensity was run on Unit 371-18. The superimposed recovered probability histograms appear in Fig. 36, and the equivalent plot of the recovered probabilities for each bin width appears in Fig. 37.

Figure 36 illustrates that the probabilities increase regularly with intensity for the first portion of the large peak. At the highest three intensities these probabilities are about equal, though the probabilities in the smaller, earlier peak increase at these intensities. In the later portion of the large peak, the probabilities actually decrease. Examination of Fig. 37 confirms that the probabilities corresponding to times late in the peak are diminished at the higher intensities. In this figure bar 44 increases regularly throughout; bar 46 levls off at -62 db; bar 48 starts decreasing at -68 db. It is as if the recovered probability at a given time were reduced by large recovered probabilities preceding it. However, this is not a refractory effect in the ordinary sense – these are recovered probabilities. (This effect has been identified and studied in click data from at least a dozen other units, and the data from Units 360-54 and 371-18 may be regarded as representative.)

This is an important result and deserves some amplification. The conventional PST histogram provided a good deal of information about the firing patterns of auditory nerve fibers when short acoustic clicks are presented as stimuli. From the histograms, it appeared that the effective stimulus was some sort of rectified version of the mechanical motion. To study more directly the mechanical motion, the form of the rectifier, and some properties of the probabilistic device, the recovered probability calculations were performed. These calculations indicated that

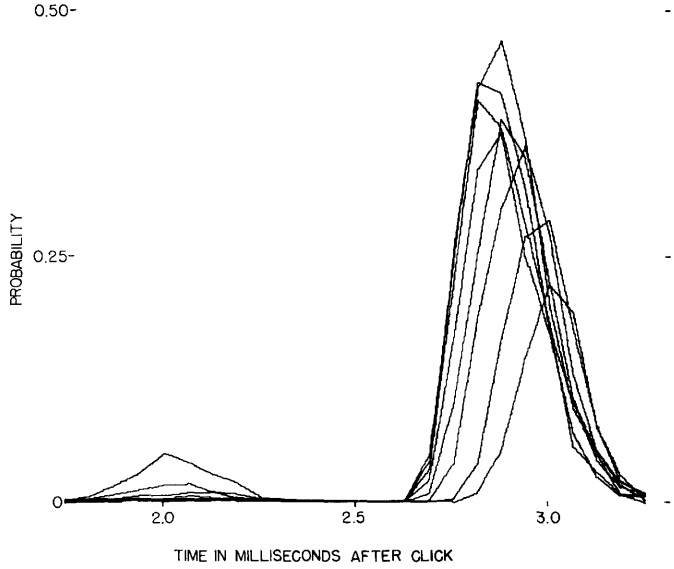

Fig. 36. Unit 371-18. Superimposed recovered probability histograms (bin width 0.0625 msec, straight-line interpolations between the tops of bars 28-42, recovered condition: -30 msec). Stimuli: 10/sec rarefaction clicks, several intensities, 4.5 minutes.

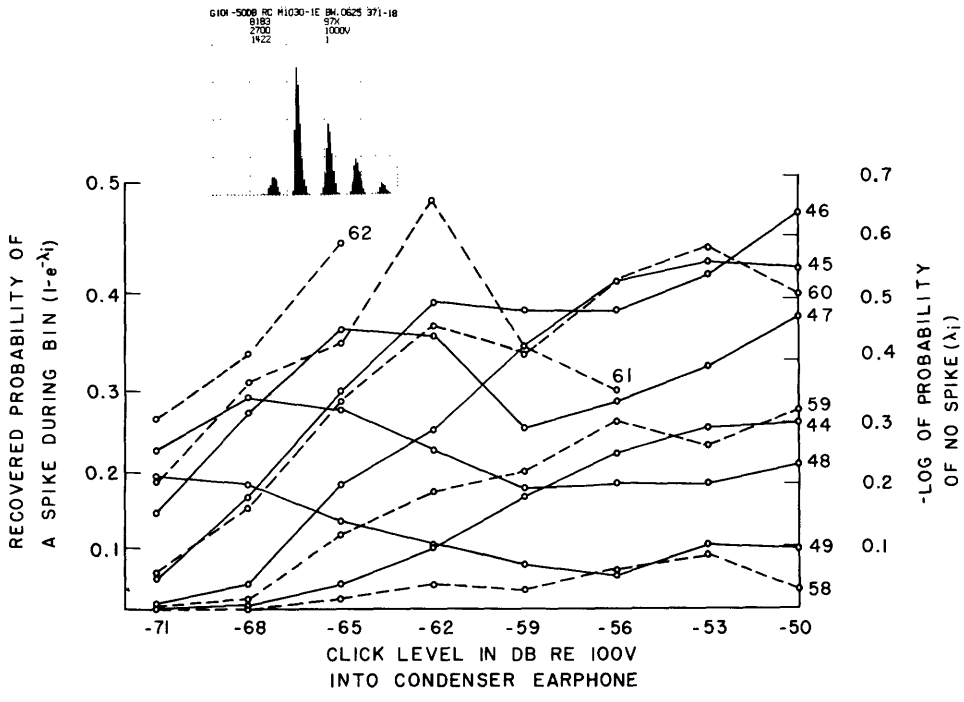

Fig. 37. Unit 371-18. Recovered probabilities associated with single bin widths (bin width 0.0625 msec, recovered condition: -30 msec). Stimuli: 10/sec rarefaction clicks, several intensities, 4.5 minutes. Separate curves are identified by bar number (the dotted vertical lines in the PST histogram go through bar numbers 0, 20, 40, 60, 80, and 100). See text for explanation of vertical scale.

some irregularities in the PST histograms resulted from the refractory characteristics of the neuron, not directly from an effective stimulus. Having temporarily removed the refractory complications from consideration, the problem remained to relate the acoustic input to the recovered probability curves. The simplest assumption here would have been that the recovered probability per unit time is an instantaneous function of the output of the mechanical system, but this assumption is contradicted by Figs. 34-37. The data presented in these figures suggest that something is depleted when moderate to large values of recovered probability occur – even when the unit does not fire. The effect of this depletion is to diminish the recovered probabilities that follow. The use of the word "depletion" is purely descriptive, and is not intended to imply that any physiological quantity is in fact depleted. Nevertheless, since it is convenient to refer to this phenomenon by some name, "depletion effect" is used for this purpose.

If the input to the probabilistics device is still to be identified as recovered probability per unit time, the "depletion effect" implies that the "rectifier" cannot have an output that is simply an instantaneous function of its input. Rather, a state variable might be associated with the "rectifier." This variable would be affected by the stimulus independently of what firings actually occurred. The ouput of the rectifier, r(t), would then depend on both the instantaneous value of the output of the mechanical system, x(t),

and the current value of this state variable; the occurrence of large recovered probabilities would affect this variable in such a way that recovered probabilities resulting from subsequent mechanical motion would be diminished.

IV. DATA OBTAINED WITH VARIOUS STIMULI OTHER THAN SIMPLE CLICKS

All of the data discussed in Section III were obtained with simple acoustic clicks as stimuli. These have proved to be very useful stimuli because of the role of the impulse response in linear time-invariant systems and because the transient nature of the stimulus minimizes some of the long-term effects that are present with other stimuli. There are many other stimuli that are useful in studying the system, and, of course, the eventual hope is to be able to describe, in one framework, the behavior of this system for a variety of stimuli. Several other stimulus situations will now be discussed briefly. The presentation is not as detailed as that of Section III: the data presented are typical, but not comprehensive. While the conclusions presented here are few in number, there are two of importance. The first result is that some of the characteristics which have previously been observed, and might have been thought to be simply refractory effects, are not. This statement applies to the transient in the PST histograms obtained with tone-burst stimuli and to the reduction of peak sizes in the PST histograms obtained with clicks masked by noise. The second conclusion is negative in nature: it does not appear to be possible to describe the low-frequency continuous tone situation in terms of the simplified model of Fig. 8.

4.1 CONTINUOUS TONES

The continuous sinusoidal stimulus is a particularly appropriate one for studying this system, because of the assumption that the mechanical system is linear and time-invariant. With a linear time-invariant system, a sinusoidal input implies a sinusoidal output. Hence, by assumption, with continuous tone stimuli, the output of the mechanical system is known, except for amplitude and phase, and even these are thought to be at least qualitatively understood.

Interval histograms and hazard functions obtained with continuous tone stimuli of several intensities are presented in Fig. 38. All of these data are from Unit 419-24, which had a CF of 11.9 kc, and this was also the frequency of the continuous-tone stimulus. At this high frequency, no stimulus-related time structure can be detected in the firing patterns. In fact, these patterns appear to be statistically quite similar to those obtained in the spontaneous case. (Compare this figure with Figs. 10 and 11.)

The data from Unit 419-24 may be regarded as typical, and the following observations, which are based on Fig. 38, are representative of the characteristics of other units. (i) In general, the rate increases with increasing intensity, except at higher intensities where it sometimes decreases. (The fact that the rate at -80 db is less than the spontaneous rate in this example is not regarded as significant, since the difference is so small.) (ii) The interval histograms all have a mode at less than 10 msec, followed by a roughly exponential decay; the time constant of this decay, as well as the location of the mode, are influenced by the intensity of the stimulus. (iii) The hazard functions appear to level off at an asymptotic value within 25 msec, but there are considerable

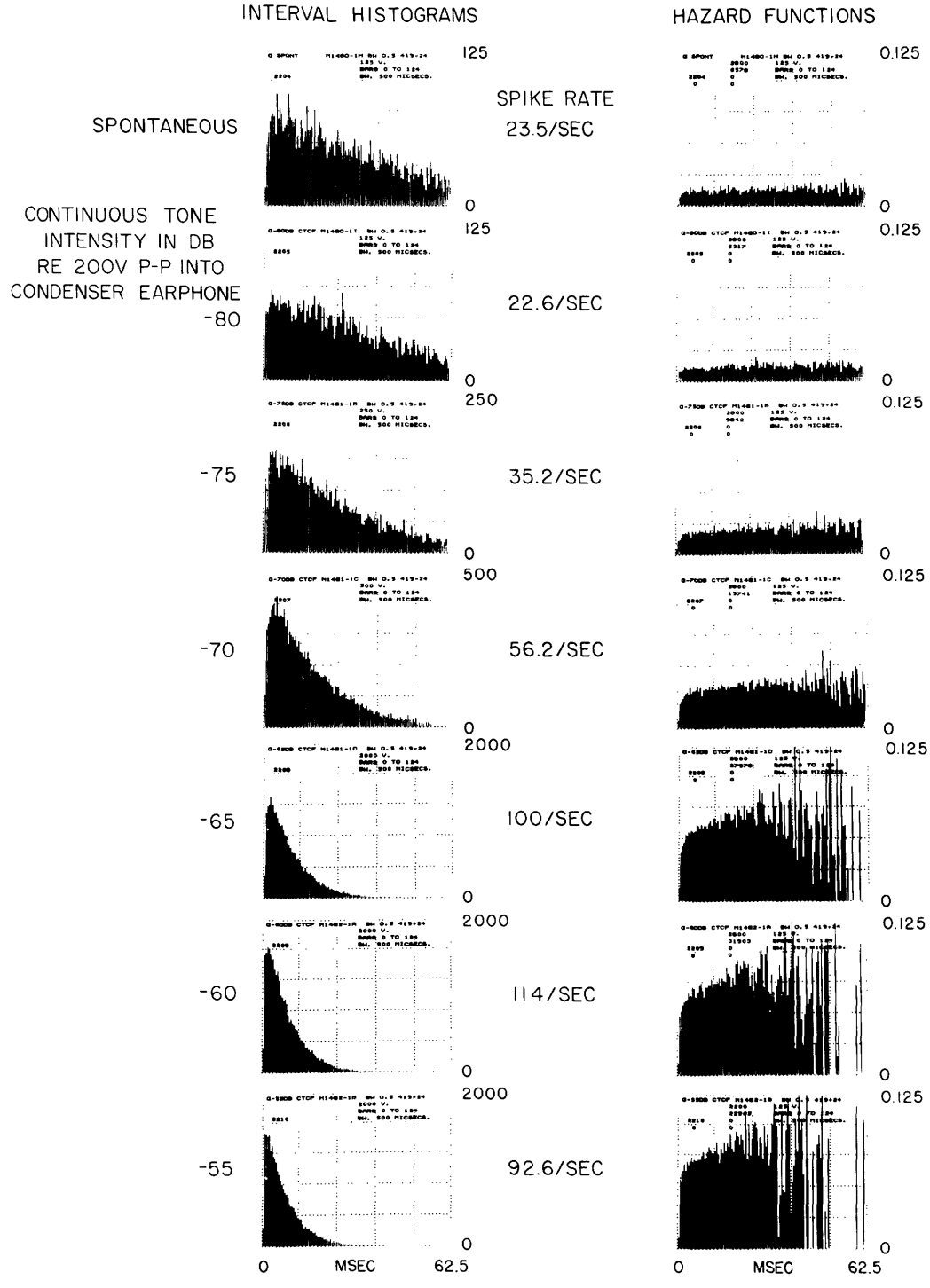

Fig. 38. Unit 419-24. Interval histograms and hazard functions (bin width 0.5 msec, 124 bars). Stimuli: continuous tones at CF of the unit (11.9 kc), several intensities, 4.67 minutes, except 3.67 minutes for −55 db run.

statistical fluctuations about this asymptote at the higher rates because, at these rates, there are relatively few intervals longer than 25 msec. In general, the asymptotic value of the hazard function is larger for the higher rates, but it is not necessarily proportional to the rate.

At frequencies below ~5 kc a stimulus-related time structure may be observed in the firing patterns of these units. This time structure may be observed in the Post Zero Crossing histogram, which is simply a PST histogram calculated by treating all positive (or all negative) going zero crossings of the sine wave in the same way as the click presentations are treated in the calculation of PST histograms from click data. The time structure may also be observed in an interval histogram, provided the bin width is small enough that intervals equal to integral multiples of the sine wave period may be identified.

PST histograms obtained from a low-frequency continuous tone intensity run are presented in Fig. 39. The stimulus frequency was chosen to equal the characteristic frequency of the unit, 0.65 kc. The full horizontal scale of the histograms represents a 1.25-msec time interval beginning 0.31 msec after a negative-going zero crossing of the stimulus; the 0.31-msec interval is not represented in the histograms. The last few bars of the histograms are zero, since the period of the stimulus is slightly less than the 1.56-msec full-scale value, and the PST calculation "resets" at each negative-going zero crossing. All of the histograms are based on 50,000 periods of the stimulus, and are presented with a vertical scale of 500.

The recovered probabilities associated with several intervals, corresponding to the adjacent sets of 8 bars in the PST histograms, were calculated from these same data. Some of the resulting recovered probability histograms are superimposed in Fig. 40. Except for the factor of 8 difference in bin width, the recovered probability curves of Fig. 40 and the PST histograms of Fig. 39 appear quite similar, and the observations that follow are suggested by both figures.

Examination of the data at any single intensity indicates that the unit tends to fire during approximately one-half of the period of the stimulus. Outside of this region, there is a lower probability of firing than in the spontaneous case; inside, it is considerably higher. Typically, the unit fires only once every several cycles, but there is a clear preferred time structure within a cycle.

In the context of the model of Fig. 8, in which a rectifier operates on the output of the mechanical system, these data are a little disturbing. If only the lower intensities were considered, these data would appear to be consistent with the model; however, the latency change that occurs with increasing intensity does not appear to be consistent with this model. To illustrate, consider the time 0.6 msec after the negative-going zero crossing. At the lower intensities there is a lower recovered probability than in the spontaneous case, which suggests a negative output of the mechanical system at this time. At the higher intensities there is a higher recovered probability than in the spontaneous case, which suggests a positive output of the mechanical system. The reverse of this

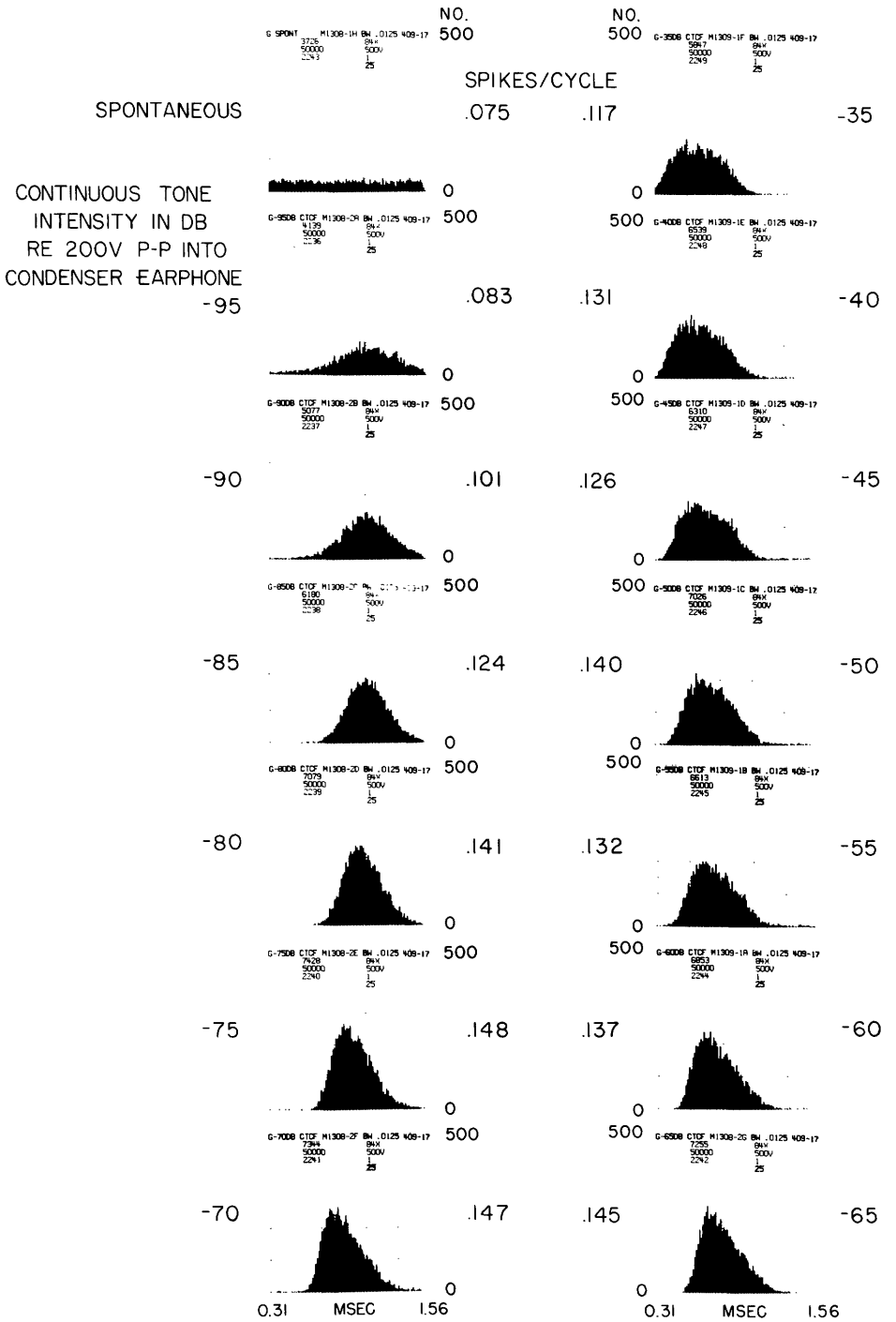

Fig. 39. Unit 409-17. PST histograms (bin width 0.0125 msec, bars 25-125). Bar 0 (not displayed) corresponds to a negative going zero crossing of the sine wave stimulus. The display begins with bar 25, which corresponds to 0.31 msec after a negative-going zero crossing. Stimuli: continuous tones at the CF of unit (0.65 kc), several intensities, approximately 77 seconds.

observation (i. e. , higher recovered probabilities at lower intensities) applies to the time 1. 1 msec. Since the mechanical system is assumed to be linear, a change in stimulus intensity should not lead to a change in the polarity of the output.

There are some similarities among Figs. 40, 34, and 36. The last two figures, which

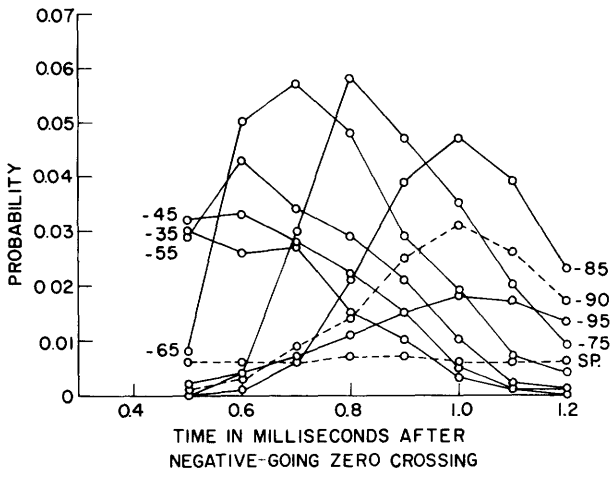

Fig. 40.

Unit 409-17. Superimposed recovered probability histograms (bin width 0. 1 msec, straight-line interpolations between the tops of bars 5-12, recovered condition: -20 msec). Stimuli: continuous tones at CF of unit (0.65 kc), several intensities, approximately 77 seconds.

contain superimposed recovered probability histograms obtained with click stimuli, led to the identification of the "depletion effect." It is possible that the latency shift in the low-frequency continuous tone data and the "depletion effect" in the click data are both manifestations of the same phenomenon, but it is certainly not obvious what the phenomenon would be. A relatively simple modification of the model of Fig. 8 will handle the "depletion effect," but a more drastic modification may be necessary to handle the low-frequency continuous tone data.

Another puzzling effect which sometimes appears in low-frequency continuous tone data can be seen in Fig. 41. In this figure the PST histograms obtained with a stimulus of 0. 30 kc are presented; the CF of this unit is 0. 43 kc. While the PST histograms for the -80 db through -50 db runs seem all right, the next three are a little disturbing. At -40 db a large dip separates the bars into two sections, at -30 db the separation is even more pronounced, and at -20 db there is a large change in latency. It was thought at first that the separation at -40 db and -30 db might be a refractory effect. This could occur if the unit usually fired in the first portion, and then could not be fired again until the later portion. It was thought alternatively that this separation might be a reflection of the tendency toward second firings after 3/4 to 1 msec, which was observed with click stimuli. That neither of these explanations is valid is easily demonstrated by calculating the recovered probability histograms from the same data. The recovered probability histograms turn out to have essentially the same shape as the PST histograms, with the dip, or separation, developing in the same way at -40 db and -30 db. (Typical numbers here are recovered probability of firing in a 0. 05-msec bin width on either side

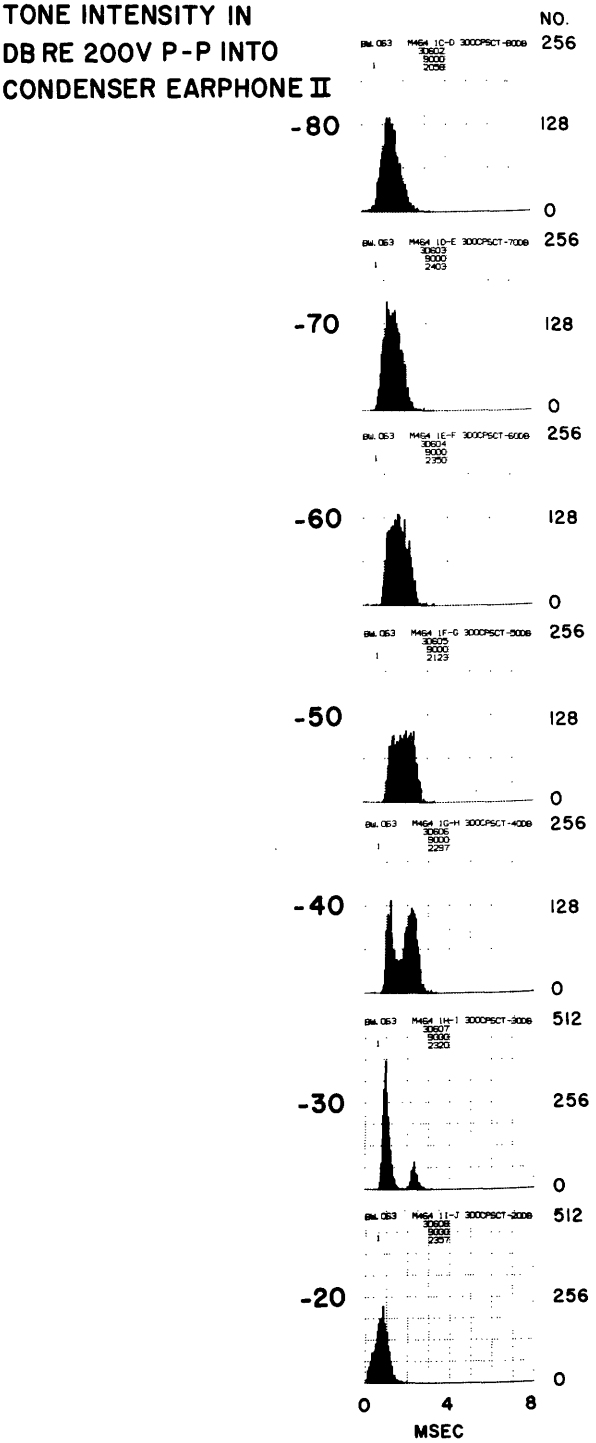

Fig. 41.

Unit 303-6. PST histograms (bin width 0.0625 msec, 128 bars). Stimuli: 0.30 kc, continuous tones, (CF of unit, 0.43 kc), several intensities, approximately 30 seconds. The origin of the horizontal axis corresponds to a positive-going zero crossing of the sine-wave stimulus. (N. Y. S. Kiang, unpublished data.)

of the dip in the -40 db run, 0.014; in the dip itself, 0.005. These estimates are based on approximately 2000 trials.)

The latency change at -20 db seems reasonable in terms of the latency changes observed with Unit 409-17, but the "separation" at -40 db and -30 db is a little surprising. There are as yet relatively few low-frequency continuous tone data available, but, thus far, this "separation" has only been observed at frequencies below the CF, and in the few units in which it has been seen, it is not present with the data obtained at the CF. These remarks are based on very little data, and are only intended to indicate that frequency may be a useful parameter to explore. It has already been suggested that it might be necessary to remove the assumption that the fiber is affected by the mechanical motion at only one point on the cochlear partition, in order to handle "inhibitory" effects. The low-frequency continuous tone stimulus may be another case in which this assumption is unworkable. If so, varying the frequency of the stimulus may give some hints as to how to modify the model of Fig. 8.

4.2 TONE BURSTS

Tone bursts have been presented as stimuli by using an electronic switch to gate a continuous tone. Typically, rise and fall times have been set at 2.5 msec, duration between 25 msec and 50 msec, and repetition rate at 10 per second. Typical results from two different units are presented in Fig. 42. In both cases the stimulus was a tone burst at the CF of the unit. The tone bursts were roughly 50 msec in length and were presented at a rate of 10 per second. The normalized PST histograms are given as light lines and the recovered probability histograms are indicated by the heavy lines. Where the number of trials available for an estimate becomes less than 50, the recovered probability histogram is terminated.

In the PST histogram for Unit 385-35 there is a clear transient at the beginning of the burst. This transient is typical of tone-burst and noise-burst PST histograms. As no such transient would be expected in the mechanical motion, the presence of this transient might be a little puzzling. One hypothesis would be that the transient reflects a refractory effect that could be explained as follows. Usually at the beginning of the tone burst the unit has not fired for a long time and is easy to fire. Later in the burst, the unit has usually fired recently and is relatively harder to fire. Hence, even with the same effective stimulus at both times, more events would be expected at the beginning of the burst than at the end. While this phenomenon might contribute to the transient in the tone burst, it does not seem to be the only contributing factor. One way to remove the refractory complication is to look at recovered probabilities, but this is not very useful in this case. Even with a full 6 minutes of data, the recovered probabilities cannot be reliably estimated except at the very beginning of the burst. Another way to deal with the refractory problem is to attempt to control it, by comparing similar conditional probabilities. The conditional probability matrix for this run is presented in Table 5. Among the entries in this table are several conditional probabilities of firing

UNIT 385-26 UNIT 385-35

NORMALIZED PST HISTOGRAMS

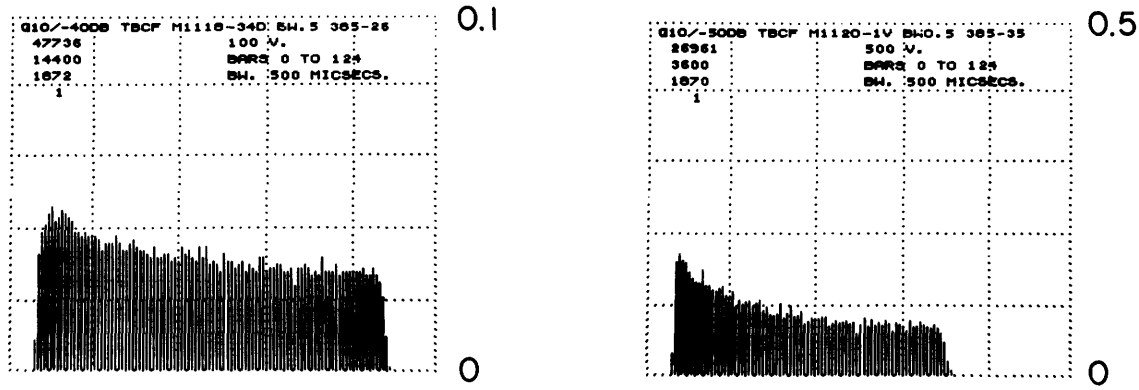

NORMALIZED PST HISTOGRAMS
AND
RECOVERED PROBABILITY HISTOGRAMS

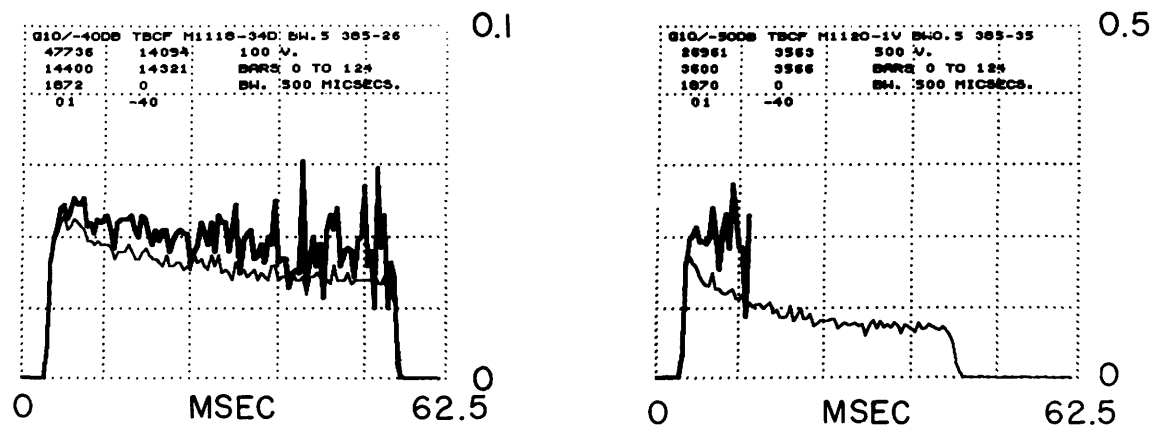

Fig. 42. Units 385-26 and 35. Upper row: normalized PST histogram (bin width 0.5 msec, 124 bars). Lower row: normalized PST histogram (heavy line) and recovered probability histogram (light line), bin width 0.5 msec, straight-line interpolations between tops of bars 0-123, recovered condition: -20 msec, probability curve given only when at least 50 trials were available for the estimate. Stimuli: 10/sec tone bursts at CF of unit. Unit 26: -40 db, 17.5 kc; Unit 35: -50 db, 9.3 kc.

Table 5. Unit 385-35. Conditional probability matrix.

Stimulus: 10/sec, -50 db tone bursts

Given last event during bars	Conditional probability of event during bars								
	0-10	11-12	13-14	15-16	17-18	19-58	59-60	61-62	63-64
$-\infty$ to -80	.352 3541	.374 2293	.351 1436	.351 932	.397 605	.992 365	0 3	0 3	0 3
0-10		.212 1263	.267 995	.287 729	.312 520	.994 358	0 2	1.0 2	0 0
11-12			.207 1143	.251 906	.306 679	.996 471	.500 2	0 1	1.0 1
13-14				.163 1014	.234 849	.991 650	.500 6	0 3	0 3
15-16					.184 935	.996 763	.333 3	0 2	0 2
17-18						.998 985	.500 2	0 1	0 1
19-58							.152 3582	.146 3036	.178 2592
59-60								.083 552	.095 506
61-62									.083 492

"Bars x-y" refers to times larger than x/2, and less than or equal to y/2 msec.
The lower number in each pair is the number of trials on which the probability estimate is based.

in a 1-msec interval, given that the last firing occurred during the previous millisecond. Typical values of this conditional probability are 0.212 near the beginning of the burst and 0.083 later in the burst. From these comparisons it does seem that as the burst continues either the stimulus strength is effectively diminished or the unit becomes less sensitive.

Unit 385-26 differs from Unit 385-35 in sensitivity. A typical recovered probability of an event in a 0.5-msec interval for Unit 35 is 0.2; for Unit 26 it is only 0.05. Because of this reduced probability of firing, it is possible to calculate the recovered probabilities for the entire tone burst. The PST histogram for Unit 385-26 has a transient, though it is less pronounced than that of Unit 385-35. It appears that the recovered probability histogram also has a transient, but statistical fluctuations cloud the issue somewhat. Further information may be obtained from the conditional probability matrix which

Table 6. Unit 385-26. Conditional probability matrix.

Stimulus: 10/sec, -40 db tone bursts

Given last event during bars	Conditional probability of event during bars								
	0-10	11-12	13-14	15-16	17-18	19-58	59-60	61-62	63-64
$-\infty$ to -80	.082 14262	.089 13091	.092 11925	.095 10829	.096 9798	.820 8861	.085 1594	.077 1459	.077 1347
0-10		.042 1177	.070 1127	.074 1048	.076 970	.786 896	.109 192	.088 171	.071 156
11-12			.053 1224	.047 1159	.090 1104	.779 1005	.045 222	.066 212	.061 198
13-14				.065 1253	.062 1172	.789 1099	.086 232	.066 212	.066 198
15-16					.050 1254	.788 1191	.063 252	.068 236	.068 220
17-18						.749 1256	.035 315	.053 304	.076 288
19-58							.058 11575	.057 10904	.065 10278
59-60								.026 886	.050 863
61-62									.030 837

"Bars x-y" refers to times larger than x/2, and less than or equal to y/2 msec.
The lower number in each pair is the number of trials on which the probability estimate is based.

is given in Table 6. Here it can be seen that recovered probabilities associated with 1-msec intervals are approximately 0.095 at the beginning of the burst, and 0.077 later in the burst. Conditional probabilities of an event in a millisecond interval, given that the last event occurred during the previous millisecond, diminish from approximately 0.055 to 0.03 as the burst proceeds. Other numbers in the matrix could also be compared, but it already seems clear that the observed transient is more than an ordinary refractory effect.

It is felt that this reduction in sensitivity is the same phenomenon as the "depletion effect" that was discussed with reference to Fig. 36. In both the click situation of Fig. 36 and the current tone-burst situation it appears that moderately large values of recovered probability diminish subsequent values, even when no firings occur. It may also be that the large number of firings that occur with Unit 385-35 fatigue the unit and

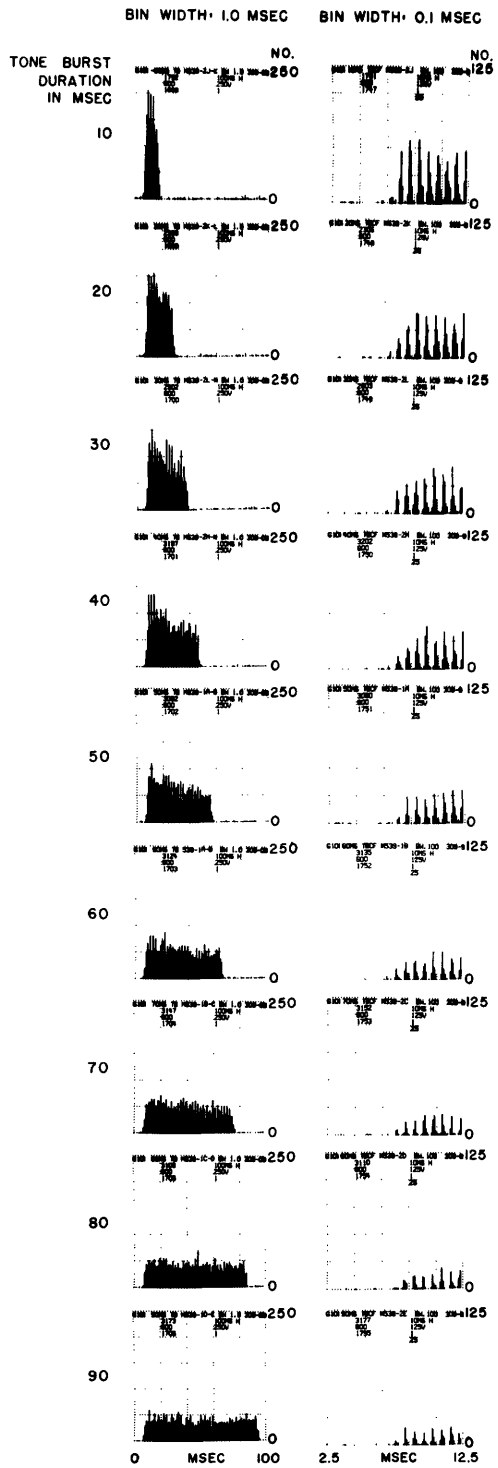

Fig. 43. Unit 309-9. PST histograms (left column: bin width 1 msec, bars 0-99; right column: bin width 0.1 msec, bars 25-124). Stimuli: 10/sec -80 db tone bursts at CF of unit (1.45 kc), several durations, 1 minute.

diminish its sensitivity, but this phenomenon has not been isolated.

In summary, there are two important and related points to be concluded from these tone-burst data. The conditional probability calculations indicate that the transient present in the tone-burst response is not simply a refractory effect in the ordinary sense. Furthermore, at least part of the transient is apparently due to the same phenomenon that was first observed with click stimuli: the "depletion effect."

Two important parameters of the tone-burst stimuli are the duration and the repetition rate. Some further information about these units may be obtained by examining data obtained with various values of these two parameters. In Fig. 43 the PST histograms obtained from Unit 309-9 for several different durations are presented; the repetition rate for all runs in Fig. 43 is 10 per second. In the left column the calculations were performed by using a bin width of 1 msec, and the entire 100-msec period of the stimulus is shown. The CF of this unit is 1.45 kc, and this is the frequency that was chosen

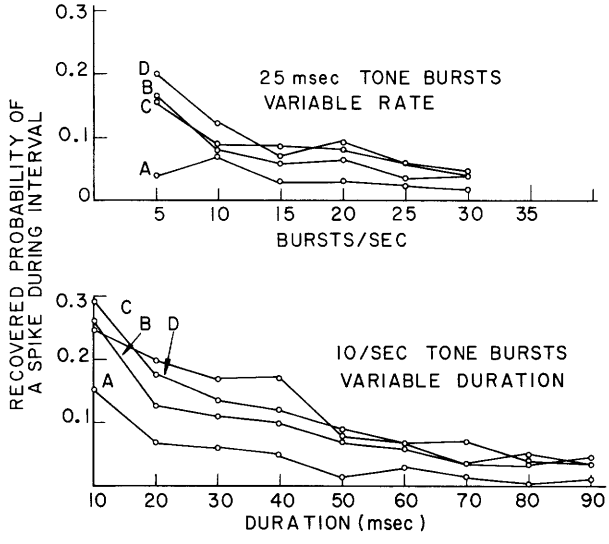

Fig. 44.

Unit 309-9. Recovered probabilities associated with four cycles of tone burst as functions of rate and duration. Stimuli: -80 db tone bursts at CF of unit (1.45 kc), several rates and durations. Interval definition: (bin width 0.1 msec) A = bars 73-79, B = 80-86, C = 87-93, D = 94-100, recovered condition: -13.5 msec.

for the tone burst. At this frequency, there is a time structure in the responses which is related to the individual cycles of the tone burst. This time structure is visible in the histograms in the right column, for which a bin width of 0.1 msec was employed.

In general the bar heights in these histograms decrease with increasing duration of the tone burst. In Fig. 44 the recovered probabilities associated with four of the first cycles in each burst are plotted as a function of duration. Here also there is a decrease with increasing tone-burst duration.

A similar effect is apparent when the repetition rate of the tone bursts is varied. In Fig. 45 histograms obtained with several different repetition rates are presented; again, two different bin widths are employed. All of the calculations in this figure are based on one minute of data; hence the number of stimuli involved in each histogram is proportional to the repetition rate. Examination of this figure indicates that the bar

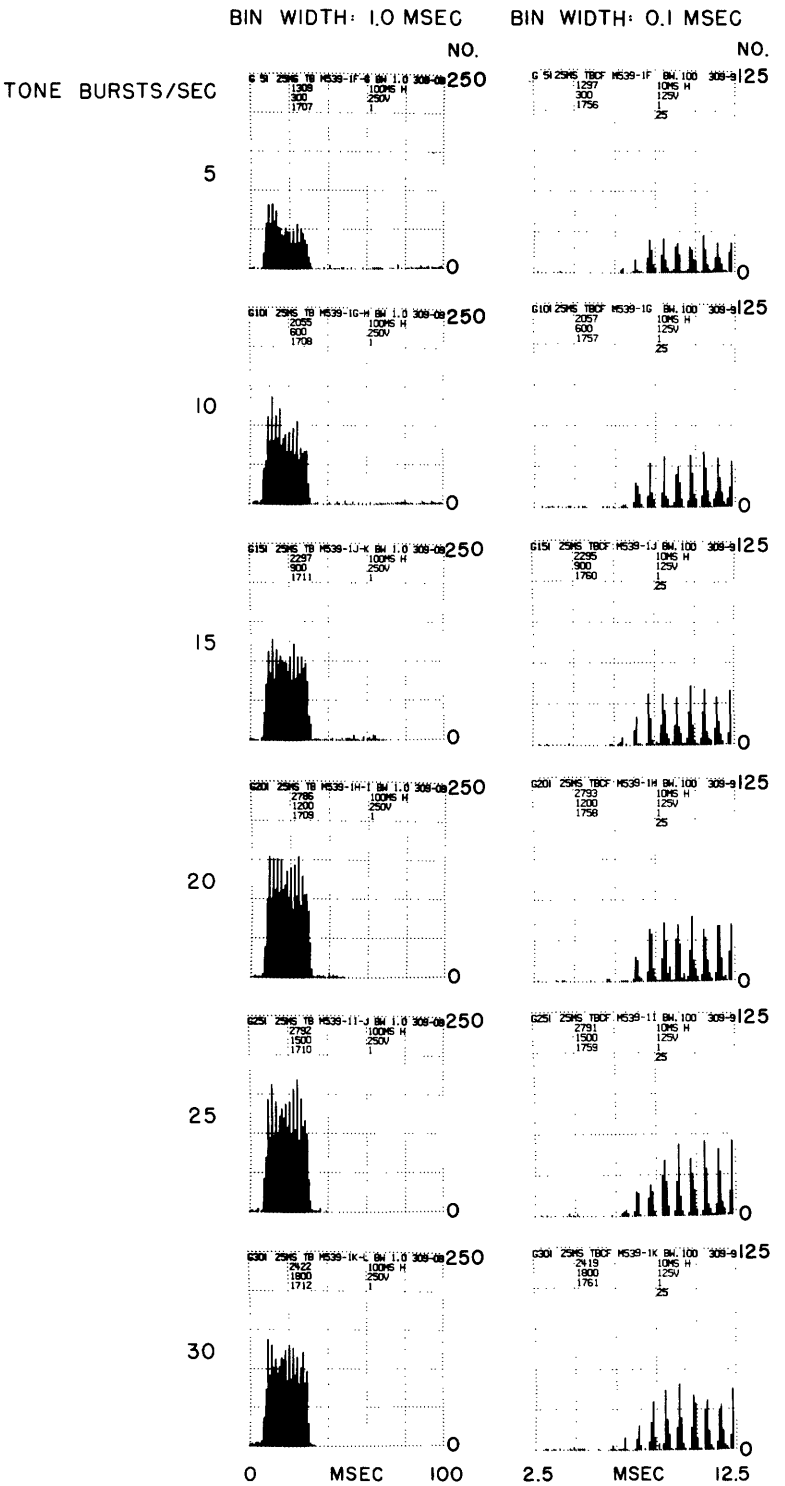

Fig. 45. Unit 309-9. PST histograms (left column: bin width 1 msec, bars 0-99; right column: bin width 0.1 msec, bars 25-124). Stimuli: -80 db, 25-msec tone bursts at CF of unit (1.45 kc), several rates, 1 minute.

heights grow more slowly than the stimulus count as repetition rate increases. Slightly restated, the spikes per bin per stimulus decrease as rate increases. The corresponding effect also appears in the recovered probabilities, which are presented in Fig. 44. In this figure it is easily seen that the recovered probabilities decrease with increasing click rate.

In summary, both the PST histograms and the recovered probabilities show variations in sensitivity with rate and duration. With the possible exception of the longest duration, the mechanical response to the previous tone burst should be over by the time the next burst begins. Apparently identical mechanical motions, at the beginning of the burst, yield different recovered probabilities depending, perhaps indirectly, on the presence of a stimulus tens of milliseconds previously. If a tone-burst rate were to be selected by the same criterion as the click rate, it appears it would have to be less than 5 per second for a 25-msec duration.

By coincidence all of the units used to illustrate tone-burst effects in the discussion above have low spontaneous rates. This precludes illustrating one more interesting phenomenon – the suppression of the spontaneous level after a tone burst. Since the noise-burst data are very similar to the tone-burst data, however, it seems sufficient to illustrate this phenomenon with only the noise-burst data.

4.3 NOISE BURSTS

The firing patterns that result when bursts of noise are presented are very similar to those obtained with tone bursts. In Fig. 46, the PST histograms obtained with three different intensities of noise bursts are presented. The horizontal scale represents the full 100-msec period of the 10 per second repetition rate. Two observations should be made from this figure. The first is that, just as with tone bursts, there is a clear transient in the response to the noise burst; the second observation is that the spontaneous level is suppressed following the noise bursts. Careful examination of the three histograms indicates that the level to which the spontaneous activity recovers before the next noise burst depends on the intensity of the noise; the higher the intensity the lower the spontaneous level just before the burst. This temporary suppression of spontaneous activity, as measured by the PST histogram, is typical of both noise and tone-burst stimulation. It was not apparent in the tone-burst data presented above only because all of the units had relatively low spontaneous rates.

Portions of the conditional probability matrices for these three runs are presented in Table 7. In this table the transient may be observed in the various conditional probabilities, which are indicated. The recovered probabilities in this table are not statistically reliable beyond 6 or 8 msec after the origin of the histogram, but the recovered probabilities that are reliable are of some interest. The recovered probability of an event within bars 7 and 8, which are at the beginning of the burst, increases with intensity as would be expected. The recovered probabilities associated with bars 1 and 2 and bars 3 and 4, which are before the burst, decrease as intensity increases. This

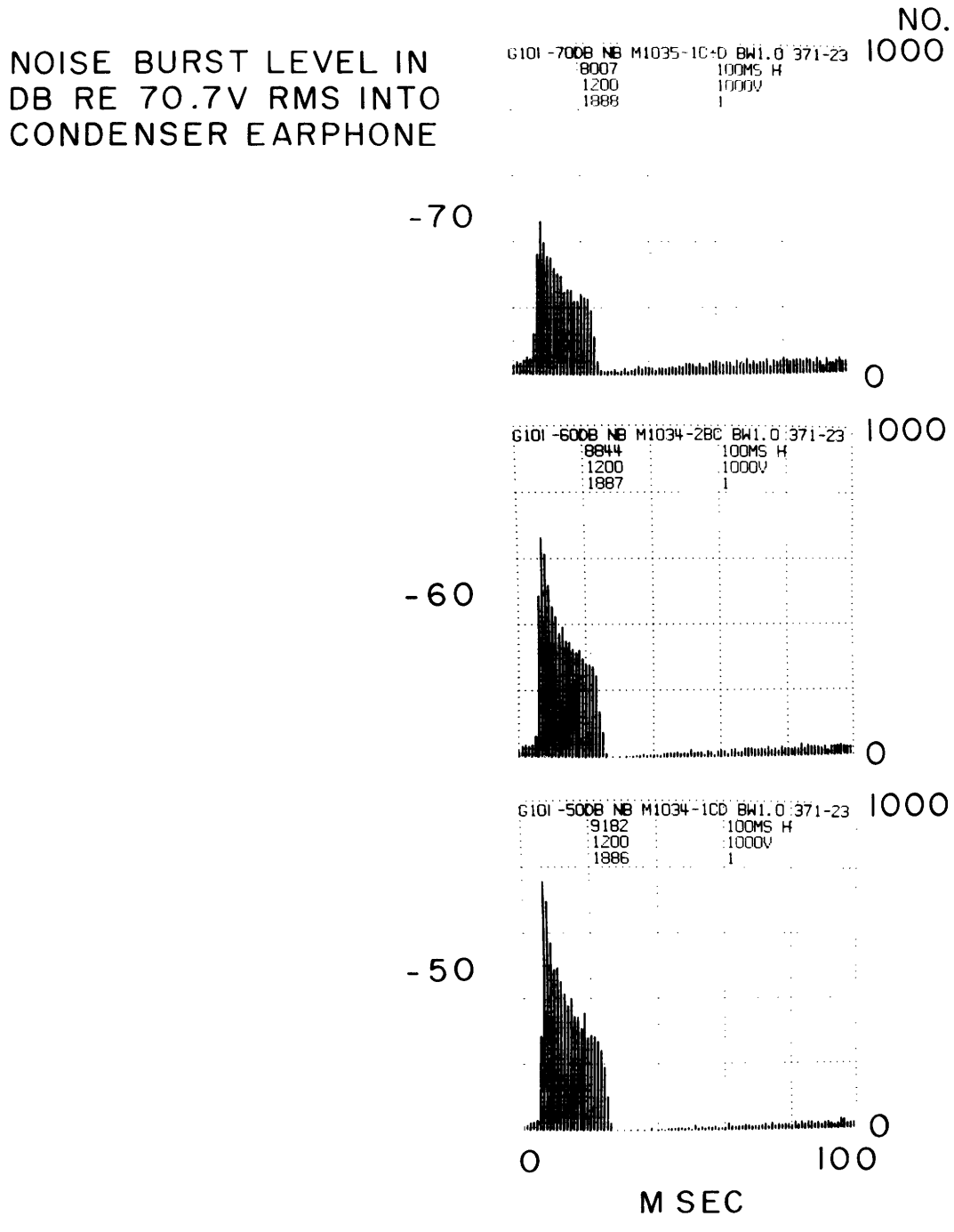

Fig. 46. Unit 371-23. PST histograms (bin width 1.0 msec, 100 bars). Stimuli: 10/sec, -70, -60, and -50 db noise bursts, 2 minutes.

Table 7. Unit 371-23. Conditional probability matrix.

Stimulus: 10/sec, -70 db noise bursts

Given last event during bars	Conditional probability of event during bars								
	0-2	3-4	5-6	7-8	9-10	11-12	13-14	15-16	17-18
-∞ to -20	.090 579	.100 527	.146 474	.620 405	.682 154	.634 49	.500 18	.778 9	.500 2
0-2		.058 104	.112 98	.632 87	.656 32	.364 11	.429 7	.250 4	.333 3
3-4			.119 101	.494 89	.578 45	.474 19	.500 10	.800 5	0 1
5-6				.512 170	.518 83	.550 40	.333 18	.083 12	.727 11
7-8					.491 700	.528 356	.494 168	.424 85	.571 49
9-10						.456 658	.497 358	.444 180	.440 100
11-12							.398 588	.407 354	.414 210
13-14								.313 536	.389 368
15-16									.272 448

(Table 7 continued on next page.)

Table 7. Unit 371-23 (continued).

Stimulus: 10/sec, -60 db noise bursts

Given last event during bars	Conditional probability of event during bars								
	0-2	3-4	5-6	7-8	9-10	11-12	13-14	15-16	17-18
$-\infty$ to -20	.076 732	.061 676	.465 635	.886 340	.821 39	.857 7	0 1	0 1	0 1
0-2		.023 87	.447 85	.979 47	0 1	1.0 1	0	0	0
3-4			.423 71	.854 41	.667 6	1.0 2	0	0	0
5-6				.709 519	.695 151	.652 46	.500 16	.375 8	.800 5
7-8					.643 962	.636 343	.664 125	.762 42	.500 10
9-10						.545 796	.591 362	.514 148	.500 72
11-12							.500 694	.519 347	.581 167
13-14								.430 654	.504 373
15-16									.409 572

(Table 7 continued on next page.)

Table 7. Unit 371-23 (concluded).

Stimulus: 10/sec, -50 db noise bursts

Given last event during bars	Conditional probability of event during bars								
	0-2	3-4	5-6	7-8	9-10	11-12	13-14	15-16	17-18
$-\infty$ to -20	.058 811	.052 764	.744 724	.948 185	.900 10	0 1	0 1	0 1	0 1
0-2		.016 63	.677 62	.900 20	1.0 2	0	0	0	0
3-4			.738 61	.625 16	1.0 6	0	0	0	0
5-6				.763 864	.741 205	.792 53	.636 11	.500 4	.500 2
7-8					.663 963	.686 325	.667 102	.647 34	.583 12
9-10						.570 821	.606 353	.547 139	.476 63
11-12							.532 733	.525 343	.546 163
13-14								.462 679	.534 365
15-16									.439 594

"Bars x-y" refers to times larger than x, and less than or equal to y msec.
The lower number in each pair is the number of trials on which the probability estimate is based.

corresponds to the effect suggested by the histogram; the level to which the spontaneous activity recovers is smaller at the higher intensities.

4.4 CLICKS PLUS NOISE

Various combinations of broadband noise and rarefaction clicks were used as stimuli to explore some effects of typical masking stimuli. PST histograms obtained from five different stimulus situations are presented in Fig. 47 and some probabilities associated with the peaks in these histograms are presented in Table 8. There are several qualitative observations to be made from these data, but first it is necessary to describe the various stimulus situations that were employed.

For the generation of these stimuli, the basic timing element was a stimulus-marker pulse which occurred periodically at a rate of 10 per second. This pulse, which was recorded along with the action potentials, marks the origin of the histogram time axis. The histograms display the interval from 2.5 msec to 12.5 msec after this pulse. After a delay of approximately 7.5 msec this marker pulse was used to trigger the click generator. It is this delay that accounts for the unusual latency of the click response in the first histogram. In all cases in which the click was used, the same delay and the same

Table 8. Unit 371-23. Probabilities associated with peaks of the PST histograms.

	Click	Click + noise burst 1	Click + continuous noise	Click + noise burst 2	Noise burst 1
p(A/R)	0.79	0.67	0.26	0.31	0.25
p(B/R)	0.76	0.69	0.29	0.33	0.33
p(B/A)	0.38	0.29	0.13	0.14	0.15
p(C/R)	x	x	0.23	0.20	0.20
p(C/A)	0.33	0.31	0.15	0.18	0.16
p(C/B)	0.14	0.15	0.09	0.10	0.08
p(D/R)	x	x	0.16	0.23	0.23
p(D/A)	0.35	0.31	0.16	0.18	0.17
p(D/B)	0.23	0.20	0.13	0.11	0.10
p(D/C)	0.10	0.08	0.04	0.07	0.07

$p(x|y)$ = conditional probability of an event in x, given last event was in y.
Interval definition: A, bars 91-97; B, bars 98-103; C, bars 104-108; D, bars 109-113; R, all times at least 10 msec before stimulus marker.
"Bars x-y" refers to times larger than x/10, and less than or equal to y/10 msec.
An "x" indicates that fewer than 100 trials were available for the probability estimate.

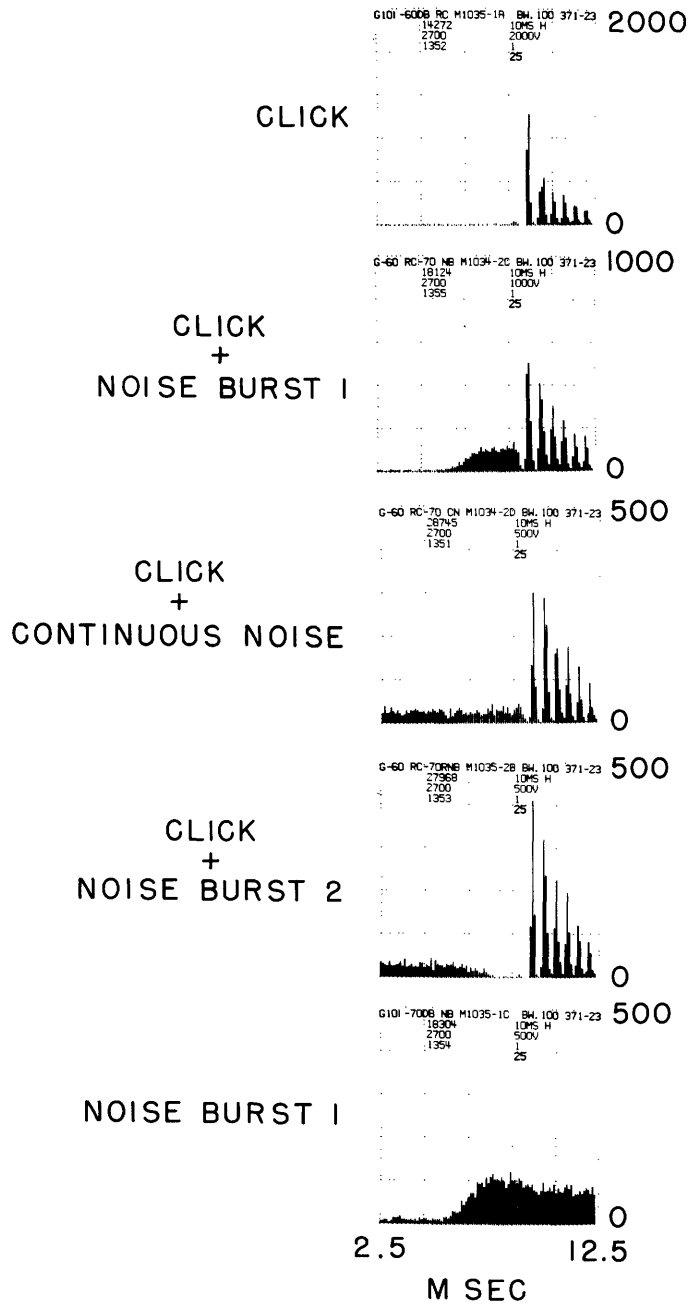

Fig. 47. Unit 371-23. PST histograms (bin width 0.1 msec, bars 25-124). Stimuli include 10/sec, -60 db rarefaction clicks and -70 db noise either continuously or in 10/sec noise bursts. Noise burst 1 is "on" in the region of the click; noise burst 2 is "on" except in the region of the click. All histograms based on 4.5 minutes.

click level were employed. The stimulus marker pulse was also used to trigger an electronic switch. The input to the electronic switch was broadband noise, and the same noise level was used in all of these runs. When continuous noise was desired, the switch was disabled. When a conventional noise burst (noise burst 1) was desired, the switch was adjusted so that its output was a 20-msec noise burst which began approximately 2.5 msec after the stimulus marker. The rise and fall times were also 2.5 msec. To generate noise burst 2 the function of this switch was reversed; in this case the noise was on until approximately 2.5 msec after the stimulus marker, at which time it was turned off with a fall time of 2.5 msec. Approximately 15 msec later, the noise was turned on again with a rise time of 2.5 msec. Finally, the outputs of the click generator and the electronic switch were added to provide the drive for the earphone. All of the histograms are based on 4.5 minutes of data. The vertical scales vary as indicated.

The first histogram was obtained with just the click as stimulus and except for the peculiar latency, which is due to the delays in the stimulus generating equipment, it is a typical click response. In the third histogram, continuous noise is added to the click, and the result is a considerable reduction in the size of the peaks. The second histogram is the same, except that rather than continuous noise, only a burst of noise surrounding the click is used. During the burst, the noise level is the same as that of the continuous noise. With the noise burst also, the peak sizes are reduced, but not as much as with the continuous noise.

One might guess that the reduction in peak size with masking noise is a simple refractory effect. Because the unit fires in response to the masking noise it is likely to be in a refractory state when the click occurs and consequently relatively fewer spikes will occur in response to the click. This explanation would not account for the reduction of the probabilities presented in Table 8. Both recovered and conditional probabilities are smaller in the noise-burst case than with the click alone, and they are still smaller in the continuous noise case.

It is curious that the probabilities in the continuous noise case are smaller than in the noise-burst case, for during the time intervals considered, the noise burst and continuous noise stimuli are equivalent. Apparently, the presence or absence of the noise tens of milliseconds before the click affects these probabilities. The same phenomenon can also be seen by comparing the histograms and the probabilities obtained with click alone with those obtained with click plus noise burst 2. These two stimuli differ only in the presence of noise outside the region of the click response. but the probabilities related to the region of the click response are clearly affected by the presence of this noise.

In summary, there are two conclusions to be made from these data. First, reductions in the sizes of PST histogram peaks in the presence of masking noise are not simply refractory effects; the probabilities are also reduced. Second, the data obtained with masking stimuli reflect at least two effects: in addition to changes caused by the different acoustic waveform, and hence mechanical motion, in the temporal proximity of

the click, the firing patterns in this region of time are strongly affected by the masking noise that occurred tens of milliseconds earlier.

V. SUMMARY AND CONCLUSIONS

This study began under the framework of a simplified model that represents the transformation from sound pressure at the eardrum to firing patterns in an auditory nerve fiber. This model has three stages: a mechanical system, a rectifier, and a probabilistic device. The output of the mechanical system is associated with the motion of the cochlear partition, but it is not specifically identified as displacement or any other physical variable. Based primarily on the data of von Békésy, this system is assumed to be linear and to be "tuned" to one frequency, the value of this most sensitive frequency varying smoothly with position along the cochlear partition.

Operating on the output of the mechanical system is a rectifier. This stage of the model was suggested by the electrophysiological data obtained with click stimuli. These data suggest that some rectified version of the mechanical motion may be regarded as an effective stimulus. Although it is tempting to identify this rectifier with the hair cell, this identification cannot be considered more than a reasonable possibility, since the "output" of the hair cell has not been clearly identified. The final stage of the model is a probabilistic device, which is intended to include the refractory characteristics of the neural unit. The probability of this device producing a spike during some time interval increases as the input increases, but decreases temporarily after each spike.

This simple model is based on data obtained with single sine waves and with short acoustic clicks, and it appears to be consistent with these data as they are presented in the form of tuning curves, interval histograms, and PST histograms. In order to test and refine this model, additional calculations, which are based primarily on the concept of a recovered neural unit, have been performed on these data. This concept is suggested by the exponential decay of the interval histograms obtained from spontaneous activity and is supported by conditional probability calculations performed on data obtained with click stimuli. The word "recovered" has been used here in a strictly operational way to refer to the state of the neural unit when the probability of firing is no longer a function of the time since the last firing. The term "refractory effects" has also been used in an operational way to refer to the effects associated with the temporarily diminished probabilities following a firing. The concept of a recovered neural unit provides a means of studying the model and data when the probabilistic device is in its simplest state. The calculations of recovered probabilities have indicated that some previously puzzling features of the PST histograms are refractory effects or other effects associated with the period shortly after a firing. By eliminating these effects, the recovered probability histograms provide a more direct measure of the mechanical system and rectifier than would be possible with conventional PST histograms alone.

A simple assumption to make concerning the model would have been that the recovered probability per unit time is an instantaneous function of the output of the mechanical system. With this assumption, the output of the rectifier could be identified as the recovered probability (per unit time) and regarded as an effective stimulus for the probabilistic

device. This assumption is contradicted, however, by the recovered probability histograms calculated as a function of intensity from data obtained with click stimuli.

The effect that contradicts this assumption has been labeled arbitrarily as the "depletion effect." Apparently, the presence of moderately large values of recovered probability diminish subsequent values, and the effect becomes increasingly important at times corresponding to the later portion of the PST histogram peaks and at higher intensities. In a descriptive way, it is useful to think of something being "used up" by the presence of moderate values of recovered probability; hence, the label "depletion effect." The important characteristic of this effect is that it occurs in the absence of firings and therefore is not a refractory effect in the ordinary sense.

In terms of the mathematics of a model, the depletion effect implies the necessity of an additional state variable. At least one state variable would be necessary to represent the time course of recovery of the probabilistic device following a firing. Unlike the state variable(s) associated with the refractory state of the probabilistic device, the additional variable could be affected even when there had not been any firings for a long period of time. One way to include this additional state variable in the model would be to incorporate the state variable into the rectifier in such a way that the output of the rectifier could still be identified as recovered probability (per unit time). Of course, there might be still more state variables necessary, and even if not, it is not clear that this formulation would be valid. Since it places the additional state variable in the deterministic portion of the model, this formulation represents a relatively easy way to include the depletion effect, and therefore seems to be a reasonable working hypothesis for the purposes of this discussion.

The "modified rectifier" might be described in the following way. The output is a function of the instantaneous output of the mechanical system and the current value of the state variable. This state variable is diminished at a rate determined by the output (or perhaps the input) of the rectifier, and increased toward its resting value at a rate that depends on its current value. When the state variable is near its resting value, and the input to the rectifier is relatively small (for example, at the beginning of a click presentation), the output of the modified rectifier is simply a nonlinear, no-memory function of the input, which is positive for zero input, increases with increasing values of the input, and decreases toward zero with decreasing values of the input. When the state variable is below its resting value, the output of the rectifier is reduced. As before, the output of the rectifier can be identified as the recovered probability per unit time.

The "depletion effect," which has been tentatively assigned to the modified rectifier, might also account for the transients observed with tone and noise bursts, including the suppression of spontaneous activity following the burst; the variation with rate and duration of the tone bursts; the click-rate data; and the masking data. In some of these cases, however, many firings are involved in each period of the stimulus, and it is

possible that still another effect could be present: When the probabilistic device fires a great deal it becomes less sensitive. The existence or extent of this possible additional effect has not been specifically investigated.

The nonrecovered properties of the probabilistic device are not well understood. While it seems reasonably clear that the device may be regarded as recovered after approximately 20 msec, what happens during that 20 msec is not clear. In terms of completing the mathematical form of the model, one possibility would be to assume that the probability of an event in an incremental unit of time is proportional to the output of the modified rectifier (recovered probability per unit of time) and a "recovery function." This recovery function would have a value of zero immediately after the firing and a value of one when the unit is recovered. The behavior of this function between the firing and complete recovery is less clear. Siebert and Gray assumed that the presence of a stimulus accelerates the recovery, and this may be consistent with (though not obvious from) the existing data. In any case, the form of recovery assumed by Siebert and Gray will not work, because of some further implications of its particular form; there may be some modification of this model that would be consistent with these data and would also be mathematically manageable.

The "second firings" are a further complication in the characteristics of the probabilistic device. Since these firings do not seem to be related to the instantaneous value of the effective stimulus (recovered probability), it may be that they should be described quite separately from the normal refractory effects. One possibility would be to assume that whenever a firing results from moderately large values of the effective stimulus, there is some probability (which depends on the strength of the effective stimulus) that a second firing will follow in 3/4 to 1 msec. The probability would not depend on the value of the effective stimulus at the time of the second firing.

The discussion suggests one way in which the model might be modified and completed to conform with some of the results of this study. Unfortunately, as already suggested, these modifications will not suffice to handle the low-frequency continuous tone data. For this reason, the model and the suggested modifications can, at best, be regarded as characterizing the data obtained with stimuli other than low-frequency continuous tones. How the model should be modified to account for the low-frequency continuous data is not now clear, but it is hoped that additional data in the future may provide some useful clues.

Acknowledgment

I wish to thank the many people in the Communications Biophysics Group of the Research Laboratory of Electronics and the Eaton-Peabody Laboratory of Auditory Physiology of the Massachusetts Eye and Ear Infirmary who have assisted in a variety of ways with this study. Professor W. M. Siebert, Professor W. A. Rosenblith, Professor T. F. Weiss, and Dr. N. Y. S. Kiang all provided useful criticisms and ideas as the study progressed. Mr. M. B. Sachs gave up many hours of his own experimental time to gather (with some assistance from me) the data on which much of this study is based. Mrs. Jenot W. Shipley prepared the majority of the figures and assisted in obtaining some of the data. Mrs. Louise F. C. Smith prepared several of the figures. Mr. F. H. Byers did much of the data processing and some of the programming. To all of these people and the many others who have contributed to this study, I am most grateful.

References

1. G. von Békésy, Experiments in Hearing, edited by E. G. Wever (McGraw-Hill Book Company, Inc., New York, 1960), pp. 446-464.
2. Ibid., pp. 99-100.
3. J. J. Guinan, Jr. and W. T. Peake, "Motion of Middle-Ear Bones," Quarterly Progress Report No. 74, Research Laboratory of Electronics, M. I. T., Cambridge, Mass., July 15, 1964, pp. 1526-1534.
4. A. Møller, "Transfer Function of the Middle Ear," J. Acoust. Soc. Am. 35, 1526-1534 (1963).
5. J. L. Flanagan, "Computational Model for Basilar Membrane Displacement," J. Acoust. Soc. Am. 34, 1370-1376 (1962).
6. W. M. Siebert, "Models for the Dynamic Behavior of the Cochlear Partition," Quarterly Progress Report No. 64, Research Laboratory of Electronics, M. I. T., Cambridge, Mass., January 15, 1962, pp. 242-258.
7. G. von Békésy, op. cit., pp. 485-500.
8. N. Y. S. Kiang with the assistance of T. Watanabe, Eleanor C. Thomas, and Louise F. Clark, Discharge Patterns of Single Fibers in the Cat's Auditory Nerve (The M. I. T. Press, Cambridge, Mass., 1965).
9. Ibid., p. 13.
10. G. L. Rasmussen, "Efferent Fibers of the Cochlear Nerve and Cochlear Nucleus," in Neural Mechanisms of the Auditory and Vestibular Systems, edited by G. L. Rasmussen and W. F. Windle (Charles C. Thomas, Publisher, Springfield, Illinois, 1960), pp. 105-115.
11. R. R. Gacek and G. L. Rasmussen, "Fiber Analysis of the Statoacoustic Nerve of Guinea Pig, Cat, and Monkey," Anat. Rec. 139, 455-463 (1961).
12. H. H. Spoendlin and R. R. Gacek, "Electronmicroscopic Study of the Efferent and Afferent Innervation of the Organ of Corti in the Cat," Ann. Otol. Rhinol. Laryngol. 72, pp. 660-686 (1963).
13. J. Fex, "Auditory Activity in Centrifugal and Centripetal Cochlear Fibers in Cat," Acta Physiol. Scand. (Stockholm) Vol. 55, Suppl. 189, 1962.
14. J. W. Woodbury and H. D. Patton, "Action Potential; Cable and Excitable Properties of the Cell Membrane," in Medical Physiology and Biophysics, edited by T. C. Ruch and J. F. Fulton (W. B. Saunders Company, Philadelphia and London, 1960), pp. 32-65.
15. S. Ochs, Elements of Neurophysiology (John Wiley and Sons, Inc., New York, 1965), pp. 18-132.
16. H. Davis, "Advances in the Neurophysiology and Neuroanatomy of the Cochlea," J. Acoust. Soc. Am. 34, 1377-1385 (1962).
17. N. Y. S. Kiang and others, op. cit., pp. 3-9.
18. Ibid., pp. 100-101.
19. Ibid., pp. 94-95.
20. A. Rupert, G. Moushegian, and R. Galambos, "Unit Responses to Sound from Auditory Nerve of the Cat," J. Neurophysiol. 26, 449-465 (1963).
21. N. Y. S. Kiang and others, op. cit., p. 126.
22. Ibid., p. 85.
23. Ibid., pp. 112-117.
24. Ibid., pp. 124-126.
25. M. Momoto, N. Suga, and Y. Katsuki, "Discharge Pattern and Inhibition of Primary Auditory Nerve Fibers in Monkey," J. Neurophysiol. 27, 768-787 (1964).

26. T. F. Weiss, "A Model for Firing Patterns of Auditory Nerve Fibers," Technical Report 418, Research Laboratory of Electronics, M. I. T., Cambridge, Mass., March 2, 1964.

27. W. M. Siebert and P. R. Gray, "Random Process Model for the Firing Pattern of Single Auditory Neurons," Quarterly Progress Report No. 71, Research Laboratory of Electronics, M. I. T., Cambridge, Mass., October 15, 1963, pp. 241-245.

28. P. R. Gray, "A Design Philosophy for Psychophysical Experiments," S. M. Thesis, Department of Electrical Engineering, M. I. T., January 1963.

29. W. M. Siebert, "Some Implications of the Stochastic Behavior of Primary Auditory Neurons," Kybernetik 2, 206-215, (1965).

30. G. L. Gerstein and N. Y. S. Kiang, "An Approach to the Quantitative Analysis of Electrophysiological Data from Single Neurons," Biophys. J. 1, 15-28 (1960).

31. D. R. Cox, Renewal Theory (John Wiley and Sons, Inc., New York, 1962).

32. E. Parzen, Stochastic Processes (Holden-Day, Inc., San Francisco, 1962), pp. 160-186.

33. J. M. Goldberg, H. O. Adrian, and F. D. Smith, "Response of Neurons of the Superior Olivary Complex to Acoustic Stimuli of Long Duration," J. Neurophysiol. 27, 706-749 (1964).

JOINT SERVICES ELECTRONICS PROGRAM
REPORTS DISTRIBUTION LIST

Department of Defense

Dr. Edward M. Reilley
Asst Director (Research)
Ofc of Defense Res & Eng
Department of Defense
Washington, D.C. 20301

Office of Deputy Director
(Research and Information Room 3D1037)
Department of Defense
The Pentagon
Washington, D.C. 20301

Director
Advanced Research Projects Agency
Department of Defense
Washington, D.C. 20301

Director for Materials Sciences
Advanced Research Projects Agency
Department of Defense
Washington, D.C. 20301

Headquarters
Defense Communications Agency (333)
The Pentagon
Washington, D.C. 20305

Defense Documentation Center
Attn: TISIA
Cameron Station, Bldg. 5
Alexandria, Virginia 22314

Director
National Security Agency
Attn: C3/TDL
Fort George G. Meade, Maryland 20755

Weapons Systems Evaluation Group
Attn: Col. Finis G. Johnson
Department of Defense
Washington, D.C. 20305

National Security Agency
Attn: R4-James Tippet
Office of Research
Fort George G. Meade, Maryland 20755

Central Intelligence Agency
Attn: OCR/DD Publications
Washington, D.C. 20505

Department of the Air Force

AUL3T-9663
Maxwell AFB, Alabama 36112

AFRSTE
Hqs. USAF
Room ID-429, The Pentagon
Washington, D.C. 20330

AFFTC (FTBPP-2)
Technical Library
Edwards AFB, Calif. 93523

Space Systems Division
Air Force Systems Command
Los Angeles Air Force Station
Los Angeles, California 90045
Attn: SSSD

SSD(SSTRT/Lt. Starbuck)
AFUPO
Los Angeles, California 90045

Det #6, OAR (LOOAR)
Air Force Unit Post Office
Los Angeles, California 90045

Systems Engineering Group (RTD)
Technical Information Reference Branch
Attn: SEPIR
Directorate of Engineering Standards
and Technical Information
Wright-Patterson AFB, Ohio 45433

ARL (ARIY)
Wright-Patterson AFB, Ohio 45433

AFAL (AVT)
Wright-Patterson AFB, Ohio 45433

AFAL (AVTE/R. D. Larson)
Wright-Patterson AFB, Ohio 45433

Commanding General
Attn: STEWS-WS-VT
White Sands Missile Range
New Mexico 88002

RADC (EMLAL-1)
Griffiss AFB, New York 13442
Attn: Documents Library

AFCRL (CRMXLR)
AFCRL Research Library, Stop 29
L. G. Hanscom Field
Bedford, Massachusetts 01731

Academy Library DFSLB)
U.S. Air Force Academy
Colorado 80840

FJSRL
USAF Academy, Colorado 80840

APGC (PGBPS-12)
Eglin AFB, Florida 32542

AFETR Technical Library
(ETV, MU-135)
Patrick AFB, Florida 32925

AFETR (ETLLG-1)
STINFO Officer (for Library)
Patrick AFB, Florida 32925

ESD (ESTI)
L. G. Hanscom Field
Bedford, Massachusetts 01731

AEDC (ARO, INC)
Attn: Library/Documents
Arnold AFS, Tennessee 37389

European Office of Aerospace Research
Shell Building
47 Rue Cantersteen
Brussels, Belgium

Lt. Col. E. P. Gaines, Jr.
Chief, Electronics Division
Directorate of Engineering Sciences
Air Force Office of Scientific Research
Washington, D.C. 20333

Department of the Army

U.S. Army Research Office
Attn: Physical Sciences Division
3045 Columbia Pike
Arlington, Virginia 22204

Research Plans Office
U.S. Army Research Office
3045 Columbia Pike
Arlington, Virginia 22204

Commanding General
U.S. Army Materiel Command
Attn: AMCRD-DE-E
Washington, D.C. 20315

Commanding General
U.S. Army Strategic Communications
Command
Washington, D.C. 20315

Commanding Officer
U.S. Army Materials Research Agency
Watertown Arsenal
Watertown, Massachusetts 02172

Commanding Officer
U.S. Army Ballistics Research Laboratory
Attn: V. W. Richards
Aberdeen Proving Ground
Aberdeen, Maryland 21005

Commandant
U.S. Army Air Defense School
Attn: Missile Sciences Division C&S Dept.
P.O. Box 9390
Fort Bliss, Texas 79916

Commanding General
Frankford Arsenal
Attn: SMUFA-L6000 (Dr. Sidney Ross)
Philadelphia, Pennsylvania 19137

Commanding General
U.S. Army Missile Command
Attn: Technical Library
Redstone Arsenal, Alabama 35809

U.S. Army Munitions Command
Attn: Technical Information Branch
Picatinney Arsenal
Dover, New Jersey 07801

Commanding Officer
Harry Diamond Laboratories
Attn: Mr. Berthold Altman
Connecticut Avenue and Van Ness St. N.W.
Washington, D.C. 20438

Commanding Officer
U.S. Army Security Agency
Arlington Hall
Arlington, Virginia 22212

Commanding Officer
U.S. Army Limited War Laboratory
Attn: Technical Director
Aberdeen Proving Ground
Aberdeen, Maryland 21005

Commanding Officer
Human Engineering Laboratories
Aberdeen Proving Ground, Maryland 21005

Director
U.S. Army Engineer
Geodesy, Intelligence and Mapping
Research and Development Agency
Fort Belvoir, Virginia 22060

Commandant
U.S. Army Command and General
Staff College
Attn: Secretary
Fort Leavenworth, Kansas 66270

Dr. H. Robl, Deputy Chief Scientist
U.S. Army Research Office (Durham)
Box CM, Duke Station
Durham, North Carolina 27706

Commanding Officer
U.S. Army Research Office (Durham)
Attn: CRD-AA-IP (Richard O. Ulsh)
Box CM, Duke Station
Durham, North Carolina 27706

Superintendent
U.S. Army Military Academy
West Point, New York 10996

The Walter Reed Institute of Research
Walter Reed Medical Center
Washington, D.C. 20012

Commanding Officer
U.S. Army Engineer R&D Laboratory
Attn: STINFO Branch
Fort Belvoir, Virginia 22060

Commanding Officer
U.S. Army Electronics R&D Activity
White Sands Missile Range,
New Mexico 88002

Dr. S. Benedict Levin, Director
Institute for Exploratory Research
U.S. Army Electronics Command
Attn: Mr. Robert O. Parker, Executive
Secretary, JSTAC (AMSEL-XL-D)
Fort Monmouth, New Jersey 07703

Commanding General
U.S. Army Electronics Command
Fort Monmouth, New Jersey 07703
Attn: AMSEL-SC

AMSEL-RD-D	HL-O
RD-G	HL-R
RD-MAF-1	NL-D
RD-MAT	NL-A
RD-GF	NL-P
XL-D	NL-R
XL-E	NL-S
XL-C	KL-D
XL-S	KL-E
HL-D	KL-S
HL-L	KL-T
HL-J	VL-D
HL-P	WL-D

Department of the Navy

Chief of Naval Research
Department of the Navy
Washington, D.C. 20360
Attn: Code 427

Chief, Bureau of Ships
Department of the Navy
Washington, D.C. 20360

Chief, Bureau of Weapons
Department of the Navy
Washington, D.C. 20360

Commanding Officer
Office of Naval Research Branch Office
Box 39, Navy No 100 F.P.O.
New York, New York 09510

Commanding Officer
Office of Naval Research Branch Office
1030 East Green Street
Pasadena, California

Commanding Officer
Office of Naval Research Branch Office
219 South Dearborn Street
Chicago, Illinois 60604

Commanding Officer
Office of Naval Research Branch Office
207 West 42nd Street
New York, New York 10011

Commanding Officer
Office of Naval Research Branch Office
495 Summer Street
Boston, Massachusetts 02210

Director, Naval Research Laboratory
Technical Information Officer
Washington, D.C.
Attn: Code 2000

Commander
Naval Air Development and Material Center
Johnsville, Pennsylvania 18974

Librarian, U.S. Electronics Laboratory
San Diego, California 95152

Commanding Officer and Director
U.S. Naval Underwater Sound Laboratory
Fort Trumbull
New London, Connecticut 06840

Librarian, U.S. Naval Post Graduate School
Monterey, California

Commander
U.S. Naval Air Missile Test Center
Point Magu, California

Director
U.S. Naval Observatory
Washington, D.C.

Chief of Naval Operations
OP-07
Washington, D.C.

Director, U.S. Naval Security Group
Attn: G43
3801 Nebraska Avenue
Washington, D.C.

Commanding Officer
Naval Ordnance Laboratory
White Oak, Maryland

Commanding Officer
Naval Ordnance Laboratory
Corona, California

Commanding Officer
Naval Ordnance Test Station
China Lake, California

Commanding Officer
Naval Avionics Facility
Indianapolis, Indiana

Commanding Officer
Naval Training Device Center
Orlando, Florida

U.S. Naval Weapons Laboratory
Dahlgren, Virginia

Weapons Systems Test Division
Naval Air Test Center
Patuxtent River, Maryland
Attn: Library

Other Government Agencies

Mr. Charles F. Yost
Special Assistant to the Director
of Research
NASA
Washington, D.C. 20546

NASA Lewis Research Center
Attn: Library
21000 Brookpark Road
Cleveland, Ohio 44135

Dr. H. Harrison, Code RRE
Chief, Electrophysics Branch
NASA, Washington, D.C. 20546

Goddard Space Flight Center
NASA
Attn: Library, Documents Section Code 252
Green Belt, Maryland 20771

National Science Foundation
Attn: Dr. John R. Lehmann
Division of Engineering
1800 G Street N.W.
Washington, D.C. 20550

U.S. Atomic Energy Commission
Division of Technical Information Extension
P.O. Box 62
Oak Ridge, Tennessee 37831

Los Alamos Scientific Library
Attn: Reports Library
P.O. Box 1663
Los Alamos, New Mexico 87544

NASA Scientific & Technical Information
Facility
Attn: Acquisitions Branch (S/AK/DL)
P.O. Box 33
College Park, Maryland 20740

Non-Government Agencies

Director
Research Laboratory for Electronics
Massachusetts Institute of Technology
Cambridge, Massachusetts 02139

Polytechnic Institute of Brooklyn
55 Johnson Street
Brooklyn, New York 11201
Attn: Mr. Jerome Fox
Research Coordinator

Director
Columbia Radiation Laboratory
Columbia University
538 West 120th Street
New York, New York 10027

Director
Stanford Electronics Laboratories
Stanford University
Stanford, California

Director
Coordinated Science Laboratory
University of Illinois
Urbana, Illinois 61803

Director
Electronics Research Laboratory
University of California
Berkeley 4, California

Director
Electronics Sciences Laboratory
University of Southern California
Los Angeles, California 90007

Professor A. A. Dougal, Director
Laboratories for Electronics and
Related Sciences Research
University of Texas
Austin, Texas 78712

Division of Engineering and Applied
Physics
210 Pierce Hall
Harvard University
Cambridge, Massachusetts 02138

Aerospace Corporation
P.O. Box 95085
Los Angeles, California 90045
Attn: Library Acquisitions Group

Professor Nicholas George
California Institute of Technology
Pasadena, California

Aeronautics Library
Graduate Aeronautical Laboratories
California Institute of Technology
1201 E. California Blvd.
Pasadena, California 91109

Director, USAF Project RAND
Via: Air Force Liaison Office
The RAND Corporation
1700 Main Street
Santa Monica, California 90406
Attn: Library

The Johns Hopkins University
Applied Physics Laboratory
8621 Georgia Avenue
Silver Spring, Maryland
Attn: Boris W. Kuvshinoff
Document Librarian

School of Engineering Sciences
Arizona State University
Tempe, Arizona

Dr. Leo Young
Stanford Research Institute
Menlo Park, California

Hunt Library
Carnegie Institute of Technology
Schenley Park
Pittsburgh, Pennsylvania 15213

Mr. Henry L. Bachmann
Assistant Chief Engineer
Wheeler Laboratories
122 Cuttermill Road
Great Neck, New York

University of Liege
Electronic Institute
15, Avenue Des Tilleuls
Val-Benoit, Liege
Belgium

University of California at Los Angeles
Department of Engineering
Los Angeles, California

California Institute of Technology
Pasadena, California
Attn: Documents Library

University of California
Santa Barbara, California
Attn: Library

Carnegie Institute of Technology
Electrical Engineering Department
Pittsburgh, Pennsylvania

University of Michigan
Electrical Engineering Department
Ann Arbor, Michigan

New York University
College of Engineering
New York, New York

Syracuse University
Dept. of Electrical Engineering
Syracuse, New York

Yale University
Engineering Department
New Haven, Connecticut

Bendix Pacific Division
11600 Sherman Way
North Hollywood, California

General Electric Company
Research Laboratories
Schenectady, New York

Airborne Instruments Laboratory
Deerpark, New York

Lockheed Aircraft Corporation
P.O. Box 504
Sunnyvale, California

Raytheon Company
Bedford, Massachusetts
Attn: Librarian

UNCLASSIFIED
Security Classification

DOCUMENT CONTROL DATA - R&D

(Security classification of title, body of abstract and indexing annotation must be entered when the overall report is classified)

1. ORIGINATING ACTIVITY (Corporate author) Research Laboratory of Electronics Massachusetts Institute of Technology Cambridge, Massachusetts	2a. REPORT SECURITY CLASSIFICATION Unclassified 2b GROUP

3. REPORT TITLE

A Statistical Analysis of Electrophysiological Data from Auditory Nerve Fibers in Cat

4. DESCRIPTIVE NOTES (Type of report and inclusive dates)

Technical report

5. AUTHOR(S) (Last name, first name, initial)

Gray, Peter R.

6. REPORT DATE	7a. TOTAL NO. OF PAGES	7b. NO. OF REFS
June 21, 1966	104	33

8a. CONTRACT OR GRANT NO.	9a. ORIGINATOR'S REPORT NUMBER(S)
DA 36-039-AMC-03200(E) b. PROJECT NO. 200-14501-B31F NSF Grant GK-835 NIH Grant 2 PO1 MH-04737-06 NASA Grant NsG-496	Technical Report 451 9b. OTHER REPORT NO(S) (Any other numbers that may be assigned this report) None

10. AVAILABILITY/LIMITATION NOTICES

Distribution of this report is unlimited

11. SUPPLEMENTARY NOTES	12. SPONSORING MILITARY ACTIVITY
	Joint Services Electronics Program thru USAECOM, Fort Monmouth, N. J.

13. ABSTRACT Electrophysiological data from single auditory nerve fibers have been analyzed with the objective of developing a random-process model for the firing patterns of these fibers. This study differs from earlier attempts at modeling these data in that new data-processing methods have been employed in order to more directly test and refine assumptions relating to models. In addition to calculating conventional post stimulus time (PST) and interval histograms, various conditional probabilities associated with the firing patterns have been estimated. These analyses suggest that a fiber recovers from the refractory effects that follow a firing within 20 msec after the firing. The effect of the stimulus on a fiber that has apparently recovered can be studied by estimating the conditional probability of a spike in a particular interval of time, given some minimum time since the last firing. Analysis of these "recovered probabilities" allows a more direct comparison of some aspects of model and data than is possible with other calculations such as the PST histogram. Results from these and other conditional probability analyses are presented with particular emphasis on data obtained with short acoustic clicks as stimuli. The use of these calculations to study the non-refractory aspects of the data has provided a somewhat simpler picture of the relation between these firing patterns and the mechanical motion of cochlear structures, but it has also exposed some unexpected phenomena. The implications of these results for possible models are reviewed.

DD FORM 1 JAN 64 1473

UNCLASSIFIED
Security Classification

UNCLASSIFIED

Security Classification

14. KEY WORDS	LINK A		LINK B		LINK C	
	ROLE	WT	ROLE	WT	ROLE	WT
auditory physiology neuron models analysis of neuronal spike data						

INSTRUCTIONS

1. ORIGINATING ACTIVITY: Enter the name and address of the contractor, subcontractor, grantee, Department of Defense activity or other organization *(corporate author)* issuing the report.

2a. REPORT SECURITY CLASSIFICATION: Enter the overall security classification of the report. Indicate whether "Restricted Data" is included. Marking is to be in accordance with appropriate security regulations.

2b. GROUP: Automatic downgrading is specified in DoD Directive 5200.10 and Armed Forces Industrial Manual. Enter the group number. Also, when applicable, show that optional markings have been used for Group 3 and Group 4 as authorized.

3. REPORT TITLE: Enter the complete report title in all capital letters. Titles in all cases should be unclassified. If a meaningful title cannot be selected without classification, show title classification in all capitals in parenthesis immediately following the title.

4. DESCRIPTIVE NOTES: If appropriate, enter the type of report, e.g., interim, progress, summary, annual, or final. Give the inclusive dates when a specific reporting period is covered.

5. AUTHOR(S): Enter the name(s) of author(s) as shown on or in the report. Enter last name, first name, middle initial. If military, show rank and branch of service. The name of the principal author is an absolute minimum requirement.

6. REPORT DATE: Enter the date of the report as day, month, year; or month, year. If more than one date appears on the report, use date of publication.

7a. TOTAL NUMBER OF PAGES: The total page count should follow normal pagination procedures, i.e., enter the number of pages containing information.

7b. NUMBER OF REFERENCES: Enter the total number of references cited in the report.

8a. CONTRACT OR GRANT NUMBER: If appropriate, enter the applicable number of the contract or grant under which the report was written.

8b, 8c, & 8d. PROJECT NUMBER: Enter the appropriate military department identification, such as project number, subproject number, system numbers, task number, etc.

9a. ORIGINATOR'S REPORT NUMBER(S): Enter the official report number by which the document will be identified and controlled by the originating activity. This number must be unique to this report.

9b. OTHER REPORT NUMBER(S): If the report has been assigned any other report numbers *(either by the originator or by the sponsor)*, also enter this number(s).

10. AVAILABILITY/LIMITATION NOTICES: Enter any limitations on further dissemination of the report, other than those imposed by security classification, using standard statements such as:

(1) "Qualified requesters may obtain copies of this report from DDC."

(2) "Foreign announcement and dissemination of this report by DDC is not authorized."

(3) "U. S. Government agencies may obtain copies of this report directly from DDC. Other qualified DDC users shall request through _____."

(4) "U. S. military agencies may obtain copies of this report directly from DDC. Other qualified users shall request through _____."

(5) "All distribution of this report is controlled. Qualified DDC users shall request through _____."

If the report has been furnished to the Office of Technical Services, Department of Commerce, for sale to the public, indicate this fact and enter the price, if known.

11. SUPPLEMENTARY NOTES: Use for additional explanatory notes.

12. SPONSORING MILITARY ACTIVITY: Enter the name of the departmental project office or laboratory sponsoring *(paying for)* the research and development. Include address.

13. ABSTRACT: Enter an abstract giving a brief and factual summary of the document indicative of the report, even though it may also appear elsewhere in the body of the technical report. If additional space is required, a continuation sheet shall be attached.

It is highly desirable that the abstract of classified reports be unclassified. Each paragraph of the abstract shall end with an indication of the military security classification of the information in the paragraph, represented as *(TS), (S), (C), or (U)*

There is no limitation on the length of the abstract. However, the suggested length is from 150 to 225 words.

14. KEY WORDS: Key words are technically meaningful terms or short phrases that characterize a report and may be used as index entries for cataloging the report. Key words must be selected so that no security classification is required. Identifiers, such as equipment model designation, trade name, military project code name, geographic location, may be used as key words but will be followed by an indication of technical context. The assignment of links, rules, and weights is optional.

UNCLASSIFIED

Security Classification